MATERNAL NUTRITION AND INFLAMMATION AS A RISK FACTOR FOR FUTURE MENTAL HEALTH DISORDERS.

By

Julian Sergej Benedikt Ramirez

A DISSERTATION

Presented to the Department of Behavioral Neuroscience and the

Oregon Health & Science University School of Medicine

In partial fulfillment of the requirements for the degree of

Doctor of Philosophy

November 13th, 2019

School of Medicine

Oregon Health & Science University

CERTIFICATE OF APPROVAL

This is to certify that the PhD Dissertation of

Julian Sergej Benedikt Ramirez

Has been approved

Dr. Damien Fair, Mentor/Advisor

Dr. Joel Nigg, Oral Exam Committee Chair

Dr. Elinor Sullivan, Member

Dr. Bonnie Nagel, Member

Table of Contents

Figures Contents

Table Contents

Abbreviations

IL-6 – Interleukin-6

MRI – Magnetic Resonance Imaging

rs-fcMRI – resting state functional connectivity magnetic resonance imaging

ASD – Autism Spectrum Disorder

ADHD – Attention Deficit Hyperactivity Disorder

SCZ – Schizophrenia

BD – Bipolar disorder

NHP – non-human primates

WSD – Western-Style Diet

CTR – Control Diet

PET – Positron Emission Tomography

EEG – electroencephalograms

ROI – Region of interest

BOLD – blood oxygen level dependent

RSN – resting-state network

VIS – Visual network

SMN – Somatomotor network

DMN – Default mode network

DAN – Dorsal Attention network

INO – Insular-opercular network

LIM – Limbic network

AUD – Auditory network

SNR – Signal-to-noise ratio

BIDS – Brain Imaging Data Structure

MSM – Multimodal Surface Matching

PLSR – partial least squares regression

LLOQ – lower limit of quantification

HCP – human connectome project

FSL – FMRIB Software Library

ANTs – Advanced Normalization Tools

T1w – T_1-weighted

asegs – automated segmented brain images

ABCD – Adolescent Brain Cognitive Development

SEM – structural equation modeling

LGM – Latent Growth Model

CFI – Comparative Fit Index

TLI – Tucker-Lewis index

RMSEA – Root Mean Square Error of Approximation

LA – Left Amygdala

RA – Right Amygdala

TBV – Total brain volume

PRIME-DE – Primate Data Exchange

ONPRC – Oregon National Primate Research Center

LGC – latent growth curve

Ia – anterior insula

Ip – posterior insula

EPI – echoplanar imaging

FD – framewise displacement

SVD – singular value decomposition

FEF – Frontal eye field

dlPMC – dorsal lateral premotor cortex

PCm – medial parietal cortex

FHI – functional homology index

PFC – prefrontal cortex

mPFC – medial prefrontal cortex

DOHaD – developmental origins of health and disease

DREADDs – Designer receptors exclusively activated by designer drugs

Acknowledgments

This dissertation was only possible through a conglomeration of collaborative and supportive efforts from numerous incredible individuals. The best science comes when you work together as a team. First and foremost, I would like to extend a tremendous thank you to my mentor Dr. Damien Fair. Damien. He not only supported me throughout my graduate career through guidance and creative input, but he also helped shape me to be the person I am today. They say to lead by example, and Damien has been a mentor to be proud and inspired by. Damien made consistent efforts to drive and push me to overcome my challenges and weaknesses, and also created an environment of driven, smart creative and well-intentioned scientists that I now consider my family. To the Developmental Cognition and Neuroimaging Lab (DCAN), you all have been amazing, and I have learned so much from all of you scientifically and socially. I was tremendously lucky to have you all by my side, helping me when I needed help, and distracting me when I needed to take my mind off of things.

Along these lines, I would like to thank all of the collaborators on these three studies whom have contributed to the work in a number of ways. Dr. Elinor Sullivan, Darrick, Sturgeon, Eric Earl, Dr. Eric Feczko, Aj Mitchell, Anders Perrone, Kathy Snider, Dr. Oscar Miranda-Dominguez, Dr. Claudia Buss, Dr. Alice Graham, Dr. Jarod Rasmussen, Dr. Alice Graham, Mollie Marr, Anthony Galassi, Samantha Papadakis, Muhammed Bah, Jacqueline Thompson, Jennifer Bagley, Michael Reusz, Elina Thomas, Jennifer Zhu, and many many more, have all been instrumental in the data acquisition, organization and data processing for this dissertation, for which I am forever grateful and impressed with.

The non-human primate subjects used for this dissertation where part of an ongoing collaboration between Dr. Sullivan and Dr. Damien Fair and their labs. This acknowledgement section only scratches the surface to the amount of work that Dr. Sullivan and her team have put into the development, care, maintenance acquisition and synthesis of the macaque data set. This data set was at the core of all of the work presented in the current dissertation, without it none of this would have been possible. This type of work encompasses a tremendous amount of planning, coordination, and time just to maintain the macaques, organize the experimental groups, the different aspects of the diet, the experimental schedules, and the type of behavioral and imaging data that needs to be collected. This involves a team of people and daily monitoring of the animal's behavior and health, troubleshooting health and behavioral issues, and being responsible for the health and safety of the animals 24 hours a day, seven days a week. Furthermore, planning the procedures, collecting, scoring and analyzing the behavioral and inflammatory data not only takes a significant amount of time, but also takes years and years of expertise to accomplish successfully. Similar efforts need to be taken into account when it comes to collecting the imaging data. All of this work was made possible by Dr. Sullivan and her amazing team. I had the pleasure and honor of collaborating with Dr. Sullivan, Jennifer Bagley, Jacqueline Thompson, Michael Reusz and many others from the Sullivan Lab that made all of this work possible. I can't thank you enough and wouldn't be here without you. Macaque imaging and behavioral tests have been ongoing since before I started graduate school. The behavioral data was collected, scored and composited by the Sullivan lab. The imaging data was also collected by the Sullivan lab

and collaborators with my role only being minor regarding fine tuning and testing of some of the imaging acquisition parameters.

The data processing was also a collaborative effort by many of the people mentioned above. When starting this dissertation, a surface-based non-human primate pipeline did not exist in our lab, so together we helped develop the pipeline to get the data processed and quality controlled. A special thanks to Darrick, Eric and Jen for the tremendous efforts that went into this, I cannot thank you enough. Furthermore, a special help to Dr. Alice Graham, Elina Thomas, Mollie Marr and Dr. Joel Nigg for the guidance on learning and running the Latent Growth Curve Models, I could not have done it without you. Similarly, thank you to David Ball and Anthony Galassi helping with the "master GUI" parts of the dissertation, which enabled me to start running the multiple models throughout the cortex. Similarly, a huge thank you to Dr. Oscar Miranda-Dominguez and Marc Rudolf for the tremendous help in getting the Partial Least Scares Regression running for the Study 3 work of this dissertation.

Study 3 also contained a human infant data which came of a valuable collaboration between Dr. Claudia Buss, Dr. Pathik Wadhwa, Dr. Alice Graham and Dr. Damien Fair. The data was collected at the University of California Irvine, by Dr. Claudia Buss and colleagues. The amount of work that went into collecting this unique and immensely useful infant data set is enormous. Very few studies have gone above and beyond to perfect infant imaging procedures, and Dr. Buss and her team are forging ahead making this difficult data set an incalculably valuable contribution to the scientific field. I am privileged and grateful to have been given the chance to utilize these data to further my graduate studies. Furthermore, the infant surface-based processing pipeline

that enabled my analyses came out of the tireless efforts of the Infant Team in the DCAN lab including Dr. Alice Graham, Darrick Sturgeon, Mollie Marr, Elina Thomas, Eric Feczko, Kathy Snider and Luci Moore.

Study 3 also contained work done by Dr. Ting Xu, my now postdoctoral mentor, who helped provide the monkey to human deformation maps, and also helped with other collaborative work along the way. I am very grateful for the support and excited to continue to work together as I continue my scientific career. Additionally, I would like to thank Dr. Elinor Sullivan for the mentoring and support throughout graduate school. Our meetings were tremendously helpful and helped me grow as I scientist. Similarly, I would like to thank Dr. Eric Feczko and Dr. Alice Graham for mentoring me and helping me overcome a number of problems I thought were not possible to overcome. I would also like to extend a magnificent thank you to my dissertation and oral exam committee. Thank you Dr. Joel Nigg, Dr. Bonnie Nagle, Dr. Elinor Sullivan, Dr. Alice Graham and Dr. Damien Fair for all of the help along the way, I am honored to have learned from such impressive and awesome people, and am excited you all could help shape my dissertation work, and scientific ambitions along the way.

I would like to extend my gratitude to the Behavioral Neuroscience Department, and all of my friends that helped make graduate school a healthy learning environment and an incredible time in my life. You know who you are, and I thank you! Amy (and Luna Blu), I cannot begin to describe how instrumental you have been throughout all of this. You make me a better person and continue to impress me in every way imaginable. Thank you for being my sun and inspiration. Finally, a big thank you to my family! As someone studying development, and developmental trajectories, I cannot be more

grateful to have such an awesome family to grow up with and help shape my trajectories as I grow as a scientist and a person.

Abstract

Mental health disorders are a serious public health issue with a largely unknown etiology. Developmental programming is the idea that genetic and environmental stimuli interact during fetal development to shape the individual and create an avenue for adverse outcomes. Animal and human studies can capitalize on this framework to study potential risk processes for neuropsychiatric disorders. Maternal inflammation, obesity, and diet are candidate risk factors for which prior studies have described a link with subsequent offspring disorders. However, how these affect specific aspects of behavior or brain development is unclear. The present work investigated this question in three studies using non-invasive imaging techniques in Japanese macaque and human subjects. Study 1 investigated how the maternal pro-inflammatory cytokine interleukin-6 (IL-6) may relate to Japanese macaque offspring amygdala volume development and anxiety-like behavior. Study 2 expanded on this and investigated how maternal IL-6, maternal diet, and offspring sex relate to cortical thickness development. Finally, Study 3 used patterns in macaque offspring functional connectivity to 1) make inferences about maternal levels of IL-6 and 2) translate the most significant models across species to make predictions in human infants from macaque functional connectivity.

Findings indicated that maternal IL-6 was associated with decrease macaque offspring amygdala volumes at 4-months of age, but an increased rate of growth from 4 to 36-months of age (Study 1). Further, IL-6 concentrations indirectly associated with 11-month anxiety-like behavior via the 4-month amygdala volumes. Second, maternal IL-6 and diet related to offspring cortical thickness development from 4, 11, 21 and 36-month MRI scans while controlling for sex. Typical macaque cortical thickness development

was characterized by identifying best-fitting models describing the different patterns of growth trajectories throughout the cortex. The predictors (diet, IL-6 and sex) independently related to the cortical growth trajectories highlighting unique patterns in significant clusters of this association. Finally, 4-month macaque resting state functional connectivity MRI (rs-fcMRI) results indicated there was enough information in infant brain connectivity to make inferences about maternal IL-6 concentrations. The top models from this analysis in part translated across-species significantly predicting human maternal IL-6 levels from macaque-derived models. Together, these three studies improve an understanding of the structural and functional consequences of changes in the maternal environment and open the door for the use of cross-species translational research.

Chapter 1: Introduction

1.1 Neuropsychiatric disorders

Neuropsychiatric disorders such as Autism Spectrum Disorder (ASD), Attention Deficit Hyperactivity Disorder (ADHD), and Schizophrenia (SCZ) pose a substantial impact on a personal, societal and economic scale (Costello et al. 2003; Kessler et al. 2005; Elsabbagh et al. 2012; Polanczyk et al. 2014; Atladottir et al. 2015). The mechanisms and etiology of these disorders are continually being studied bringing us closer to identifying treatment and prevention strategies to mitigate various risk factors and contributing components. While genetics play an important role, they are not solely responsible for these disorders. Genetic studies revealed a strong heritability component; additive interactions with genetic factors may explain the phenotypic variance for 75-90 percent in ADHD (Levy et al. 1997; Faraone et al. 2005; Hawi et al. 2015), ~80 percent in ASD (Bailey et al. 1995; O'Roak and State 2008) and 60-85% in SCZ (Lichtenstein et al. 2009; Escudero and Johnstone 2014). These disorders manifest during the development of the brain, a complex process that closely interacts with internal and external environmental factors and that results in behavioral traits and atypical manifestations (Zhao and Castellanos 2016).

1.2 Developmental Programming

While the general concept of how these neuropsychiatric disorders might manifest is understood, the exact etiology of how they form is principally unknown. Contributing factors can be multifold, interrelated and heterogeneous depending on the disorder, symptom or characteristic of interest. One concept, however, which is often studied in this field is the idea of "developmental programming". Developmental programming is

the notion that stressors of the maternal uterine environment in pregnancy or the neonatal period influence the epigenetic control of multiple bodily systems and developmental processes (Reynolds et al. 2010; Kwon and Kim 2017). Dramatic transformations occur during fetal brain development, processes such as cellular proliferation, neurogenesis, neural migration, apoptosis, synaptogenesis, myelination and microglia and immune cell colonization (Sidman and Rakic 1973; Toga et al. 2006; Knuesel et al. 2014; Nayak et al. 2014). Environmental and genetic interactions can influence this critical window in development and ultimately shape an individual's constitution (Entringer 2007; Bale et al. 2010; Kwon and Kim 2017; DeCapo et al. 2019). Prior research has investigated the nature in which environmental factors may interact with brain behavioral development. The general heuristic of etiology entails multiple feedback loops along a developmental chain of events from genes→molecules→cells→brain→behavior outcomes, during which environmental factors may intervene at various points (Miller and Rockstroh 2013). Epigenetic modifications, or de novo mutations can influence RNA or protein-coding and alter gene expression leading to downstream changes in brain development (Miller and Rockstroh 2013).

Consequently, the maternal environmental state may play a fundamental role in offspring development. There are several maternal factors that may modify fetal brain development during this early period of life. Studies have implicated maternal intake of substances such as alcohol (Kodituwakku 2007; Popova et al. 2017), nicotine (England et al. 2015) and other drugs (dos Santos et al. 2018) with subsequent changes in the offspring's brain and behavioral characteristics. Additional factors often experienced during pregnancy such as stress (Ronald et al. 2010; Buss et al. 2012; Entringer et al.

2015; Gumusoglu et al. 2017; Graham et al. 2019), psychological state (Qiu et al. 2015a), and environmental toxins (Ostrea et al. 2002; Crinnion 2009) also have been shown to impact fetal development. Finally, maternal inflammation and diet/nutrition are two key elements that have gained major scientific traction throughout the years of studying developmental programming.

Inflammation: Maternal inflammation during pregnancy has repeatedly been linked to altered offspring outcomes in animal and human studies (Estes and McAllister 2016; Careaga et al. 2017; Bergdolt and Dunaevsky 2019; Dunn et al. 2019; Guma et al. 2019; Gumusoglu and Stevens 2019). However, it is important to note that inflammation is also a normal part of pregnancy as immunosuppression may enable the fetus to not be rejected (Warning et al. 2011). Immune mediators, or neuropoietic cytokines play a critical role in typical brain development via endocrine, paracrine and autocrine signaling, and transcriptional activation (Stolp 2013). They help with processes such as cell fate determination and differentiation, cell survival and proliferation, neuronal and glial migration as well as playing a role in synaptic function (Stolp 2013). While maternal immune activation (MIA) is part of typical development, atypical levels often associated with factors such as stress, environmental toxins or diet have been associated with negative outcomes as well (Ostrea et al. 2002; Crinnion 2009; Ronald et al. 2010; Buss et al. 2012; Entringer et al. 2015; Qiu et al. 2015a; Gumusoglu et al. 2017; DeCapo et al. 2019; Graham et al. 2019). Broadly, maternal inflammation during pregnancy has been associated with an increased risk in offspring exhibiting symptoms of neurodevelopmental disorders such as autism spectrum disorder (ASD) (Parker-Athill and Tan 2010; Careaga et al. 2017; Guma et al. 2019), attention deficit hyperactivity

disorder (ADHD) (Dunn et al. 2019), and schizophrenia (SCZ)(Estes and McAllister 2016; Scola and Duong 2017; Guma et al. 2019).

Maternal inflammation during pregnancy is often studied by promoting maternal MIA. MIA is frequently induced for research purposes via administration of lipopolysaccharide (LPS) or polyinosinic: polycytidylic acid (PolyI:C). These act as a bacterial or viral infection and consequently activate endogenous pro-inflammatory cytokines such as interkeukin-6 (IL-6), IL-1b, IL-12, IL-18, tumor necrosis factor alpha (TNFα) and interferon gamma (IFNγ) which can stimulate immune cell production in the mother (Homan et al. 1972; Alexander and Rietschel 2001; Gumusoglu and Stevens 2019). The placenta plays a fundamental role in regulating immune protection, nutrient and endocrine factor availability for the offspring, controlling factors often linked to neurological disorders, such as autoimmunity, hypoxia and growth restriction (Hsiao and Patterson 2012). Research is still in the process of identifying the extent to which all of these maternal cytokines pass through the placenta and their specific influence on fetal outcomes. However, extensive work has been conducted by generally inducing MIA as well as investigating the role of individual pro or anti-inflammatory cytokines by blocking or activating them individually (Gumusoglu and Stevens 2019). For example, injecting IL-6 during pregnancy is sufficient enough to change subsequent prepulse and latent inhibition behaviors in adult offspring mice (Smith et al. 2007). Furthermore, blocking the effects of IL-6 via an IL-6 receptor knock out or a coadministration of an anti-IL-6 antibody during PolyI:C induced MIA can rescue multiple behavioral outcomes associated with the PolyI:C treatment (Smith et al. 2007). While IL-6 has frequently been characterizes as a central candidate in this regard, it is important to note that other

cytokines have also been extensively investigated and shown to play similar and unique roles in fetal development (Guma et al. 2019; Gumusoglu and Stevens 2019). IL-6 is one of many cytokines, operating dynamically, which should ultimately be understood systematically, and not in isolation. However, as a "proof of concept" studying individual cytokines can be informative in linking maternal and offspring outcomes until more comprehensive studies are performed.

Maternal concentrations of IL-6, have been extensively studied as a crucial intermediary pathway linked to negative outcomes in animal and human offspring (Smith et al. 2007; Hunter and Jones 2015; Glaus et al. 2017; Wu et al. 2017; Graham et al. 2018). IL-6 is often referred to as a *sensor*, *transducer* and *effector* of the dynamic environmental interactions with brain development and associated conditions (Entringer et al. 2015; Graham et al. 2018). Increased levels of inflammatory cytokines in the fetal brain, placental tissue, and amniotic fluid have been related to proliferation, synaptogenesis, axonal growth, and cell survival during early development (Challis et al. 2009). In rodent models, blocking or increasing IL-6 was sufficient in mitigating or prompting inhibitory, repetitive, anxiety-like, and social behaviors accompanied by changes in gene expression and cellular density in the brain (Smith et al. 2007; Wu et al. 2017).

Maternal IL-6 and offspring outcomes have also been characterized in more complex models involving human and non-human primates (NHPs). In humans, maternal IL-6 links to developmental features of the amygdala, subcortical and cortical structural and functional connectivity (Graham et al. 2018; Rasmussen et al. 2018; Rudolph et al. 2018; Spann et al. 2018). These and other studies also directly or indirectly connect

maternal IL-6 to offspring inhibitory, working memory, cognitive, and negative affect behaviors (Graham et al. 2018; Gustafsson et al. 2018; Rasmussen et al. 2018; Rudolph et al. 2018). Maternal inflammation is one factor that may play a critical role in influencing fetal developmental programming. Whereas, factors such as stress, sickness, environmental toxins, maternal diet and nutrition may in part elevate neuroinflammation, but may also independently impact fetal development via other processes (Ostrea et al. 2002; Crinnion 2009; Ronald et al. 2010; Buss et al. 2012; Entringer et al. 2015; Qiu et al. 2015a; Gumusoglu et al. 2017; DeCapo et al. 2019; Graham et al. 2019)

Diet/Nutrition: Maternal diet and nutrition are also associated with subsequent neurodevelopmental and behavioral outcomes in offspring (DeCapo et al. 2019). As discussed in a review by DeCapo et al., 2019, fat, protein, and carbohydrate rich foods increase levels of fatty acids, amino acids and glucose respectively in the maternal circulatory system. Active and passive mechanisms of placental transport expose fetal circulation to these micronutrients. In part, the placental tissue allows for fatty acids originating from triglycerides to freely diffuse across, however, transport proteins can also provide further energy dependent transfer. Furthermore, fatty acids not entering the circulatory system can be converted back to triglycerides to be stored in lipid droplets. Amino acids and glucose can utilize active transport across the placenta facilitated in part by glucose transport proteins. These micronutrients can then cross the blood brain barrier via similar active and passive diffusion processes and result in altered neuronal function and development. Potential mechanisms for this include impaired cell signaling, reductions in myelination as a result of delayed glial maturation, dendritic

instability and atrophy as well as altering inflammatory cytokine concentrations. (DeCapo et al. 2019). Hence, during gestation and lactation, the mother can deliver varying nutritional content to the offspring. Insufficient or excess access to most nutrients can impact fetal development (Morrison and Regnault 2016). Maternal metabolic conditions often associated with diet, such as obesity and diabetes, can also alter the nutrient balance and function of the placenta (Higgins et al. 2011; Morrison and Regnault 2016). Indeed, animal and clinical models have linked maternal obesity and diabetes to higher risks for offspring developing neuropsychiatric disorders (Van Lieshout and Voruganti 2008; Krakowiak et al. 2012; Van Lieshout et al. 2013; Rivera, Christiansen, et al. 2015). With rising levels in obesity and a "Western-Style" diet (WSD) intake, evidence from clinical and preclinical models have begun to establish concrete support that both of these factors can be associated with distinct components of neuropsychiatric disorders (Sullivan et al. 2014; Baker et al. 2017; Contu and Hawkes 2017; DeCapo et al. 2019). However, until recently, few studies have been able to truly dissociate these two and link them each to specific aspects of behavioral change (Thompson, Gustafsson, DeCapo, et al. 2018).

These studies are instrumental in linking maternal factors such as IL-6 or WSD to subsequent brain and behavior characteristics. However, the majority of studies focus on one or two time points to measure their outcome of interest (Smith et al. 2007; Bilbo and Schwarz 2009; Enayati et al. 2012; Kalmady et al. 2014; Wu et al. 2017; Graham et al. 2018; Gustafsson et al. 2018; Rasmussen et al. 2018; Rudolph et al. 2018). Limited efforts have been made to demonstrate these relationships in the light of developmental

trajectories. Offspring developmental growth trajectories can play an important role in characterizing developmental shifts in components of neuropsychiatric disorders (Shaw et al. 2010, 2013).

1.3 Developmental trajectories

A number of neuropsychiatric disorders are characterized and explained by delayed or accelerated components of brain and behavioral development (Gogtay et al. 2007; Nugent et al. 2007; Shaw et al. 2007, 2013; Nordahl et al. 2012; Alexander-Bloch et al. 2014; Friedman and Rapoport 2015; Musser et al. 2016; Hazlett et al. 2017; Karalunas et al. 2017). This can be a critical element to consider when studying the outcome of alterations in developmental programming. For instance, if there is an early decrease in the rate of development, followed by an accelerated "catch-up" trajectory, depending on the timing of outcome data collection, the conclusions may differ significantly. For instance, a meta-analysis investigating the relationship between mood disorders and amygdala volumes (Hajek et al. 2009), initially found no differences in amygdala volumes of patients with and without a diagnosis of bipolar disorder (BD). However, when separating the data into groups of children & adolescents vs. adults (> 20 yrs.) the left amygdala volumes were found to be significantly smaller in the young BD subjects compared to controls. Interestingly, there was a trend (p=0.07) towards adult left amygdala volumes being larger in BD subjects (Hajek et al. 2009). These findings and others are a testament to the importance of using a longitudinal design when studying developmental disorders, as complex growth trajectories are impossible to capture with only one time-point.

With regards to developmental disorders such as ADHD, ASD and SCZ (Owen and O'Donovan 2017), these findings are especially relevant for this dissertation, as growth trajectories can differ before and after diagnosis in all of these populations (Gogtay et al. 2007; Nugent et al. 2007; Shaw et al. 2007, 2013; Nordahl et al. 2012; Alexander-Bloch et al. 2014; Friedman and Rapoport 2015; Musser et al. 2016; Hazlett et al. 2017; Karalunas et al. 2017). In ADHD, diverse heterogeneous developmental trajectories have been described in longitudinal studies characterizing brain and behavioral components (Shaw et al. 2007, 2013; Friedman and Rapoport 2015; Musser et al. 2016; Karalunas et al. 2017). In ASD, findings have shown increased rates of growth in amygdala volumes (Nordahl et al. 2012) as well as increased rates in early cortical surface area and late total brain volume growth (Hazlett et al. 2017). Even in SCZ, these distinctly variable developmental trajectories can be observed in subsections of hippocampal (Nugent et al. 2007) or cortical change over time (Gogtay et al. 2007; Alexander-Bloch et al. 2014).

1.4 Translational Research

Demonstrating how consequences from developmental programming connect to differential brain growth trajectories after birth can be difficult. The current understanding of how neuropsychiatric disorders may be associated with the maternal environment has been fueled by research conducted in animal and human models. However, each model comes with its particular advantages and disadvantages when studying these relationships.

For instance, it is essential to use a human model when making direct inferences about neuropsychiatric disorders such as ADHD or ASD. These disorders are immensely

complex and unique to the human population. Technological advances in research enable us to characterize these disorders using in-depth behavioral assays, genetic testing and neuroimaging techniques such as Positron Emission Tomography (PET) electroencephalograms (EEG) and magnetic resonance imaging (MRI). These methods have been used extensively to gain a better understanding of the heterogeneous landscape of human nature. However, these intricacies that make humans so unique are accompanied by circumstances such as socioeconomic status, food intake, family history and numerous other environmental factors that make it hard to account for specific factors in a controlled experimental design. Even observational or interventional studies researching developmental trajectories in humans can be difficult due to their long lifespans, issues with attrition and retention, high costs, and age-specific tools used to collect the data.

Animal models often bypass these complications and still contribute valuable insights by modeling specific components representative in these disorders. Rodent models can be extremely beneficial for laying the groundwork in causal relationships. Short lifespans, high reproduction rates, and low maintenance have made rodents an ideal model to study genetic manipulations, basic circuitry, fundamental behavioral mechanisms and in-depth neuronal characterizations across development. However, critical components can often be lost when using these "simple" research subjects.

Rodents are limited in regard to generalizability to human brain development for studying how the maternal environment during pregnancy may relate to fetal and infant brain development. Core components of fetal brain formation such as neurogenesis, migration, formation of the blood brain barrier, synaptogenesis, and immune

development occur predominantly after birth in rodents (DeCapo et al. 2019). Non-human primates (NHPs) may be worthwhile candidates to bridge the gap between rodent and human research. NHPs have a similar gestational and developmental timeline to humans, with these fetal brain formation processes occurring prior to birth. Additionally, NHPs have similar placental structure and function which ensures comparable fetal exposure to maternal inflammatory factors, secreted lipids, and nutrition (Sullivan and Kievit 2016). Finally, NHPs share various multifaceted brain and behavioral characteristics with humans, making them tremendously valuable for translational research (Orban et al. 2004; Hutchison and Everling 2012; Miranda-Dominguez, Mills, Grayson, et al. 2014; Ausderau et al. 2017; Casimo et al. 2017; Donahue et al. 2018; Van Essen and Glasser 2018; Xu et al. 2018; Xu, Nenning, et al. 2019; Xu, Sturgeon, Ramirez, Froudist-Walsh, Margulies, Schroeder, Fair, et al. 2019a).

1.5 MRI in research

Non-invasively studying structural and functional brain characteristics across multiple species has been facilitated by rapidly expanding advances in MRI technology. MRI can be used to measure the structural and functional components of the brain. Structurally, three-dimensional volumes of specific predefined regions of interest (ROIs) in the brain, or structural differences in the brain on a voxel-wise level can be measured. Surface-based registrations have also enabled us to characterize the cortex measurements of surface area, sulci depth, myelination or cortical thickness (Glasser et al. 2013).

Functionally, MRI has enabled us to investigate regional patterns of brain connectivity, large-scale functional network organization and how these interact with patterns in behavior. Resting-state functional connectivity MRI (rs-fcMRI) is a powerful

tool that may allow us to bridge the gap between human and animal research. Rs-fcMRI measures the spontaneous fluctuations in the blood oxygen level dependent (BOLD) signal at rest and correlates these across regions in the brain. The BOLD signal has been validated as a tool to indirectly measure brain activity. It relies on the ability to measure the magnetic properties of hemoglobin in the blood. As blood flow increases at a higher rate than oxygen metabolism during local neuronal activity, MRI can indirectly measure this activity (Huettel et al. 2008). Hemoglobin becomes deoxyhemoglobin by losing an oxygen making its iron paramagnetic. This change in the magnetic field then influences the protons in surrounding water molecules (Ogawa et al. 1990; Attwell and Iadecola 2002). The BOLD signal often measured via a T1*-sensitive MRI sequence, identifies the transverse magnetization decay (faster signal loss) which occurs around deoxyhemoglobin (Chavhan et al. 2009). Deoxygenated hemoglobin is actually decreased during neuronal activity, as an initial increase in oxygen usage, is followed by a gradient increase in blood flow and blood volume seconds later (Malonek et al. 1997).

Rs-fcMRI has enabled us to measure synchronized neuronal activity between spatially diverse regions across the brain. Large bodies of work have characterized these patterns in synchronized neuronal activity across development that make up different modules or "resting-state networks" (RSNs) (Grayson and Fair 2017). These intrinsic properties have been instrumental in understanding functional and structural relationships in the brain across development and different populations of interest. It typically takes a network of various scattered regions to perform specific cognitive abilities, rather than spawning from one individual area in the brain (Petersen and Sporns 2015).

The types of networks have been refined and reproduced using a technique called "Community Detection" which optimizes the "modularity" of activity by maximizing the ratio of within- and between-network connectivity (Doucet et al. 2011; Power et al. 2011; Yeo et al. 2011; Lohse et al. 2014; Gordon et al. 2016). These communities can be categorized into various broad modules comprising of the visual (VIS), somatomotor (SMN) and default mode network (DMN), the dorsal attention (DAN), singulo-opercular salience, and the frontoparietal executive networks (Doucet et al. 2011; Power et al. 2011; Yeo et al. 2011; Gordon et al. 2016; Grayson and Fair 2017). However, smaller specialized subdivisions exist within this framework such as the limbic (LIM), insular-opercular (INO), ventral attention, and auditory (AUD) networks. Recent advances in the field have even allowed us to identify subject-specific areal-level parcellations that are stable and unique to a single subject (Laumann et al. 2015).

1.6 Non-Human MRI research

In the past, the majority of these functional characterizations and methodologies have predominantly been established in the human population, with fewer developments in animal models. While there are some benefits associated with imaging NHPs, there are also substantial difficulties that have to be overcome and taken into consideration. Naturally, macaques have much smaller heads, which makes acquiring quality images much more difficult. For example, the macaques used in this dissertation were scanned in a 15-channel knee coil, adapted for the use in macaques, consequently resulting in a lower signal-to-noise ratio (SNR) in the data. For this scenario, four structural images are acquired and averaged together to overcome some of the SNR issues. Additional complications can arise from larger orbital, neck, cheek and forehead tissue, which have

similar intensities to the brain, making it hard for processing pipelines to identify what is brain and what is head. A major caveat, yet also strength in NHP imaging is that most studies necessitate the use of anesthesia for scan acquisition. This reduces systematic image artifacts caused by motion in the scanner (Fair et al. 2012; Power et al. 2012, 2014, 2015). However, a clear limitation is the anesthetic influence on the functional properties of rs-fcMRI.

For a long time, intrinsic functional networks such as the default mode network, characterized with rs-fcMRI, were thought to only be present in awake individuals and were studied in-depth in adult human subjects. It was not until much later that these properties were discovered to be present in anesthetized macaques (Vincent et al. 2007). These networks have since been repeatedly characterized and validated in macaques, and even rodent models (Bezgin et al. 2012; Markov et al. 2014; Miranda-Dominguez, Mills, Grayson, et al. 2014; Stafford et al. 2014; Grayson et al. 2016; Van Essen and Glasser 2018). Furthermore, functional connectivity organizations have recently been characterized in even more depth. Similar to the human advancements, areal brain parcellations have been delineated in individual macaques and shown to be stable and reproducible across awake and anesthetized states, serving as a sort of functional "fingerprint" (Xu et al. 2018). These functional organizations can also be investigated across individuals and anesthetic states, to identify regions in which there is more or less variability across conditions (Xu, Sturgeon, Ramirez, Froudist-Walsh, Margulies, Schroeder, and Milham 2019).

These types of studies highlight the tremendous progress that has occurred in NHP imaging over the years. Large milestones have been made in NHP image

acquisition and processing techniques, complex functional connectivity analyses, and network characterizations on a group and individual level (Miranda-Dominguez, Mills, Grayson, et al. 2014; Robinson et al. 2014; Grayson et al. 2016; Margulies et al. 2016; Donahue et al. 2018; Milham et al. 2018; Xu et al. 2018; Ramirez et al. 2019; Xu, Nenning, et al. 2019; Xu, Sturgeon, Ramirez, Froudist-Walsh, Margulies, Schroeder, and Milham 2019). Inline, the author and collaborators have been working on establishing a macaque version of the human connectome pre-processing pipeline (Glasser et al. 2013), which utilizes modern standards in neuroimaging, to study structural and functional data in surface space, using the gifti/cifti file format. This pipeline was built in the Brain Imaging Data Structure (BIDS) format and contained in a docker image to allow for easy sharing in a single contained package (Gorgolewski et al. 2016). Having established this pipeline not only allows us to stay current and investigate volume and surface-based analyses in the same space but also has made it possible to make cross-species comparisons from macaques to humans directly. In a recent paper on bioRxiv by one of the author's close collaborators and mentors Xu et al., macaque surfaces have been aligned and deformed to human space and vice versa using similarities in functional network topologies, well-documented cross-species landmarks and methods defined as joint embedding and Multimodal Surface Matching (MSM) (Robinson et al. 2014; Xu, Nenning, et al. 2019). The evolution of macaque imaging techniques has brought us one step closer to bridging the gap between animal and human research. With a similar playing field in imaging methods across these species, gaps can be filled to reproduce findings from human studies while adding to this knowledge through advantages that are unique to animal studies.

1.7 Goals of dissertation projects

Here, the author intended to utilize the benefits of a NHP model to replicate and build additional insights into findings established in the human and rodent literature. This dissertation had three research aims designed to target components of structural and functional brain development that are dependent on the maternal environment, in order to reproduce, elaborate and translate to findings established in humans.

Study 1 examined how maternal inflammation during pregnancy related to offspring amygdala development and anxiety-like behaviors. This study built and expanded on previous work in human infants showing that maternal IL-6 concentrations were associated with infant amygdala volumes and subsequent behavioral differences (Graham et al. 2018). As a result of shorter lifespans and a more controlled environment, this study expanded on these findings in a NHP model by studying the developmental trajectories of amygdala volumes in relation to maternal IL-6. This study used Japanese macaque offspring scanned at 4, 11, 21 and 36-months-of-age, and investigated how maternal IL-6 levels related to amygdala volume development and offspring anxiety-like behavior at 11-months of age. (Figure 1.1). Potential confounding variables were included in the model to identify which variables significantly impacted the outcome. Only significant covariates were included in the final model of this study, as there was not enough power to include all covariates at once without diminishing the model fit. Offspring sex, total brain volume, maternal age, maternal percent body fat, and number of prior pregnancies were all tested, but only total brain volume remained in the model as a significant covariate.

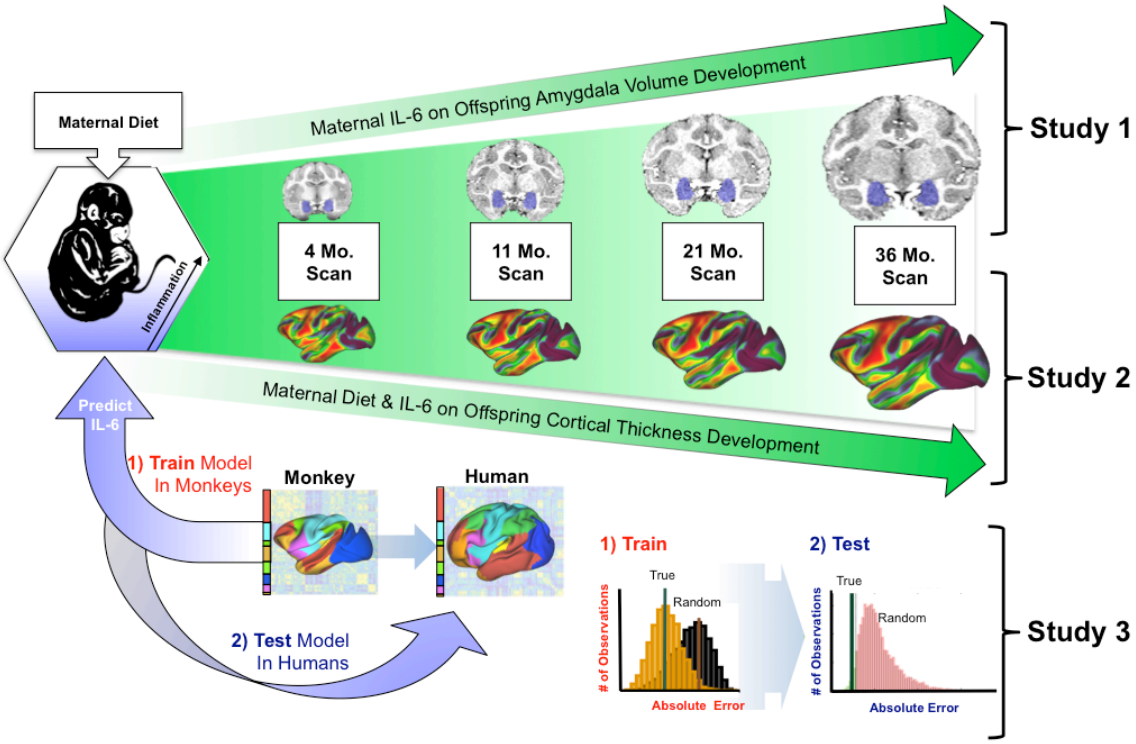

Figure 1.1: An overview of the three studies in this dissertation. Maternal diet and inflammation (measured by IL-6) were investigated in relation to offspring brain development. Study 1 investigated the association between maternal IL-6 and offspring amygdala volume development. Study 2 investigated the relationship between maternal IL-6, diet and offspring sex on cortical thickness development. And Study 3 used resting-state functional connectivity MRI in 4-month monkeys to make predictions about concentrations of maternal IL-6 as a training data set and then tested the most predictive models in the human data set to make inferences about human maternal IL-6 from the macaque models.

Study 2 expanded on these findings and researched these relationships on a whole-brain level, investigating the cortical thickness development of each individual surface gray matter vertex (grayordinate). This study first characterized typical cortical

thickness development in these macaques, a unique contribution to the field. And then, investigated how components of the maternal and offspring environment relate to this development. In addition to maternal IL-6, this study also investigated how maternal diet ("Western-style" or Control) and offspring sex related to differential cortical thickness growth trajectories depending on the region of the brain (Figure 1.1). Study 1 tested a number of different covariates in the model to see if they significantly impacted the outcome and resulted in only including the total brain volume in the model. As models in study 2 were run for each of the 56522 grayordinates of the cortical surface, this type of reduction in covariates was not possible to conduct for each grayordinate. Instead only relevant core variables of interest (Maternal IL-6, Maternal Diet and Offspring Sex) were included in the model to maximize the model fits across the brain.

Study 3 used models derived from functional connectivity in macaque offspring brains to make inferences about maternal IL-6 and then translated these findings across species to make inferences about human maternal IL-6 from macaque derived models. This study built on recent imaging advances and first aimed to replicate findings established in human infants, and then translated these findings across species. A recent paper by Rudolph et al., used infant function connectivity of within- and between-network connectivity to make inferences about maternal IL-6 concentrations via partial least squares regression (PLSR) analyses (Rudolph et al. 2018). They demonstrated that the predominant networks associated with this estimation were the Salience, the subcortical and the dorsal attention networks. This study first attempted to replicate these findings in the 4-month macaques, using a previously described macaque specific areal parcellation (Bezgin et al. 2012; Grayson et al. 2016). In collaboration with Xu et al., this

parcellation was deformed to human space for cross-species analyses. The best fitting models and parameters derived from the replication analyses were used to train models in the complete macaque data set and then tested these in the human population using the deformed parcellation. Together, the findings from these studies help build a better understanding of the relationship between the maternal environment and offspring brain development. These findings contribute valuable insights into macaque and human development, and also open the door for translational research using rs-fcMRI across macaque and human populations (Figure 1.1).

Chapter 2: Maternal interleukin-6 is associated with macaque offspring amygdala development and behavior.

2.1 Introduction of Study 1

Numerous studies in humans and animals have shown that variation in the *in utero* environment can affect fetal brain development and subsequently influence behavior (Rees and Harding 2004; Rees and Inder 2005; Sullivan et al. 2010; Piontkewitz et al. 2011; Mills, Pearce, et al. 2016). One factor receiving significant attention in this regard, in both animal and human studies, is maternal inflammation. Specifically, as noted earlier, interleukin-6 (IL-6) is one frequently studied inflammatory cytokine with prior positive findings indicating a role in fetal brain development (Smith et al. 2007; Hunter and Jones 2015; Glaus et al. 2017; Wu et al. 2017; Graham et al. 2018). Previous studies in human and animal models have linked maternal IL-6 to various behavioral outcomes and alterations in offspring brain function and structure (Smith et al. 2007; Bilbo and Schwarz 2009; Enayati et al. 2012; Kalmady et al. 2014; Wu et al. 2017; Graham et al. 2018; Gustafsson et al. 2018; Rasmussen et al. 2018; Rudolph et al. 2018). However, while neurodevelopmental trajectories have been discussed and investigated at the level of one or two time points, few studies have investigated the impact of maternal IL-6 on offspring brain development in a sufficient density to estimate growth trajectories.

The amygdala may be a suitable exemplar for measuring the effect of maternal inflammation on brain growth trajectories. Levels of the maternal pro-inflammatory cytokine IL-6 during pregnancy has been associated with infant amygdala structure and function, and related behavioral outcomes across multiple studies (Smith et al. 2007; Enayati et al. 2012; Graham et al. 2018; Gustafsson et al. 2018; Rasmussen et al. 2018).

In humans, it has been demonstrated that higher levels of maternal gestational IL-6 are associated with increased bilateral amygdala connectivity and right-amygdala volumes which mediated an effect on lower impulse control at 24 months of age (Graham et al. 2018). Other works have also recently demonstrated that infant functional connectivity between various brain networks are related to maternal IL-6 levels (Rudolph et al. 2018; Spann et al. 2018). Last, new data suggests that heightened maternal IL-6 levels relate to decreased integrity of structural connectivity between the amygdala and prefrontal cortex (uncinated fasciculus) in the neonatal time period and an increased rate of change in this structural connectivity from the neonatal period to 1-year-of-age (Rasmussen et al. 2018). In total, these human studies provide support for associations between maternal IL-6 levels during pregnancy and offspring amygdala development and emotionality. Here, this association is further investigated in a nonhuman primate (NHP) model, which offers several advantages for examining early developmental trajectories and isolating various factors of interest.

Though modern technologies have made studying brain-behavioral relationships possible in the human population, rodent and NHP models continue to be useful. Animal models allow for direct control over confounding variables such as socioeconomic status, diet, and other complex environmental influences that are often observed in human populations. For example, rodent models have been instrumental in pinpointing the initial causal relationships between maternal inflammation and brain and behavioral outcomes (Parker-Athill and Tan 2010; Wong and Hoeffer 2017; Wu et al. 2017). These types of studies set the stage for further investigation in a NHP model to offer a more accurate translational comparison. NHPs closely mirror the complex behaviors, brain structures,

and function present in humans (Orban et al. 2004; Hutchison and Everling 2012; Gottlieb and Capitanio 2013; Miranda-Dominguez, Mills, Carpenter, et al. 2014; Miranda-Dominguez, Mills, Grayson, et al. 2014; Grayson et al. 2016; Casimo et al. 2017; Xu et al. 2018). Fetal NHP exposure to maternal inflammatory factors, nutrition, and secreted lipids is also closely comparable to humans due to similar placental structure and function. Since NHPs have a similar gestational and developmental timeline to humans with the majority of brain development occurring prenatally, NHPs are beneficial for examining the association of inflammatory cytokines secreted by the placenta (Sullivan and Kievit 2016). Finally, examining neurodevelopmental processes requires repeated assessments of the brain. In humans, repeated measures in brain imaging are particularly challenging, particularly during early development. NHPs provide an opportunity for well-controlled repeated assessments that allow for capturing neurodevelopmental processes as opposed to single snapshots of development.

Here maternal IL-6 levels during pregnancy were investigated in relation to offspring amygdala structural development and behavior in a well-characterized cohort of Japanese macaque (*Macaca fuscata*) offspring (Sullivan et al. 2010, 2012; Thompson et al. 2017) Maternal IL-6 levels during pregnancy were assessed in association with offspring amygdala development over the equivalent time frame of human infancy into puberty in a longitudinal Japanese macaque model. Further, associations between maternal IL-6 and offspring and anxiety-like behavior via alterations in amygdala structure were examined.

2.2 Materials and Methods of Study 1

2.2.1 *Macaque study overview*

This study used a set of primates comprising a well-defined NHP primate model of maternal Western-style diet (WSD) or control diet (CTR) (Sullivan et al. 2010, 2012; Thompson et al. 2017). Such a sample better reflects "real world" human populations in Western and developing countries (Thompson, Gustafsson, Decapo, et al. 2018). Notably, IL-6 was previously reported as similar between the two maternal diet groups, while still displaying large individual differences (Thompson, Gustafsson, Decapo, et al. 2018). Rather than focus on diet, the current study focused on differences in maternal IL-6 concentrations, while still testing the relevance of diet in early models as a covariate. These data were obtained from a well-established ongoing study, with data collection dating back to 2010. The scan and behavioral data were collected by the Sullivan et al. laboratory, while the processing and data analyses were derived later for the dissertation. Detailed characterizations of the maternal and offspring phenotypes have been described in earlier reports (McCurdy et al. 2009; Sullivan et al. 2010, 2012, 2017; Comstock et al. 2013; Thompson et al. 2017). All aspects of the study were approved by the Oregon National Primate Research Center Institutional Animal Care and Use Committee following the National Institutes of Health guidelines on ethical use of animals.

2.2.2 Subjects

Mothers consumed either a WSD (TAD Primate Diet no. 5LOP, Test Diet, Purina Mills) or a CTR diet (Monkey Diet no. 5000; Purina Mills) for 1.2-8.5 years prior to offspring birth (age at offspring birth [mean (*M*) ± SEM]: CTR *M*=9.44 ± 0.38 years; WSD *M*=9.32 ± 0.37 years). Details on the maternal diet (Supplemental Table 1) and

offspring rearing were recently described in a prior publication (Thompson et al. 2017). Briefly, offspring stayed with their mothers until weaning (~8 months of age), at which point they were housed in peer social groups of 6-10 juveniles and 1-2 unrelated female adults. Of the total subjects (n = 56; Female n = 26; CTR n = 23), the majority (n = 41; Female n =19) consumed a CTR diet post-weaning; a subset consumed a WSD post-weaning (n =15; Female n = 7) to account for potential effects of the postnatal diet. All of these factors were considered in subsequent analyses (see below).

2.2.3 Anxiety-like behavior

Offspring underwent behavioral testing at the 11-month (M = 10.87 ± 0.03) time point (n=44, Female n=22; CTR n=18). Subjects missing behavioral data did not systematically differ in sex (sample: M=0.50, missing: M=0.66, p=0.31), maternal diet (sample: M=0.59, missing: M=0.58, p=0.96), or Amygdala Intercept (sample: M=208.13, missing: M=211.01, p=0.45) and slope (sample: M=17.87, missing: M=18.56, p=0.73) (see Analysis Overview below for details on the modeling). Behavioral tests and procedures were performed as previously described (Thompson et al. 2017). In brief, animals underwent the human intruder and the novel object test. The human intruder and novel object tests reliably assess stress induced fearful and anxiety-like behavior by characterizing behavioral responses to threatening and non-threatening stimuli (Kalin et al. 1991; Williamson et al. 2003; Sullivan et al. 2010; Raper et al. 2013). In brief, during the human intruder, a non-familiar investigator enters the testing room and displays their facial profile (nonthreatening) or makes continuous direct eye-contact (threatening) during which macaque behavioral responses are recorded. In the novel object test novel, familiar, threatening and non-threatening objects are presented to the macaques, and

latency to grab familiar foods, as well as other stress induced behaviors are recorded. Typical and atypical stress responses on these tests were scored to form a single anxiety composite expressing the percent duration of total anxiety-like behaviors exhibited. While this behavior is typically described as anxiety-like behavior, some ambiguity exists in this interpretation as others might prefer to consider this fear-related, emotional regulatory or impulse control behavior. More details are described in the supplementary materials.

2.2.4 Maternal Interleukin-6 concentrations

Plasma was collected from mothers during their third trimester (48.96 ± 1.06 days) before offspring birth (maternal age: 9.13 ± 0.39 months). These procedures have been previously described (Thompson, Gustafsson, Decapo, et al. 2018) and are further explained in the supplemental materials of this manuscript. IL-6 values below the lower limit of quantification (LLOQ) of 1.23 pg/mL were excluded, resulting in a total of 46 subjects with usable IL-6 data (Female n= 21; CTR n = 16). Subjects missing IL-6 data did not systematically differ in sex (sample: M=0.53, missing: M=0.56, p=0.90), maternal diet (sample: M=0.64, missing: M=0.33, p=0.09), or Amygdala Intercept (sample: M=207.99, missing: M=210.30, p=0.44) and slope (sample: M=17.65, missing: M=19.20, p=0.32). For the current study, IL-6 levels were logarithmically transformed across all subjects in order to normalize the distribution and center the outliers closer to the mean.

2.2.5 MRI acquisition

Offspring MRI scans were acquired at 4 (M = 4.37 ± 0.05), 11 (M = 11.09 ± 0.04), 21 (M = 21.11 ± 0.05) and 36 (M = 36.53 ± 0.09) months of age. MRI data were acquired on a Siemens TIM Trio 3 Tesla scanner using a 15-channel knee coil modified

for scanning monkey heads. Prior to scanning, macaques were sedated with a single dose of ketamine (10-15mg/kg) for intubation and maintained on <1.5% isoflurane anesthesia throughout the scan. Macaques were monitored throughout the session for abnormalities in heart rate, respiration or peripheral oxygen saturation. For each macaque, a total of 4 T_1-weighted anatomical images (TE= 3.86 ms, TR= 2500 ms, TI= 1100 ms, flip angle= 12°, 0.5 mm isotropic voxel) and one T_2-weighted anatomical image (TE= 95 ms, TR= 10240 ms, flip angle= 150°, 0.5 mm isotropic voxel) were collected. Other scans were collected at this time; however, they were not used for the present study.

2.2.6 MRI preprocessing

The current study used a modified version of the human connectome project (HCP) minimal preprocessing pipeline (Glasser et al. 2013) for use in macaques. Processing included the use of the FMRIB Software Library (FSL) (Smith et al. 2004a; Woolrich et al. 2009; Jenkinson et al. 2012) and FreeSurfer image analysis suite (http://surfer.nmr.mgh.harvard.edu/)(Dale et al. 1999; Fischl et al. 1999). Structural scans were averaged. Study-specific templates were created for each age group from averaged T_1-weighted (T1w) images using previously established methods (Scott et al. 2016a) with Advanced Normalization Tools (ANTs) (version 1.9; http://stnava.github.io/ANTs/). For each subject, age-specific templates were registered and warped to the subject's averaged T1w image using FSL and ANTs. Affine transformations and warps from this registration were then applied to the template mask and segmented in order to delineate white and grey matter structures and subcortical regions such as the amygdala. Subject automated segmented brain images (asegs) and masked structural images went through modified versions of the PreFreeSurfer, FreeSurfer and PostFreeSurfer stages of the modified HCP

pipeline (Glasser et al. 2013). Gradient distortion corrected T1w volumes were first aligned to the Yerkes19 (Donahue et al. 2016) AC-PC axis and then nonlinearly normalized to the Yerkes19 macaque surface-based atlas. AC-PC aligned T1w volumes are segmented using the recon-all FreeSurfer functions and previously defined asegs. The initial pial surface is calculated by finding voxels that are beyond ±4 standard deviations from the grey matter mean. Next, the preliminary pial surface and white matter surface were used to define an initial cortical ribbon. The original T1w volume was smoothed with the ribbon using a Gaussian filter with a sigma of 2.5mm. Then, the original T1w image was divided by the smoothed volume to account for low-frequency spatial noise. This filtered volume was used to recalculate the pial surface, but now using ±2 (instead of ±4) standard deviations as the threshold to define the pial surface. These segmentations were then used to generate an individualized 3D surface rendering, using a number of surface features including subject curvature, sulcal depth, and myelination. These surfaces were registered to the Yerkes19 macaque surface-based atlas. This registration process allows all data types (cortical thickness, sulcal depth, function activity, functional connectivity, etc.) to be aligned directly within and between individuals (Xu, Sturgeon, Ramirez, Froudist-Walsh, Margulies, Schroeder, Fair, et al. 2019a). The pipelines follow previous standards for human data and the ABCD project (available here https://github.com/DCAN-Labs/ or here https://github.com/ABCD-STUDY/abcd-hcp-pipeline) and are currently being prepped for a similar release.

A rigorous quality control assessment was conducted on the processed MRI data by quality control trained raters to determine the final MRI numbers used in the study (N=48; Female n= 22; CTR n = 19). While raters were trained via the same mechanisms,

unfortunately a rater agreement score was not calculated. The rating was conducted on a 1 to 3 scale with 1 indicating a good quality registration and image, and 3 indicating poor quality. An additional reviewer assessed the subjects that received a score of 2 to determine if they were deemed usable or excluded from the study. Quality was based on artifacts including poor surface delineations, ringing artifacts that result from movement in the scanner, abnormal warping of the brain, or excessive blurriness of the image. The amygdala volumes for this study were defined by the outputs from the FreeSurfer stage of the pipeline, which were vetted by this quality control assessment (Examples detailing the quality of the structural outputs for all of the ages have been added as supplementary material figures 1-4). Of the subjects that were determined good enough to use for analyses, a total of 30 subjects had scans for 2 or more different time points. Due to the nature of the longitudinal design, subject numbers varied for the 4 (n=17; Female n= 6; CTR n = 8), 11 (n=25; Female n= 11; CTR n = 11), 21 (n=27; Female n= 13; CTR n = 10) and 36 (N=31; Female n= 16; CTR n = 11) month time points. Subjects missing MRI data did not systematically differ in sex (sample: M=0.54, missing: M=0.5, p=0.83), maternal diet (sample: M=0.60, missing: M=0.5, p=0.59), or IL-6 level (sample: M=8.55, missing: M=6.19, p=0.41). Of the initial 56 animals, 39 animals had both IL-6 and MRI data (Female n= 18; CTR n = 13). These 39 animals (4-month n=15, 11-month n=20, 21-month n=25, and 36-month n=24) were used for the analyses of this study. Missing data from different time points were later addressed in the analysis.

2.2.7 Analysis overview

This study used latent growth curve models to investigate brain growth over time in relation to maternal IL-6. Latent growth curve models derive from the structural

equation modeling (SEM) framework and allow for the estimation of a growth trajectory over time in relation to other factors (McArdle and Epstein 1987; Meredith and Tisak 1990; Muthén 2002). This analysis framework allows one to first construct an *unconditional model* to identify the best fitting model of the typical growth trajectory. Once this is established, predictors and covariates can be added to create the *conditional model*. This conditional model can then be further refined to only include statistically relevant covariates by systematically reducing the covariates of the model to define the final model to use (Singer and Willett 2003; Lee and Thompson 2009; Curran et al. 2010; Muthén and Muthén 2017).

Data were analyzed in version 8 of Mplus (Muthén and Muthén 2017) to create the latent growth curve models using the robust maximum likelihood estimator to accommodate non-normal data, and the full information maximum likelihood method to handle missing data (Enders 2001). Extensive research has documented the utility of this method for estimating longitudinal parameters in studies with missing data at various time points (Enders 2001; Raykov 2005; Buhi 2008; Jeličić et al. 2009; Schlomer et al. 2010; Larsen 2011; Peyre et al. 2011; Gustavson et al. 2012). Model fit criteria for these analyses were based on a Comparative Fit Index (CFI) and a Tucker-Lewis index (TLI) above 0.90, and a Root Mean Square Error of Approximation (RMSEA) below 0.1 (Bentler 1990; Maccallum et al. 1996; Schumacker and Lomax 2004).

2.2.8 Establishing the unconditional model

Study 1 investigated left (LA) and right (RA) amygdala volumes separately (Figure 2.1) to account for potential lateralized effects that may occur as a result of prenatal influences (Qiu et al. 2015b). An important initial step when conducting latent

growth models is to pinpoint the optimal functional form of the developmental trajectory of your data by testing different growth forms (Curran et al. 2010). To establish this best-fitting unconditional models of typical amygdala volume development, first a linear growth curve model was tested; however, the model fit was poor (LA: $\chi 2$ (4) = 30.45, p < 0.01, CFI = 0.58, TLI = 0.48, RMSEA = 0.37, RA: $\chi 2$ (4) = 16.70, p = 0.01, CFI = 0.78, TLI = 0.73, RMSEA = 0.26). When adding a quadratic term, the model did not converge. Thus, the parameters were adjusted to a spline growth curve model as the mean amygdala volumes were not quite linear nor quadratic across the 4 (M=207.93), 11 (M=231.28), 21 (M=246.60) and 36-month (M=266.03) time-points. For the spline model, the second and third time-points were freed, and the non-significant 36-month variance and slope with intercept variance were suppressed to improve model fit. Spline models can be more accurate when describing biological growth systems and are often used to substitute asymptotic models in data sets that do not reach the asymptote (Aggrey 2002; Kahm et al. 2010). As the brain develops at different rates depending on the region (Ball and Seal 2019), spline models often best describe this non-linear trajectory, as has previously been shown in a study in marmosets (Sawiak et al. 2018). Furthermore, a chi-square difference test indicated that the spline model significantly improved the model fit (LA: $\chi 2$ (1) = 23.41, p < 0.001, RA: $\chi 2$ (1) = 11.69, p < 0.001), which was used for the rest of the analysis (LA: $\chi 2$ (5) = 7.04, p = 0.22, CFI = 0.97, TLI = 0.97, RMSEA = 0.09, RA: $\chi 2$ (5) = 5.01, p = 0.29, CFI = 0.98, TLI = 0.98, RMSEA = 0.07).

This model determined two latent growth variables, the intercept (starting point) and slope (growth over time). The 4-month time point was coded as zero in the current analysis to define the intercept. This is common practice in latent growth curve modeling.

The number given to the intercept indicates the starting point for the model to identify growth over time (Muthén 2002; Muthén et al. 2002). Hence, the intercept mean growth factor parameter indicates the average of the outcome over individuals at the time point with the time score that is coded as zero (i.e. 4 months in this case). Additionally, the intercept variance parameter indicates the variance at the 4-month time point excluding the residual variance.

2.2.9 Establishing the conditional model

Having identified the best fitting unconditional model, next the predictor of interest (maternal IL-6) and potential covariates of interest were introduced. For this, first the potential covariates to include in the final model were defined. Additional models run to determine the covariates for the final left and right amygdala models are described in more detail in the supplemental materials. In brief, all covariates were initially added to the model, however, to improve the model fit and trustworthiness of the parameter estimates, non-significant covariates for the left and right amygdala models were removed (Supplemental Table 2.1).

As amygdala size is related to total brain volume (TBV) (O'Brien et al. 2011), a typical TBV unconditional growth model was run, of which TBV slope and intercept were used as covariates in the amygdala volume analysis. Additional covariates with possible associations with offspring brain and behavioral development were introduced to the model to account for potential confounding variables. Covariates that were tested included: 1) maternal age at offspring birth, 2) maternal pre-pregnancy percent body fat, 3) the number of prior pregnancies, 4) maternal diet, 5) offspring post-weaning diet, 6) offspring sex and 7) offspring TBV slope and intercept. Offspring age at scan was not

included as a time-varying covariate as scans were scheduled to occur at the same age for all animals within each age group. Variation is measured in days (i.e., not months or years), were typically the result of scheduling conflicts or external complications, and are relatively small for each age (4-month mean age in days=133.17, SD=5.31, Min=125, Max=152, 11-month mean age in days =336.58, SD=6.62, Min=329, Max=352, 21-month mean age in days = 643.84, SD=6.74, Min=630, Max=669, and 36-month mean age in days =1114.10, SD=15.90, Min=1083, Max=1162) (further justification in supplemental materials).

2.2.10 Adding a mediation to the model

For the final refined conditional model, the relevance anxiety-like behavior in the IL-6-amygdala associations was testing using a statistical mediation. Specifically, this study tested for the indirect effect of maternal IL-6 on anxiety-like behavior via amygdala volume using the "model indirect" command in M*plus*. As anxiety-like behavior was only collected at the 11-month time point, only the 4-month amygdala volume (intercept of the model) was used for the mediation aspect of the model (Maternal IL-6 (A), 4-month amygdala volume (B), 11-month anxiety-like behavior (c)).

2.3 Results of Study 1

2.3.1 Amygdala volume increased over time and varied significantly among individuals

The development of LA and RA volumes (Figure 2.1) was first examined to determine the unconditional model, before continuing to the final conditional model that examined how IL-6 related to amygdala volume development and behavior via the amygdala. This unconditional model showed amygdala volume development with a significant positive intercept (LA: M= 208.43, p=0.001, RA: M=217.92, p<0.001) and

slope (LA: M= 17.94, p<0.001, RA: M=15.83, p<0.001), which is indicative of the observed data in Figure 2.1, Table 2.1 and Supplemental Table 2.1. Importantly, there was enough variance across subjects in both the slope and intercept terms to conduct the conditional models investigating whether amygdala trajectories were associated with maternal exposure to IL-6 and anxiety-like behavior. This finding was true for both the left (intercept: 95.17, p=0.001; slope: 22.27, p=0.001) and right (intercept: 86.18, p=0.013; slope: 18.36, p=0.001) amygdalae. These analyses defined the typical amygdala volume development and established an unconditional model to test the predictor of interest (Table 2.1 & Supplemental Table 2.1).

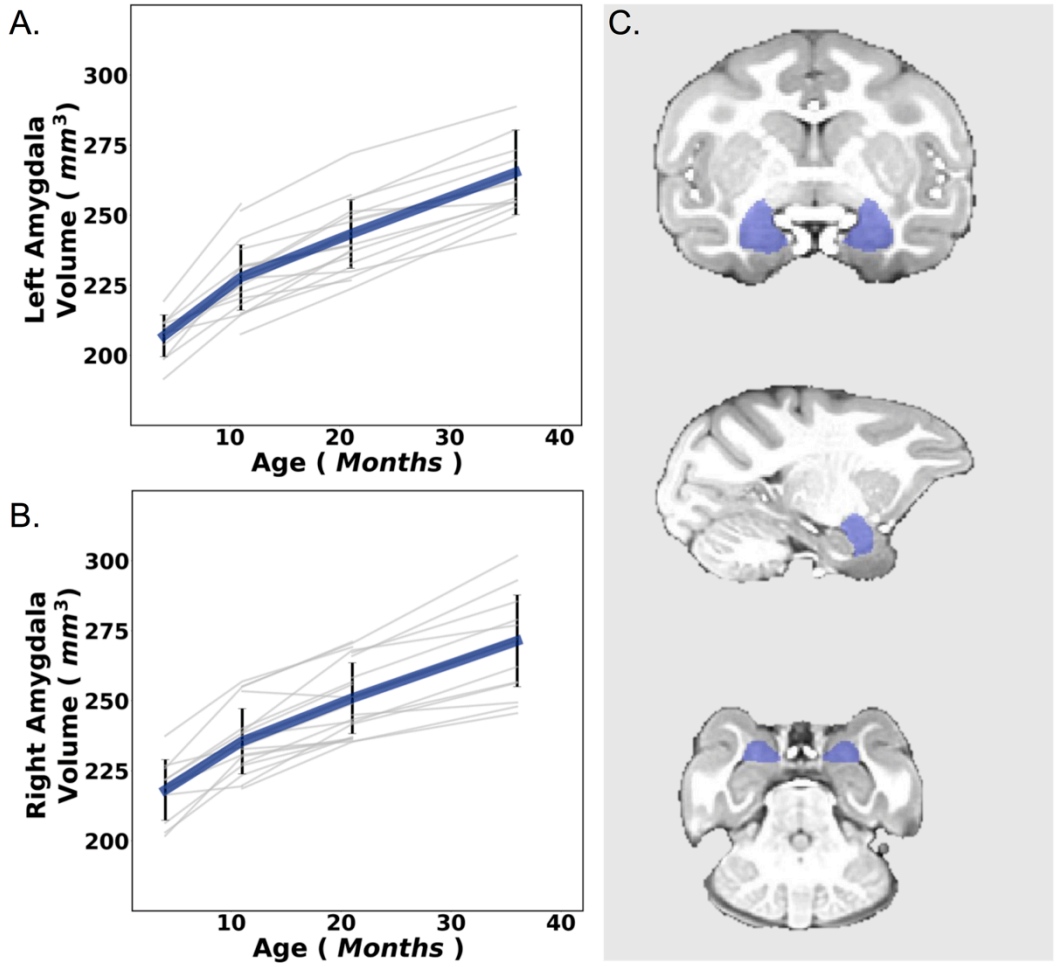

Figure 2.1: Raw left (2.1A) and right (2.1B) amygdala development over the four different time points. Error bars are depicted as SEM. Individual data points defined as non-significant outliers by the SPSS statistical software are seen above some of the bars as open circles. Macaque offspring amygdalae ROIs were defined using the modified version of the human connectome pipeline (2.1C).

Table 2.1: Model statistics for the left and right unconditional amygdala models

	Unconditional Left Amygdala		Unconditional Right Amygdala	
Parameter	Estimate	S.E.	Estimate	S.E.
Intercept Mean	***208.47	1.946	***217.917	2.302
Intercept Variance	***95.166	27.974	*86.182	34.739
Slope Mean	***17.939	0.834	***15.827	0.899
Slope Variance	***22.267	5.948	**18.364	5.657
Intercept & Slope Covariance	Restricted		Restricted	

2.3.2 Establishing the final model to use for the analysis

Once the amygdala volume trajectories were established via the unconditional models (Table 2.1) (also see LGM steps in Methods), next the conditional model was determined, which described how IL-6 related to amygdala volume development and also asked if early amygdala volumes at 4-month mediated the relationship between IL-6 and anxiety-like behavior at 11-month of age. Covariates included in the final left amygdala model were the TBV slope and intercept, and covariates included in the final right amygdala

model were TBV, maternal diet, pre-pregnancy percent body fat, maternal age and offspring sex.

Since changes in brain characteristics often drive behavioral differences, final models included anxiety-like behavior and the significantly relevant covariates for the left and right amygdala models (Table 2.2). The aim was to see if maternal IL-6 directly or indirectly associated with anxiety-like behaviors via the amygdala volume intercept of the model. Anxiety-like measures were only available at the 11-month time point; hence the mediation analysis only included the amygdala volume intercept, as the behavioral measures were not available across time.

The final model for the left amygdala volumes resulted was moderately well-fitting ($\chi 2$ (18) = 23.68, p = 0.166, CFI = 0.94, TLI = 0.92, RMSEA = 0.09). The left amygdala volume model explained 62% (R2=0.62) of variance for the intercept and 70% (R2=0.70) for the slope. However, these values need to be considered with caution, as they may be inflated with small sample sizes. A significant amount of variance in both the intercept and slope (see Table 2.2) remained unexplained in the final model. This indicates that unexamined factors also play an important role.

Table 2.2: Model statistics for the final left and right amygdala model

	Final Left Amygdala Model		Final Right Amygdala Model	
Parameter	Estimate	S.E.	Estimate	S.E.
Intercept Mean	***18.672	5.075	**17.776	5.140
Intercept Variance	*0.381	0.150	***0.688	0.148

Slope Mean	1.106	0.721	**2.394	0.811
Slope Variance	*0.305	0.141	0.121	0.074
Intercept & Slope Covariance	Restricted		Restricted	
Predictors of Intercept				
Interleukin-6	***-0.744	0.110	-0.147	0.194
TBV intercept	[1]0.255	0.144	0.295	0.255
Maternal Diet	N/A	N/A	0.228	0.270
Offspring Sex	N/A	N/A	0.352	0.243
Pre-pregnancy % body fat	N/A	N/A	0.397	0.312
Maternal age at offspring birth	N/A	N/A	-0.443	0.227
Predictors of Slope				
Interleukin-6	**0.451	0.157	0.034	0.109
TBV slope	***0.701	0.107	***0.820	0.066
Maternal Diet	N/A	N/A	-0.144	0.141
Offspring Sex	N/A	N/A	***-0.379	0.185
Pre-pregnancy % body fat	N/A	N/A	-0.348	0.185
Maternal age at offspring birth	N/A	N/A	0.034	0.174
Mediation: (Interleukin-6→Amygdala Intercept→Anxiety-like Behavior)				
Indirect	*0.580	0.281	0.024	0.047
Direct	[1]-0.574	0.307	-0.020	0.169
Intercept →Anxiety	*-0.779	0.316	-0.162	0.196

Note: ł= p <.10; *p<.05; **p<.01;***p<.001. N/A *indicates covariates not included in the final model*

For the right amygdala, model fit was inadequate, rendering those results untrustworthy ($\chi 2$ (39) = 146.31, p < 0.001, CFI = 0.38, TLI = 0.30, RMSEA = 0.27). Hence, aside from reporting the findings in Table 2.1, all further investigations focused

on the left amygdala volumes. Results from the final left amygdala model can be seen in Table 2.2 and Figure 2.2.

2.3.3 IL-6 levels relate to smaller left amygdala volume at 4-months and more rapid growth over time

In the context of the final model, maternal IL-6 levels were associated with lower left amygdala volume intercept (B=-0.744, p<0.001); the model also showed that maternal IL-6 exposure significantly predicted increased amygdala volume slope (B=0.451, p=0.004). The TBV slope and intercept latent variable covariates also predicted an increase in amygdala volume slope but not intercept (Intercept: B=0.255, p=0.078, Slope: B=0.701, p<0.001). Table 2.2 and Figure 2.2 depict these findings.

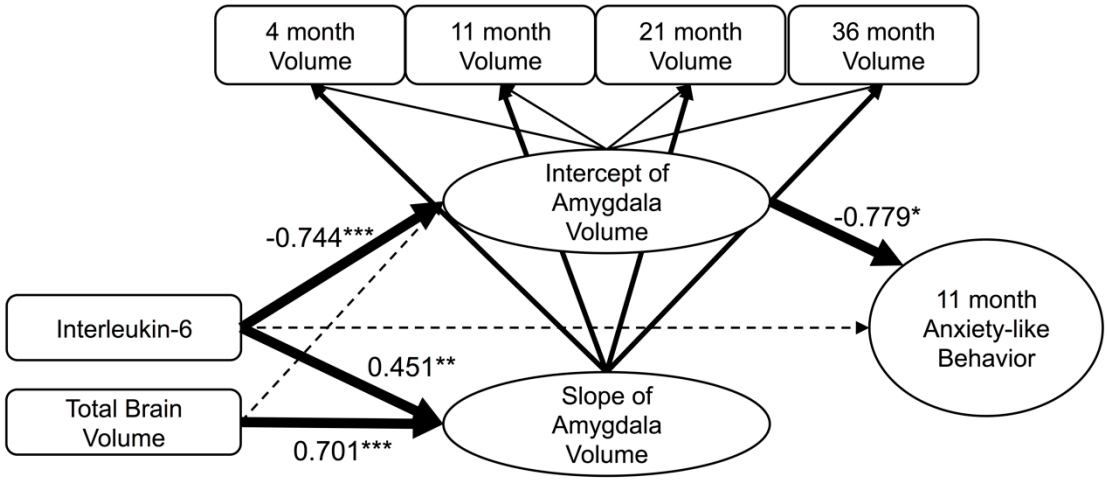

Figure 2.2: Final spline latent growth curve model for study 1. 4 (n=15), 11 (n=20), 21 (n=25) and 36 (n=24) month amygdala volumes were used to construct intercept and slope latent variables. Predictor (IL-6) and the covariate (Total Brain Volume) were introduced into the model, to determine the extent to which they related to the latent variables. Additionally, an indirect mediation effect was added to this model to see how maternal IL-6

related to anxiety-like behavior at 11-months via the 4-month amygdala volumes (intercept of this model). Only the intercept was tested in regard to the mediation of this model, as the slope contained information of later time-points (i.e. 21 and 36-month data) than the 11-month anxiety like behavior. Thick solid lines indicate that the relationship was significant ($p<0.05$) while dotted lines indicate insignificant relationships.

Although analyses were computed using dimensional measures, to facilitate visualization and interpretation, subjects were categorized into high and low IL-6 groups using a median split and compared at each time point to depict how the growth trajectories differ depending on the level of maternal IL-6 during pregnancy (Figure 2.3A). Furthermore, to visualize the relationship between IL-6 and amygdala volumes independent of the TBV effect, TBV intercept and slope values were regressed out from the amygdala volume intercept and slope respectively (Figure 2.3B&C). Having identified a link between maternal IL-6 and amygdala volumes, this study next sought to examine whether these findings related to anxiety-like behaviors.

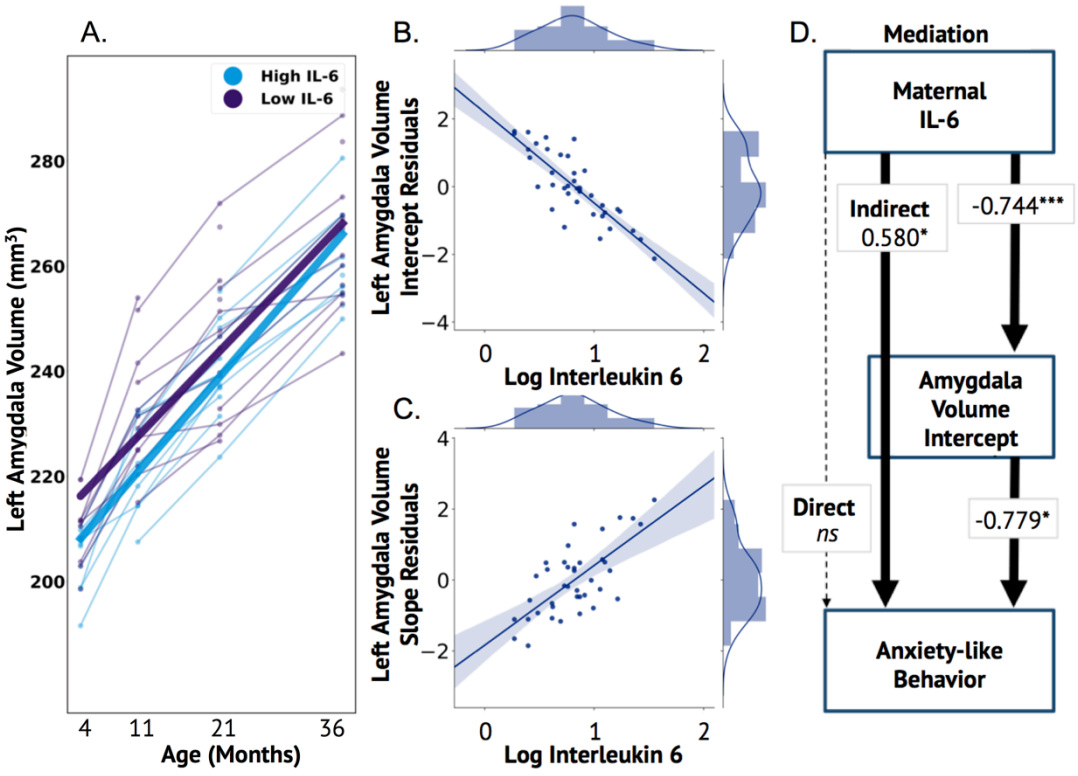

Figure 2.3: Maternal IL-6 associated with left but not right amygdala volumes and indirectly related to anxiety-like behavior via the amygdala intercept. Animals were median split into high and low IL-6 levels purely for visualization purposes in order to show that higher maternal IL-6 was associated with lower amygdala volumes at the intercept but an increased slope (A). Total brain volume values were regressed from amygdala volume values to more accurately visualize the association of the amygdala intercept (B) and slope (C) on IL-6 using these residuals. The mediation results are depicted in D and show a significant indirect, but not a direct effect of maternal IL-6 on anxiety-like behavior at 11-months via the amygdala intercept. Individual estimates are shown in text on the arrows. The total indirect effect on anxiety-like behavior is depicted in the continuous line from IL-6 to anxiety-like behavior through the amygdala volume intercept. The results of the individual connections (IL-6 to

amygdala volume intercept & amygdala volume intercept to anxiety-like behavior) are illustrated in the lines between these variables. Note: *p<.05; **p<.01;***p<.001.

2.3.4 Larger amygdala volumes at 4-months are associated with decreased anxiety-like behavior at 11-months and mediate an indirect effect of IL-6 levels on anxiety-like behavior

Results for the behavioral aspect of the final model indicated that the left amygdala intercept significantly predicted the animal's anxiety-like behavior at 11-months of age (*B*=-0.779, *p*=0.014). Higher amygdala volumes at "4-months-of-age" were associated with lower anxiety at this time point. The direct effect of IL-6 on anxiety-like behavior was shy of significance (*B*=-0.574, *p*=0.062). However, there was a significant indirect effect of IL-6 on anxiety-like behavior at 11-months via the amygdala intercept (*B*=0.580, *p*=0.039) (Figure 2.3D). Furthermore, adding an extra parameter for 11-month volumes as a sensitivity analysis did not change results (supplemental materials). Thus, higher maternal IL-6 during pregnancy was associated with elevated anxiety-like behavior at 11-months of age via differences in the 4-months amygdala volume intercept.

2.4 Discussion of Study 1

The current study offers novel insights into our present understanding of how the maternal environment affects offspring brain development and behavior. These findings are the first to demonstrate prospectively that maternal IL-6 is associated with offspring macaque amygdala volume development and indirectly related to anxiety-like behavior through effects on the amygdala. Heightened levels of IL-6 during pregnancy predicted lower left amygdala volumes at 4-months-of-age and an increased rate of amygdala volume development. Furthermore, elevated maternal IL-6 levels predicted higher

anxiety-like behavior, statistically mediated via the differences in amygdala volume at 4-months-of-age. These findings are noteworthy as they in some cases oppose, but mostly corroborate several lines of work in humans and rodent models identifying an association between 1) maternal inflammatory cytokines and behavioral outcomes in NHPs, 2) maternal inflammatory cytokines and the newborn brain and rate of development in NHPs, and 3) the relationship between brain and behavioral outcomes.

The finding of an indirect relationship between maternal IL-6 and offspring anxiety-like behavior via reduced left amygdala volume. This finding is relevant to the mental health literature, as several lines of evidence highlight negative valence systems (related to anxiety) as a key transdiagnostic dimension of several developmental psychopathologies (Schatz and Rostain 2006; Insel et al. 2010; Cuthbert 2014; Karalunas et al. 2014). Furthermore, negative valence behaviors, such as anxiety and depression symptomatology, have repeatedly been linked to heightened inflammation during pregnancy in rodents (Hava et al. 2006; Lucchina et al. 2010; Enayati et al. 2012) and humans (Kiecolt-Glaser et al. 2015; Simanek and Meier 2015) Other disorders, such as, ADHD, ASD, and schizophrenia have shown correlations to maternal inflammation in humans (Tohmi et al. 2004; Parker-Athill and Tan 2010; Bronson and Bale 2014; Wong and Hoeffer 2017) and in rodent models (Patterson 2009; Estes and McAllister 2016). The current findings add to the literature highlighting the effects of the immune system on mental health risk during the earliest periods of brain development (Estes & McAllister, 2015; xKnuesel et al., 2014).

While the findings mostly corroborate findings in humans, some relationships opposed findings from the human literature. Interestingly, the findings in the present

study were, in some ways, at odds with a previous report of higher maternal inflammation linked to larger amygdala volume in human infants (Graham et al. 2018). In that human infant study, higher maternal IL-6 during pregnancy was associated with offspring larger *right* amygdala volumes at four weeks old. In contrast, the present report associated maternal IL-6 with offspring *smaller* left amygdala volumes at the 4-month time point (intercept). While seemingly at odds with human findings, similar trends have been observed in prior primate research investigating the influence of an influenza (A/Sydney/5/97 or H3N2) infection during the third trimester. This study showed smaller (uncorrected only) amygdala volumes in infected vs control macaques at 12 months-of-age (Short et al. 2010). One reason for the seeming discrepancy in the current and human study may be that the current study used a model that incorporated the rate of change, while in the original human publication only one time-point (the neonatal period) was examined. This can enable some refinement of the interpretation of that earlier report. . In the NHP model, maternal IL-6 concentrations predicted a decrease in starting (intercept) but an increase in the rate of left amygdala volume development (slope); the human data were acquired at the "point" on the human developmental "curve" at which the NHP model could potentially predict an association between increased amygdala volumes and IL-6 after the increased growth rate.

Importantly, direct comparisons of NHP studies to human findings can often be complicated, as the brains develop at different rates. Indeed, while the human brain undergoes maximum growth right around birth, maximal brain growth happens ~60 days prior to birth in monkeys (Brambrink et al. 2010). The macaque brain is already above 50% of its full adult size at birth compared to the human infant brain, which is only ~35%

of its full adult size. Because critical developmental processes such as myelination, synaptogenesis, and neurogenesis also occur at slightly different stages (Clancy et al. 2001; Workman et al. 2013), the impact of *in utero* environmental influences may vary slightly across these two species and may influence different stages of brain development. This may in part explain the discrepancy in NHP and human findings in the early amygdala volumes. Despite this problem, it is still the case that the majority of the brain developmental timeline is much more comparable in human and macaque species as opposed to rodent and human species, where the majority of brain development happens after birth in rodent models.

Furthermore, it was interesting to observe slightly larger right than left amygdala volumes in the current study (Table 2.2). As an increased rate of development associated with IL-6 in the left amygdala, it is possible that a significant association with the right amygdala may have existed at an earlier time point before volumes increased at a greater growth rate (slope).

Support for the possibility that growth trajectories may play an important role is further strengthened in a similar collaboration investigating the association of maternal IL-6 with human infant frontolimbic white matter tract integrity across two time-points (4 weeks and 12 months of age) (Rasmussen et al. 2018). Similar to the current findings, they found that IL-6 was associated with a decrease in fractional anisotropy (FA) of the uncinate fasciculus proximal to the amygdala at the first time point. However, IL-6 was also associated with a positive increase in rate of FA across the first year of life, perhaps analogous to the findings that are reported in the current study (Rasmussen et al. 2018).

Despite the limitations of comparing across species noted earlier, the finding in study 1 that early amygdala volumes associate with later behavioral outcomes, and that the rate of amygdala growth changes across time is particularly significant because the majority of longitudinal human studies lack the dense sampling to examine this critical question. However, evidence from the available literature on human mood disorders is consistent with the overall findings, as smaller amygdala volumes have been linked to children with mood disorders, and the association either dissipates or is reversed into adulthood (Hajek et al. 2009; Warnell et al. 2017). Other neuropsychiatric disorders, such as ASD and ADHD, often share comorbidity with anxiety and are also associated with changes in amygdala volume development (Schatz and Rostain 2006; White et al. 2009). While children with ADHD have smaller amygdala volumes at early ages (Hoogman et al. 2017) (similar to the intercept findings), children with ASD (Nordahl et al. 2012) have larger and faster developing amygdala volumes (similar to the slope findings). Though amygdala volumes alone are unlikely to account for the entirety of sequela across these disorders to say the least, they may help explain specific component behaviors such as anxiety (Amaral et al. 2003). Finally, the difference in findings from previous human work (Graham et al. 2018) relating larger right amygdala volumes to impulse control behaviors and the current findings relating smaller left amygdala volumes with increased anxiety-like behaviors may further explain the complex nature of how the amygdala is associated with behavioral development.

Limitations: While these findings give promising novel insights into the association of maternal inflammation on offspring brain behavioral development, some limitations are addressed here. This study utilized NHPs as part of an ongoing

longitudinal study; however, behavioral data at the time of analysis were only available for the 11-month time point. Hence, it was not possible to control for the 4-month behavioral data or include the slope variable, as a result of lacking the 21 and 36-month behavioral data. It is likely that a more complete longitudinal behavioral assessment would greatly benefit the overall interpretation of the current findings. While "typical" amygdala development was assessed in the unconditional model, a spline model was necessary in place of a linear or quadratic model to achieve data fit. A more complete data set would likely allow the models to converge in either a linear or quadratic fashion. With only seven NIH funded primate research centers in the United States, these types of data are particularly rare and difficult to acquire. Very few studies exist that use infant monkey scans, across multiple time points. Hence, future studies will greatly benefit from open access consortium studies such as the PRIME Data Exchange (Milham et al. 2017). With the current scarcity in available data, it is important to note that due to the nature of the longitudinal design and species, a substantial portion of the subjects had missing data, with the fewest data points at the 4-month time point. However, missing data is a common occurrence in longitudinal studies, and has been extensively addressed using the full information maximum likelihood estimator used in this study (Collins et al. 2001; Enders 2001; Graham 2003; Raykov 2005; Buhi 2008; Jeličić et al. 2009; Schlomer et al. 2010; Larsen 2011; Peyre et al. 2011; Gustavson et al. 2012). While not a limitation per se, it is important to recognize that other factors not studied here, such as genetics, other cytokines, cortisol, or environmental stressors experienced post-birth likely also play an important role in explaining individual differences of amygdala volume trajectories (Graham, Pfeifer, Fisher, Carpenter, et al. 2015; Graham, Pfeifer, Fisher, Lin, et al. 2015;

Graham et al. 2016, 2019; Buss et al. 2017). In addition, even though maternal and post-weaning diet did not significantly contribute in this model, having a more complete data set of this covariate, and a more complete picture of the inflammatory 'milieu,' might offer a more comprehensive understanding of potential associations of diet on inflammation and subsequent brain development. It is important to note that other factors such as obesity, glucose/insulin homeostasis and diet can all independently contribute to different aspects of offspring neurodevelopment and should be studied in concert for future experiments.

Furthermore, this study used TBVs as covariates in the model. Though the addition of this covariate can be considered as a strength, there is still debate in the field regarding how best to handle the effect of TBV, as different correction methods may lead to different results and interpretations. Complex familial relationships between the mothers in this study could also be a potential confound. As this study did not have the power to address this problem using the batch analysis approach, the closest comparison to this measure was using the number of maternal pregnancies as a covariate, which was not a significant confounder. Similarly, this study did not control for age at scan, due to having insufficient power to address this time-varying covariate and obtain a trustworthy model (more details on this in the supplemental materials and methods section). Finally, previous research has shown that IL-6 concentrations can fluctuate over time during pregnancy; here, IL-6 concentrations during the third trimester were measured. However, this timing can also be considered a strength, as this critical window in development with regard to IL-6, has been shown to be highly influential to postnatal brain development (Rudolph et al. 2018) and, thus, may provide some specificity to the results. Nonetheless,

these findings are likely to benefit from future work that characterizes the dynamics of maternal inflammation across pregnancy using multiple measurements.

The results from the present report increase our current understanding of how maternal inflammatory cytokines may impact brain and behavior relationships over time. Previous findings independently relating maternal inflammation with anxiety-like behaviors and amygdala volume differences are supported by the current findings --- indeed, these relationships are integrated together in the context of brain development over time. Though other risk factors, brain regions, and behaviors undoubtedly contribute to these relationships, this study's findings suggest a promising avenue of study for future investigation. Finally, in light of rising obesity rates, stress, consumption of WSDs, and their effects on increased maternal inflammatory states, the current findings are timely, relevant, and offer a deeper understanding of how the maternal immune system shapes long-term brain and behavioral development in offspring. Finally, the work from study 1 was recently published online in the *Cerebral Cortex* journal (Ramirez et al. 2019).

2.5 Supplemental Materials for Study 1

2.5.1 Anxiety-like behavior

Animals underwent the human intruder and the novel object test. These are validated measures to test anxiety behavior in Non-Human Primates (NHPs) (Kalin et al. 1991; Belzung and Le Pape 1994; Williamson et al. 2003; Coleman et al. 2011). Behavioral tests were videotaped and scored by a blinded observer using a comprehensive ethogram (Thompson et al. 2017) implemented via the Observer XT software Version 11 (Noldus Information Technology). Quantified behavioral responses included anxious, abnormal, locomotive, and exploratory behaviors, along with vocalizations. For each animal, the

summed duration of all typical and atypical stress responses was used to form a single anxiety composite expressing the percent duration of total anxiety-like behaviors exhibited [further described in (Thompson et al. 2017)].

2.5.2 Maternal Interleukin-6 concentrations

Mothers underwent a fasting period for the night and morning of sample collection, for which they were sedated using Telazol (3-8mg/kg IM). Blood was collected from the saphenous vein and placed into heparinized tubes. Blood samples were centrifuged for 20 minutes at 2400 RPM and 4 C°, and plasma was aliquoted and stored in a -80 C° freezer for later use.

Maternal IL-6 cytokine concentrations were extracted from the plasma via a monkey 29-plex cytokine panel (ThermoFisher Scientific, Waltham, MA) using two different plates from the same lot (#1833398A). A Milliplex Analyzer (EMD Millipore, Billerica, MA) bead sorter was used for the samples in combination with version 3.1 of the XPonent Software (Luminez, Austin, TX). Next, calculations were performed using version 5.1 of the Milliplex Analyst Software (EMD Millipore). The lower limit of quantification (LLOQ) for IL-6 was 1.23 pg/mL with 88.79% of the values above the LLOQ. The inter-assay coefficient of variance (CV) was determined to be 2.61%. A full description of the results from the cytokine assay can be seen in a previous study (Thompson, Gustafsson, Decapo, et al. 2018).

Supplemental Table 2.1: Macaque Diet

	Percent of diet		Percent of energy	
	CTR	**WSD**	**CTR**	**WSD**
Protein	**20.6**	**17.0**	**26.8**	**18.4**
Fat	**5.0**	**15.0**	**14.7**	**36.6**
Saturated	0.89	5.42		
Polyunsaturated	3.3	2.8		
Linoleic	2.6	2.5		
Linolenic	0.34	0.10		
Arachidonic	0.0	0.06		
Omega-3	0.36	0.21		
Monounsaturated	1.1	6.2		
Carbohydrates	**44.8**	**41.5**	**58.5**	**50.0**
Glucose	0.15	0.04		
Fructose	0.19	5.5		
Sucrose	2.8	8.8		
Lactose	0.0	4.6		
Starch	26	20.5		

CTR = Monkey Diet no.5000; Purina Mills. Western Style Diet (WSD) = TAD Primate Diet no. 5LOP Test Diet, Purina Mills. Macronutrient information provided from diet specification sheets.

2.5.3 Identifying the final models to include

Once the unconditional models (Models #1) were established (Table 2.1) additional models were run to test potential confounding variables of interest in order to isolate associations between IL-6 and amygdala development for the final model. The first step

was to include all of the covariates into a model (Models #2) to identify which covariates were significantly relevant to these variables, as running a model with all covariates did not produce a good model fit and trustworthy results (Supplemental Table 2.2). The covariates tested for this analysis consisted of maternal age at offspring birth, maternal pre-pregnancy percent body fat, the number of pregnancies, maternal diet, offspring post-weaning diet, offspring sex, and offspring total brain volume (TBV). For the TBV covariate, latent variables from a separate TBV model were included, capturing TBV development over this same period. TBV development was captured by a linear growth model, which fit the data well ($\chi 2$ (6) = 7.67, p = 0.26, CFI = 0.99, TLI = 0.99, RMSEA = 0.08). The slope and intercept from this model were used as covariates in the amygdala model along with the other potential confounding variables. When running Models #2 that contained all possible covariates, the majority of covariates in the model were not significantly associated with either amygdala intercept or slope, resulting in a poor model fit for the left ($\chi 2$ (25) = 83.81, $p < 0.001$, CFI = 0.58, TLI = 0.30, RMSEA = 0.25) and right ($\chi 2$ (25) = 102.96, $p < 0.001$, CFI = 0.55, TLI = 0.26, RMSEA = 0.28) amygdala. In the context of this poor fitting model (Model #2), IL-6 was associated with the left (B=-0.529, p<0.001) but not right (B=-0.030, p=0.535) amygdala intercept and the left (B=0.300, p=0.034) but not right (B=0.012, p=0.430) amygdala growth (Supplemental Table 2.2). The next and final model (Model #3) only used the significant covariates from the previous left and right amygdala models (Models #2) and also incorporated the behavioral mediation (main text).

This study did not include time-varying covariates. Hence, age at each scan was not included as a time-varying covariate, based on the correlation findings. When correlating

the age at scan with amygdala volumes at the 4-month (RA: $r(14)=0.04, p=0.89$,LA: $r(14)=0.31, p=0.26$), 11-month (RA: $r(19)=0.46, p=0.04$,LA: $r(19)=0.11, p=0.65$), 21-month (RA: $r(24)=0.28, p=0.18$,LA: $r(24)=-0.07, p=0.75$), and 36-month (RA: $r(23)=-0.04, p=0.87$,LA: $r(23)=-0.07, p=0.75$) time points, only the 11-month RA was significantly associated with 11-month scan age. When adding this variable as a time-varying covariate to the model, the results did not significantly change, and the model was considered untrustworthy by Mplus. As the predictor IL-6 was not associated with right amygdala volume development, it was not included as a time-varying covariate to avoid overcomplicating the model.

Supplemental Table 2.2**:** Models #2. Model statistics for predictor and covariates when introduced together to determine the covariates to use in the final model.

	Left Amygdala		**Right Amygdala**	
Parameter	**Estimate**	**SE**	**Estimate**	**SE**
Intercept Mean	**15.104	5.052	**14.671	4.973
Intercept Variance	**0.276	0.100	**0.518	0.159
Slope Mean	0.410	0.687	***4.380	1.191
Slope Variance	*0.354	0.142	0.180	0.108
Intercept & Slope Covariance	Restricted		Restricted	
Predictors & Covariates of Intercept				
Interleukin-6	***-0.529	0.137	-0.108	0.172
TBV intercept	**0.469	0.190	0.261	0.221
Maternal Diet	-0.332	0.202	0.351	0.224
Offspring Sex	-0.156	0.172	0.267	0.209

Post-Weaning Diet	-0.325	0.242	-0.385	0.273
Number of prior pregnancies	-0.178	0.270	-0.057	0.348
Pre-pregnancy % body fat	-0.306	0.232	*-0.504	0.250
Maternal age at offspring birth	-0.258	0.368	0.532	0.455
Predictors & Covariates of Slope				
Interleukin-6	0.300	0.141	0.115	0.146
TBV intercept	0.501	0.210	***1.124	0.198
Maternal Diet	0.312	0.203	*-0.496	0.197
Offspring Sex	0.055	0.189	**-0.502	0.187
Post-Weaning Diet	0.270	0.201	0.348	0.234
Number of prior pregnancies	0.494	0.307	0.412	0.315
Pre-pregnancy % body fat	0.335	0.234	[1] 0.418	0.239
Maternal age at offspring birth	-0.313	0.391	**-1.232	0.408

Note: ł= p <.10; *p<.05; **p<.01;***p<.001.

Supplementary figures 1-4 show outputs from the modified NHP HCP processing pipeline. White and gray matter delineations and surface pial registrations were used to assess the quality of the images processed through the pipeline. Executive summaries from the pipeline allowed us to scroll through each slice of the brain to make sure the brain was properly delineated. Amygdala ROIs defined by ANTs Joint Label Fusion are also displayed in these figures to show how amygdala volumes were assessed. Figures indicate representative example outputs from the pipeline for the 4 (Supplemental Figure 2.1), 11(Supplemental Figure 2.2), 21 (Supplemental Figure 2.3) and 36-month (Supplemental Figure 2.4) scans.

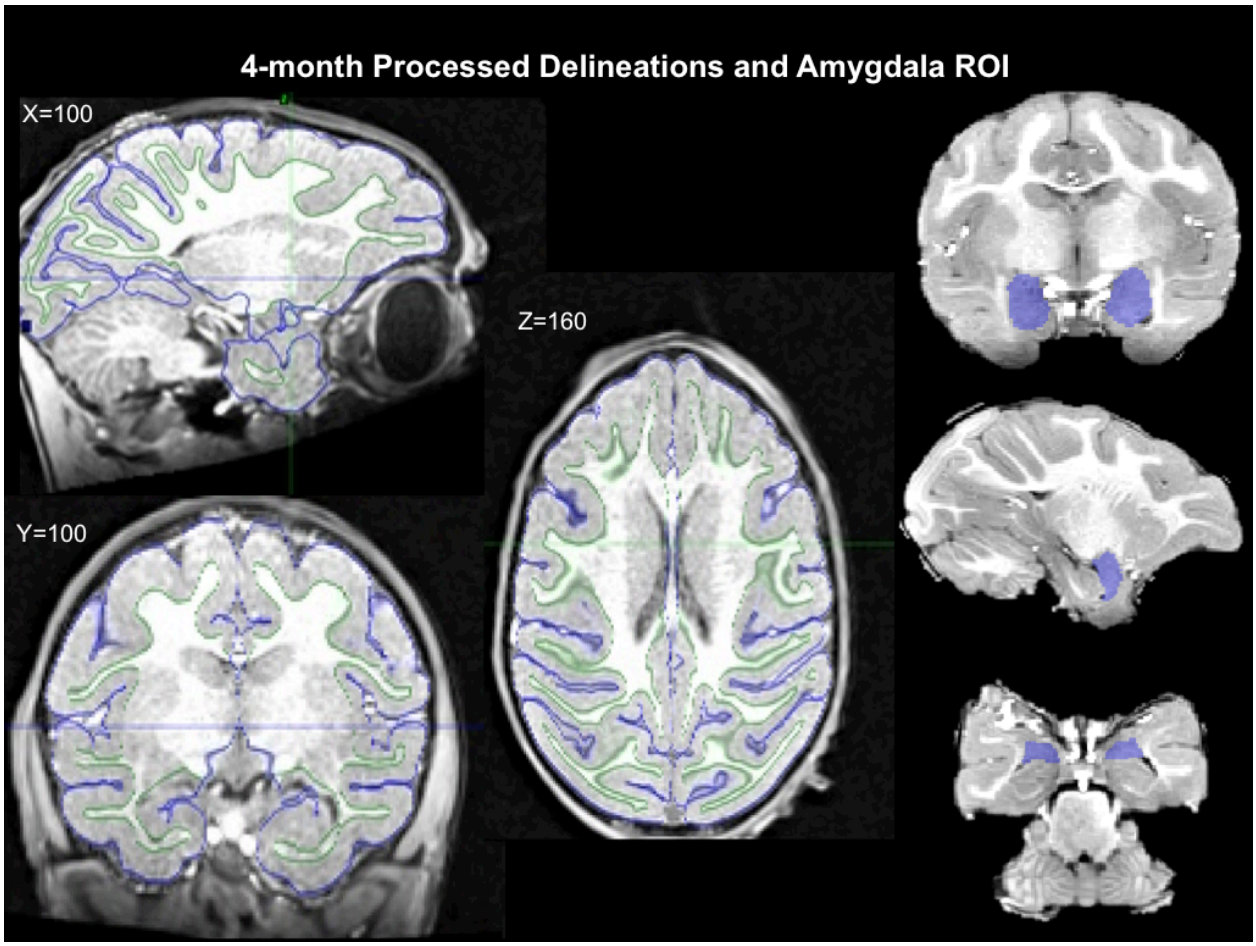

Supplemental Figure 2.1: Example of a 4-month old subject processed through the pipeline. White and gray matter delineations and surface pial registrations were used to assess the quality of the images processed through the pipeline. Amygdala ROIs defined through ANTs Joint Label Fusion are also shown.

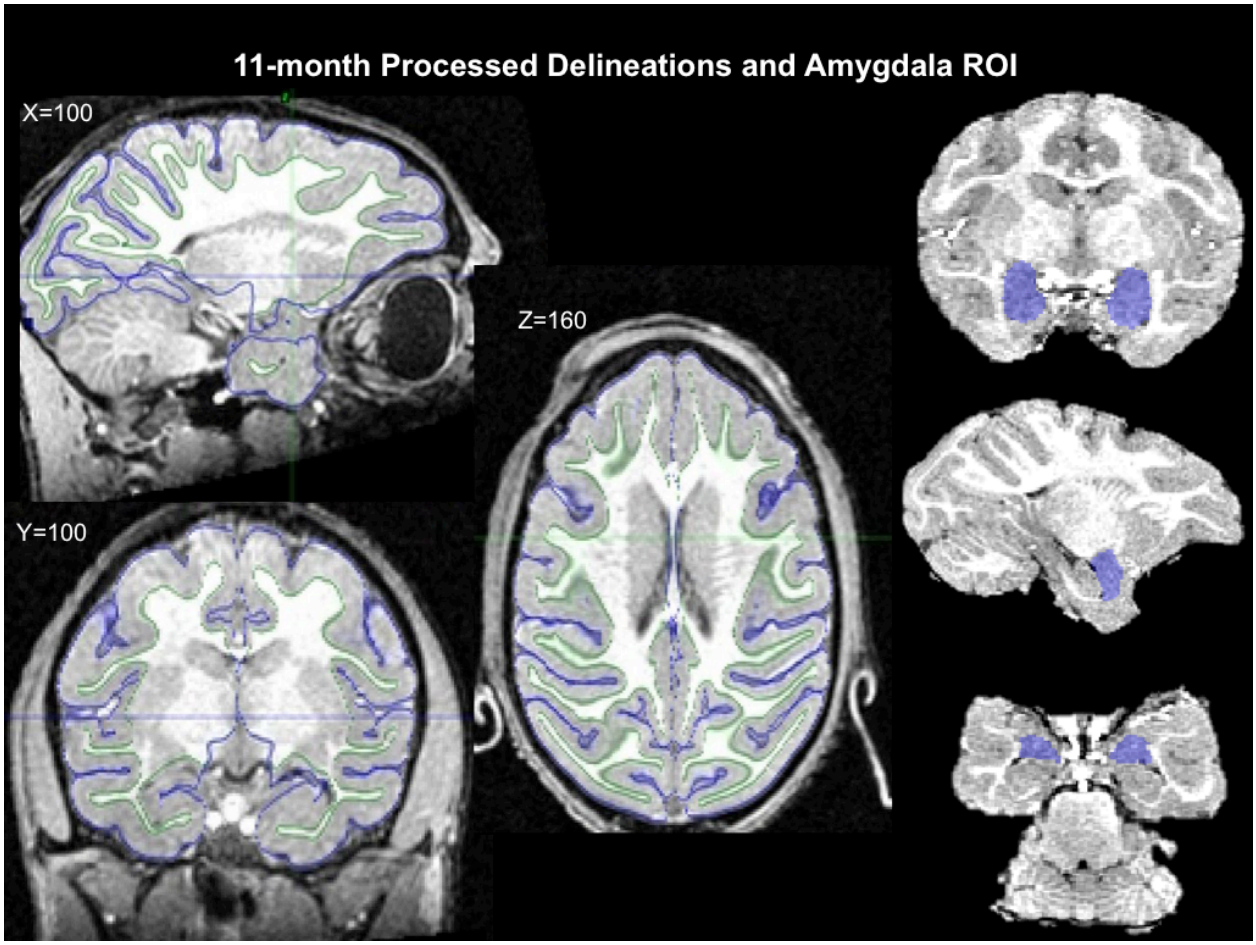

Supplemental Figure 2.2: Example of an 11-month old subject processed through the pipeline. White and gray matter delineations and surface pial registrations were used to assess the quality of the images processed through the pipeline. Amygdala ROIs defined through ANTs Joint Label Fusion are also shown.

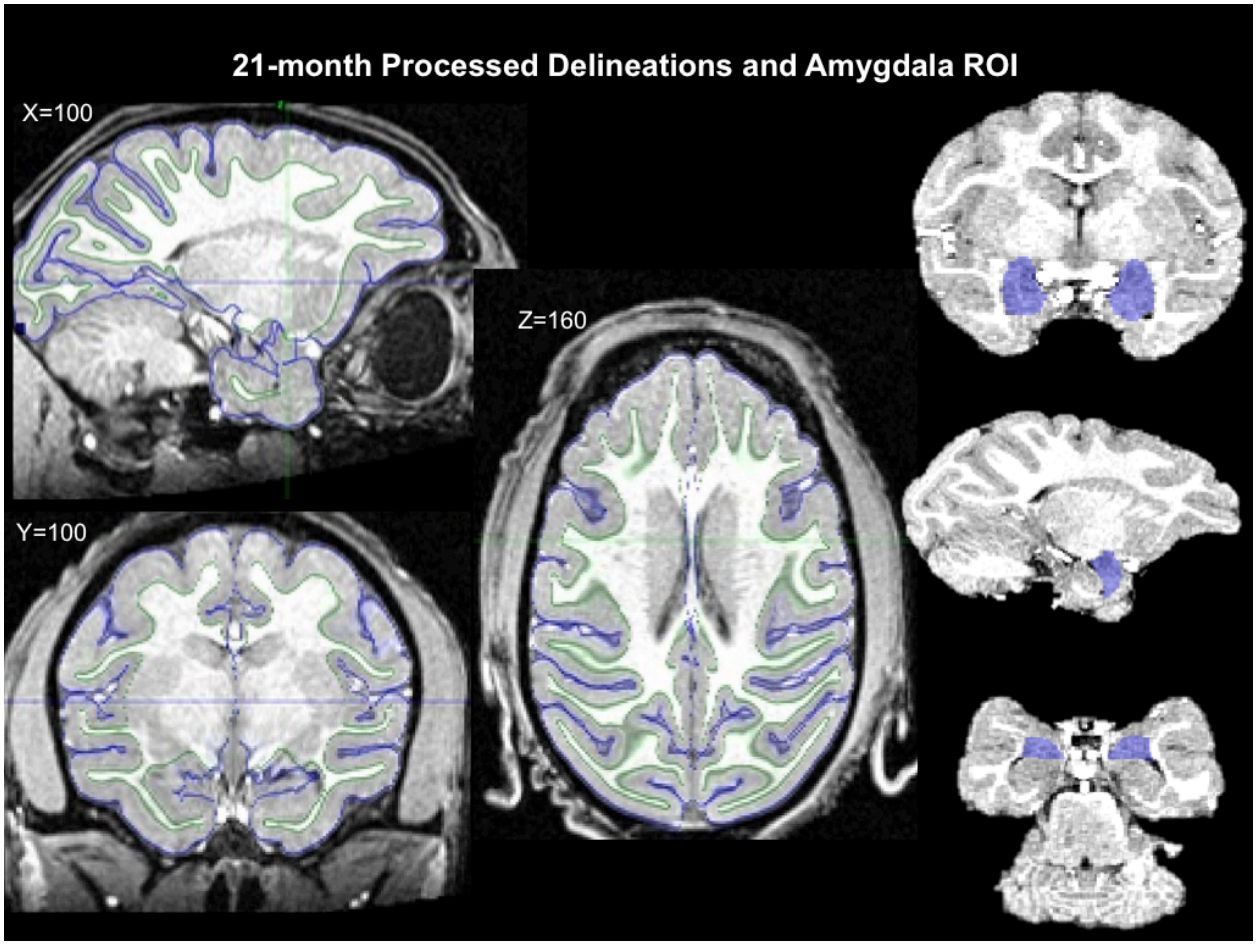

Supplemental Figure 2.3: Example of a 21-month old subject processed through the pipeline. White and gray matter delineations and surface pial registrations were used to assess the quality of the images processed through the pipeline. Amygdala ROIs defined through ANTs Joint Label Fusion are also shown.

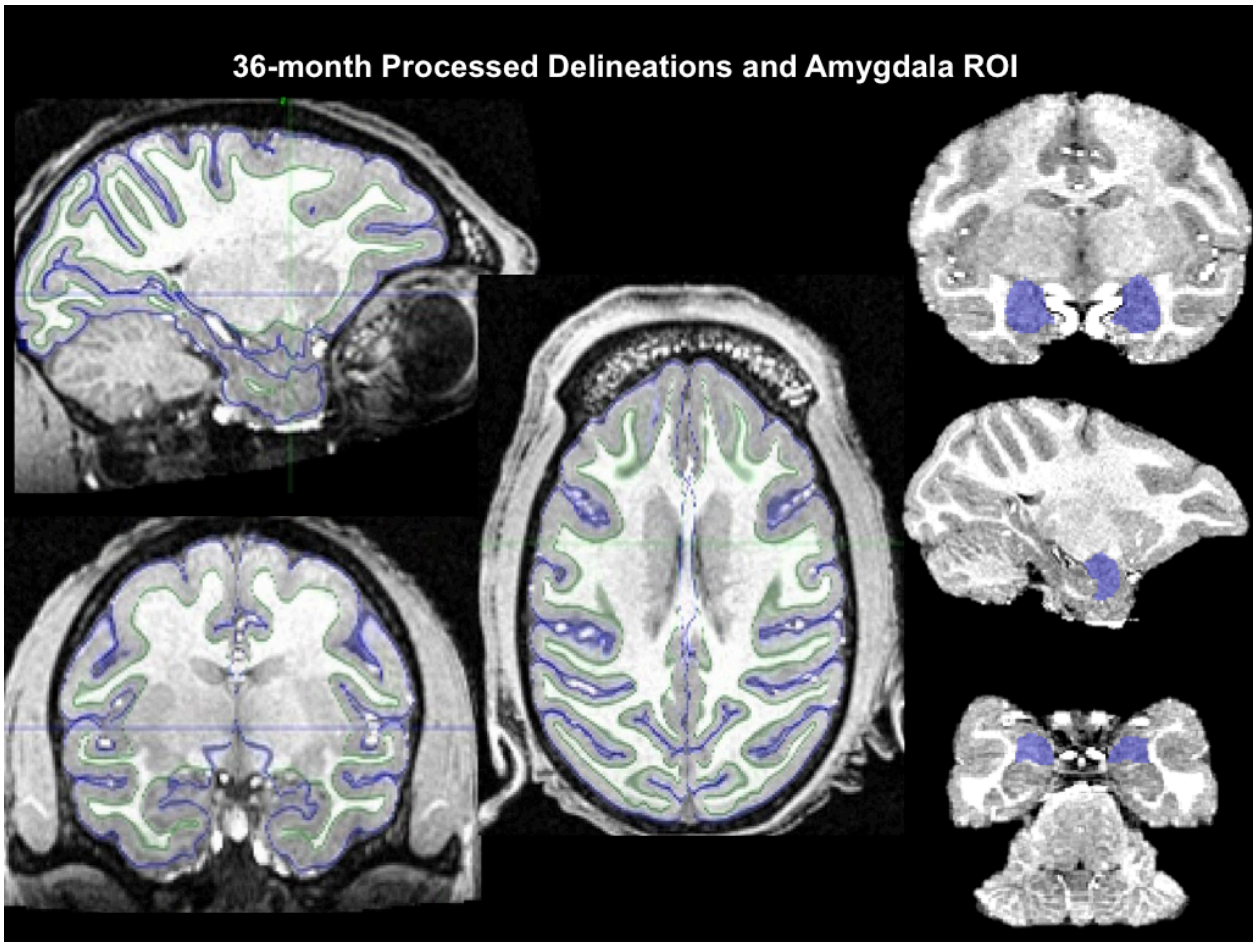

Supplemental Figure 2.4: Example of a 36-month old subject processed through the pipeline. White and gray matter delineations and surface pial registrations were used to assess the quality of the images processed through the pipeline. Amygdala ROIs defined through ANTs Joint Label Fusion are also shown.

Chapter 3: Study 2: Differential macaque cortical thickness development in the light of maternal interleukin-6 and diet and offspring sex.

3.1 Introduction

External factors such as maternal IL-6 influence not just one region such as the amygdala, but also play a more diffuse role throughout the brain. Furthermore, the brain is heavily interconnected. Thus, changes in early developing subcortical regions, such as the amygdala, have been shown to have a bi-directional relationship with cortical developmental processes (Tottenham and Gabard-Durnam 2017). Hence, it is important to also study these maternal-offspring relationships on larger cortical development. Cortical thickness measured with MRI has long been used to characterize the nature of the developing brain (Mills, Goddings, et al. 2016; Vijayakumar et al. 2016; Tamnes et al. 2017). While the underlying neurobiology supporting cortical thickness remains under investigation (Goodkind et al. 2015; Shin et al. 2018), it has been linked to a number of neurodevelopmental disorders, including attention deficit/ hyperactivity disorder (ADHD) (Shaw et al. 2006, 2007, 2013; de Zeeuw et al. 2012; Friedman and Rapoport 2015; Hoogman et al. 2019), autism spectrum disorder (ASD) (Hardan et al. 2006, 2009; Raznahan et al. 2010; Hedrick et al. 2012; Khundrakpam et al. 2017; Mensen et al. 2017; Prigge et al. 2018) and schizophrenia (Habets et al. 2011; Rapoport et al. 2012; Rimol et al. 2012). Furthermore, the impact of genetic and environmental influences are often studied in the light of cortical thickness (Panizzon et al. 2009; Kolb and Gibb 2011; Raznahan et al. 2011; Hedrick et al. 2012; Brito and Noble 2014; Avants et al. 2015; Jansen et al. 2015).

While the utility of studying cortical thickness in development is thus supported, accurate characterization in human models remains a challenge for several reasons. For example, it is well recognized that within-subject, longitudinal designs are critical for proper characterization of long-term growth trajectories (Foulkes and Blakemore 2018); however, due to the protracted nature of human brain development, few longitudinal studies exist that capture the critical developmental window from birth through adolescence. In addition, it is well documented that increased subject motion in youth complicates longitudinal data collection and analysis through subject/data loss (Dosenbach et al. 2017) and systematic image artifacts (Fair et al. 2012; Power et al. 2012, 2014, 2015). Other 'interacting' factors common to all human studies related to demographics, education, diet, and other 'covariates' also complicate the design of well-controlled longitudinal studies that measure cortical thickness.

Non-human primate models provide an opportunity to overcome some of these limitations in human longitudinal studies of cortical thickness. The developmental period from birth to early adolescence is truncated relative to humans allowing for more easily acquired repeated measurements during this time. NHPs often undergo MRI sedated and, thus, motion artifacts are limited relative to their human counterparts. In addition, data acquisition can be controlled with regard to timing and various other environmental factors. NHP, to a far greater degree than rodents, also share many complex behavioral and brain characteristics as compared to humans (Orban et al. 2004; Hutchison and Everling 2012; Miranda-Dominguez, Mills, Grayson, et al. 2014; Ausderau et al. 2017; Casimo et al. 2017; Donahue et al. 2018; Van Essen and Glasser 2018; Xu et al. 2018; Xu, Nenning, et al. 2019; Xu, Sturgeon, Ramirez, Froudist-Walsh, Margulies, Schroeder,

Fair, et al. 2019a). Last, NHPs have a similar gestational period to humans with early brain development predominantly occurring prenatally (Sullivan and Kievit 2016).

Recent work in macaques (Malkova et al. 2006; Liu et al. 2015; Scott et al. 2016a; Ball and Seal 2019) and marmosets (Seki et al. 2017; Uematsu et al. 2017; Sawiak et al. 2018) have shed some light on NHP cortical brain development from birth through early adolescence. For example, Ball and Seal have shown that total macaque cortical gray matter volume, as a proportion of intracranial volume, generally decreases from 3 to 36-months of age (Ball and Seal 2019). Scott and colleagues highlight differential growth trajectories for the frontal, parietal, occipital, temporal, cingulate and insular cortical volume development from 1 to 260 weeks-of-age (Scott et al. 2016a). While these studies primarily focus on cortical volume and require a specific parcellation schema of the cortex (a limitation aimed to avoid here – see methods), they do provide some context with which to consider cortical thickness development in the current report.

While macaque models provide an avenue to study longitudinal trajectories in typical development, they also provide several benefits when studying atypical development. Along with the factors noted above, the ability to do well-controlled experimental designs with regard to various environmental factors has made NHP models tremendously advantageous (Sullivan et al. 2010; Rivera, Kievit, et al. 2015; Sullivan and Kievit 2016; Thompson et al. 2017; Ramirez et al. 2019).

As noted in chapter 1 and study 1, several lines of evidence in humans have highlighted the role of developmental programming in shaping long-term brain trajectories in relation to maternal factors. The author's mentor and collaborators have shown in several studies that maternal diet and inflammation during pregnancy can

influence the offspring's brain after birth. Human studies found that maternal interleukin-6 (IL-6) relates to differences in growth characteristics of amygdala volumes and amygdala structural and functional connectivity (Graham et al. 2018; Rasmussen et al. 2018; Rudolph et al. 2018; Spann et al. 2018)..

As Study 1 noted, maternal IL-6 relates to decreased 4-month left amygdala volumes, but also an increased rate of growth from 4 to 36-months-of-age, with an indirect relationship to anxiety-like behavior (Ramirez et al. 2019). Other findings have implicated a maternal "Western-Style" diet high is associated with dysregulated dopamine and serotonergic systems in offspring (Thompson et al. 2017; True et al. 2018). While study 1 originally tested if maternal diet and offspring sex should be included in the model, ultimately these variables were excluded from the final model as they did not significantly associate with amygdala volume development and the data set was too small to include every possible covariate.

Study 2 sought to determine the typical developmental trajectories in cortical thickness from birth to early adolescence in a Japanese Macaque model and to examine how these trajectories might be modified by maternal diet, inflammation (i.e., IL-6), and offspring sex. Since this study investigated multiple models across each vertex of the cortex (vertex n=56522) the covariates could not be statistically reduced for each model by testing if each one related to brain development, as was done in Study 1. Instead only intuitively relevant variables of interest were included for all models (i.e. Maternal IL-6, Diet and Offspring Sex).

3.2 Materials and Methods

3.2.1 Macaque Study Overview

This study used Japanese macaques from the same NHP cohort as in Study 1, however, the total number of subjects included differed as a result of the timing and state of experimental procedures established when each study was conducted. (Sullivan et al. 2010, 2012; Thompson et al. 2017). Maternal and offspring phenotypes have been characterized and described in prior reports (McCurdy et al. 2009; Sullivan et al. 2010, 2012, 2017; Comstock et al. 2013; Thompson et al. 2017). This study and procedures have been approved by the Oregon National Primate Research Center (ONPRC) Institutional Animal Care and Use Committee, and also follow the National Institutes of Health guidelines on ethical use of animals (Figure 3.1).

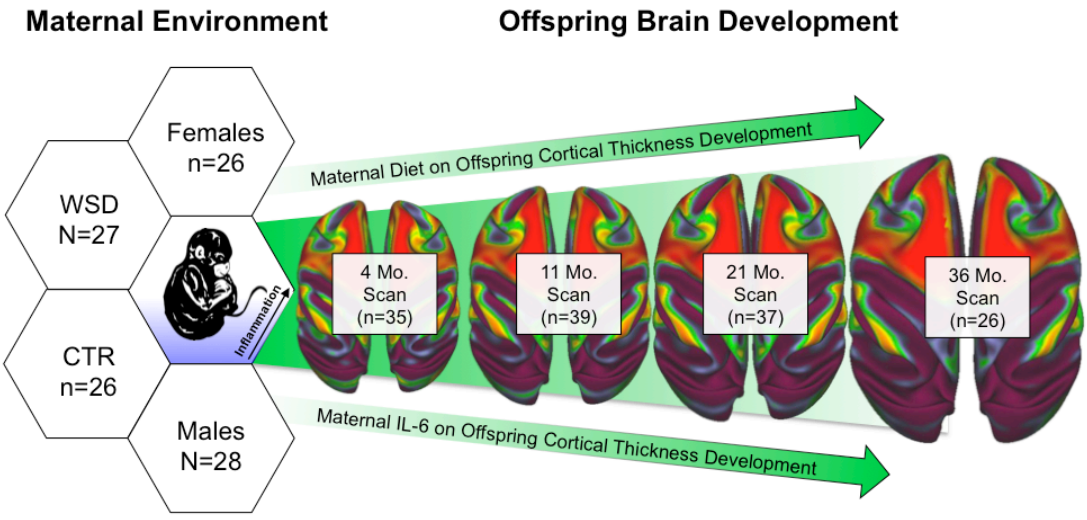

Figure 3.1: Overview of macaque study. Maternal Western-Style Diet (WSD) or Control Diet (CTR) and maternal IL-6 may influence cortical thickness development across time.

3.2.2 Subjects

Offspring mothers consumed either a CTR diet (Monkey Diet no. 5000; Purina Mills) or a WSD (TAD Primate Diet no. 5LOP, Test Diet, Purina Mills). Diet groups were determined 1.2-8.5 years before offspring birth (age at offspring birth [mean (M) ± SEM]: CTR M= 11.33 ± 3.23 years; WSD M= 8.46 ± 2.31 years). Offspring were housed with their mothers until weaning age (~8-months) and then peer social housed with 1-2 unrelated female adults and 6-10 other juveniles. Further offspring rearing and diet characteristics have been detailed in a recent publication (Thompson et al. 2017). As all three studies use the same cohort of animals, offspring and maternal procedural details are the same but repeated here for completeness.

The current study used 53 subjects (Female n=25; CTR n =26), of which the majority (n=44; Female n=19; CTR n =21) of offspring consumed a CTR diet as opposed to a WSD post-weaning. Maternal IL-6 levels were collected from plasma during the 3rd trimester (48.16 ± 9.26 days) prior to offspring birth (maternal age: 9.25 ± 2.95 years). A lower limit of quantification (LLOQ) of 1.23 pg/mL threshold was used for IL-6 levels, excluding subjects below this value. This resulted in a total, 42 (Female n = 19; CTR n = 17) subjects with usable IL-6 measurements. IL-6 concentrations were logarithmically transformed across subjects to center potential outliers and normalize the distribution. Comprehensive plasma collection and analysis procedures have previously been described in detail (Thompson, Gustafsson, Decapo, et al. 2018).

3.2.3 MRI acquisition

Partly identical to Study 1, MRI scans were acquired on a Siemens TIM Trio 3 Tesla scanner in a 15-channel knee coil adapted for monkey use. Longitudinal scans

occurred at 4 (M = 4.37 ± 0.05), 11 (M = 11.09 ± 0.04), 21 (M = 21.11 ± 0.05) and 36 (M = 36.53 ± 0.09) months of age. Monkeys were sedated with a single dose of ketamine (10-15mg/kg) for intubation before each scan followed by a <1.5% isoflurane anesthesia for the rest of the scan. Respiration, heart rate, and peripheral oxygen saturation were monitored throughout.

However, the scan acquisition was adjusted partway through the study to optimize future outputs. For this reason, some scans were acquired using scan acquisition # 1 (n=80), while other scans were acquired with scan acquisition #2 (n=56). While this was a limitation, mean cortical thickness (Supp. Fig. 1) was not significantly different between the two acquisitions while controlling for age ($F(1,133)=2.22$, $p=0.139$) and thus not included in these models.

A total of four T1-weighted anatomical images were collected for each subject either using acquisition #1 (TE= 3.86 ms, TR= 2500 ms, TI= 1100 ms, flip angle= 12°, 0.5 mm isotropic voxel) or acquisition #2 (TE= 3.33 ms, TR= 2600 ms, TI= 900 ms, flip angle= 8°, 0.5 mm isotropic voxel). Additionally, one T2-weighted anatomical image was acquired for acquisition #1 (TE= 95 ms, TR= 10240 ms, flip angle= 150°, 0.5 mm isotropic voxel) or acquisition #2 (TE= 407 ms, TR= 3200 ms, 0.5 mm isotropic voxel). Additional scan types were acquired in these sessions, but not used for this manuscript.

3.2.4 MRI preprocessing

As previously reported, this study used a macaque specific modified version of the human connectome project (HCP) minimal preprocessing pipeline (Glasser et al. 2013). Details on preprocessing have previously been described in study 1 and are also in our prior publication (Ramirez et al. 2019). In brief, this pipeline was built to analyze

outputs in surface space and used FMRIB Software Library (FSL)(Smith et al. 2004b; Woolrich et al. 2009; Jenkinson et al. 2012), the FreeSurfer image analysis suite (http://surfer.nmr.mgh.harvard.edu/)(Dale et al. 1999; Fischl et al. 1999), Advanced Normalization Tools (ANTs) (version 1.9; http://stnava.github.io/ANTs/) in combination with in-house established tools. The general structure follows the HCP stages (Glasser et al. 2013), with macaque specific modifications occurring before and in the PreFreeSurfer, FreeSurfer, and PostFreeSurfer stages. Subjects were aligned to the Yerkes19 atlas space (Donahue et al. 2016). This pipeline produced the volumetric amygdala data used for study 1 from the FreeSurfer stages, but also allowed us to get the surface-based cortical thickness measures for each surface vertex (identified as grayordinate) from the later stages of the pipeline.

3.2.5 General analysis overview

Cortical thickness development was investigated in relation to maternal diet, IL-6 and offspring sex using latent growth curve (LGC) analyses. Growth trajectories over time and related predictors/covariates were estimated with LGCs using the same procedures as in Study 1 (McArdle and Epstein 1987; Meredith and Tisak 1990; Muthén 2002) . As was described in Study 1 (and its published version,:(Ramirez et al. 2019)) and is restated here for completeness. The best-fitting model to characterize the typical growth trajectory is established as the unconditional model. Then predictors and covariates are added to the model to see how they relate to the different aspects of this typical growth trajectory (e.g. the starting point [intercept] or the growth [slope]). The best-fitting model is determined by testing out the simplest model (intercepts only), followed by more complex models (intercept & slope, or intercept, slope & quadratic). A

chi-squared difference test is used to see if adding the additional functional forms significantly improves the model. The simplest model that is not significantly improved by additional functional form/s is considered the best fitting model (Andruff et al. 2009). Individual models were analyzed using version 8 of Mplus (Muthén and Muthén 2017), with the robust maximum likelihood estimator for non-normal data and full information maximum likelihood for missing data (Enders 2001). A large body of research supports the use of this method in studies with missing data at different time points (Enders 2001; Raykov 2005; Buhi 2008; Jeličić et al. 2009; Schlomer et al. 2010; Larsen 2011; Peyre et al. 2011; Gustavson et al. 2012). Best-fitting models were identified using in-house derived code in MATLAB (The MathWorks, Inc., Natick, Massachusetts, United States) and the procedures of what this code did is explained throughout the remainder of the methods and depicted in Figure 3.2. Finally, figures were created using Jupyter Notebooks, MATLAB, PowerPoint, and the Connectome Workbench visualization software (Marcus et al. 2011).

3.2.6 Characterizing typical cortical thickness development on a grayordinate level

To establish typical cortical thickness development across four time-points the previous convention in the field (Curran et al. 2010) was followed to determine the best-fitting unconditional model on every surface grayordinate (n=56,522)(Figure 3.2). Consequently, for each grayordinate, multiple latent growth models using different functional forms (intercept, slope, quadratic, and splines on the 4, 11, 21 and 36-month time points) were computed based on prior convention (Curran et al. 2010). Chi-squared difference tests were then computed between the most simple (intercepts only) and more complex models (e.g. intercept & slope) to determine the best fitting model of each

grayordinate (Figure 3.2). This enabled characterization of the best fitting growth trajectory of each grayordinate and how the estimated mean cortical thickness of each grayordinate changed across time. For visualization purposes, a video is provided (Supp Mov. 1) of the estimated mean cortical thickness development from 4 to 36-months of age. The thickness at time points (in months) between actual scan dates was interpolated using a linear interpolation for change of thickness in each month.

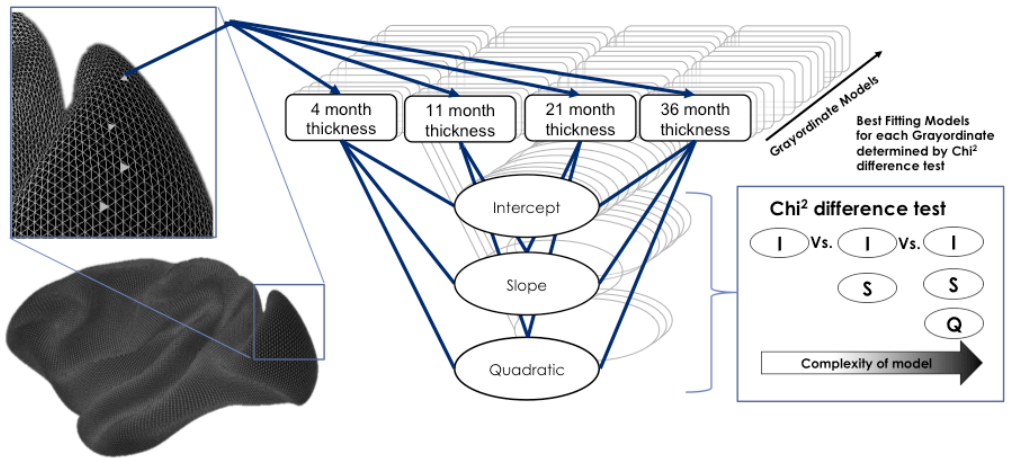

Figure 3.2: Analysis model overview. Latent growth curve models are defined for each grayordinate, indicating the cortical thickness at 4, 11, 21, and 36-months of age. The most simple model (intercepts only) is run first, and then a Chi-Squared difference test is run on more complex models to identify the best fitting model for each grayordinate. Spline models were determined by freeing the different time points one at a time and tested for inclusion with the Chi-squared difference test after the quadratic model.

3.2.7 Introducing predictors to the unconditional models

After modeling typical cortical thickness development, predictors of interest (maternal IL-6, maternal diet, offspring sex) were introduced. This allowed us to identify how each predictor related to the latent growth variables (i.e. intercept, slope, quadratic)

of each grayordinate trajectory while controlling for the impact of the other predictors. Estimates of the relationships between predictors and growth variables can be displayed on the brain for visualization purposes (Figure 3.5-Figure 3.7).

3.2.8 Cluster detection analysis

Having established estimates, p-values and standard errors for each model, the plan was to next identify which specific regions from this analysis were most notable. using a cluster detection analysis. To avoid issues with multiple comparisons and identify the most important areas, these estimates were standardized and run through a cluster detection algorithm, based on previously defined guidelines (Eklund et al. 2016). Clusters of voxels defined by estimates and standard errors, were ordered by size, permutated and top clusters were kept based on a predefined z-score threshold. In this case, clusters above/below a z-score of 2.36 yielded a corrected significance p-value of 0.01 in line with previous findings using cortical thickness data (Greve and Fischl 2018).

3.2.9 2.9 Testing how maternal diet, IL-6 and offspring sex relate to whole-brain average cortical thickness

Finally, to test whether findings were not just a function of changes in overall total cortical thickness, this same analysis was repeated on mean total brain cortical thickness development as opposed to individual vertices across the cortex. This was run as a proof that the more detailed grayordinate specific approach added information and was thus needed to identify how predictors related to changes in specific aspects of cortical development depending on the region as opposed to the total brain. To do this, the best-fitting unconditional model of typical total brain development was identified using a chi-squared difference test. Then, predictors of interest (IL-6, Diet, Sex) were

added to see how they related to the functional forms (intercept and slope) of this new conditional model (Figure 3.9, Supp Table 3.1).

3.3 Results of Study 2

3.3.1 *Characterizing typical cortical thickness development across the entire brain.*

This study first aimed to characterize typical cortical thickness development for all cortical grayordinates to identify the unconditional models. The best fitting model for each grayordinate was identified and the different growth patterns were mapped on the brain (Figure 3.3A). While the majority of regions in the brain were best characterized by an intercepts-only model (i.e. little change across time) or a linear model (intercept and slope), some region's development was best described by more complex growth models including quadratic or spline functional forms (Figure 3.3A). This map of best-fitting models can be viewed alongside the supplemental movie 1.

To further characterize these findings the age of the monkeys at which point the cortical thickness was thinnest (Figure 3.3B) and thickest (Figure 3.3C) was identified. Not all regions start the thickest at the 4-month time point or end the thinnest at the 36-month time point, but instead, in some regions, the cortical thickness is thinnest/thickest at the 11 or 21-month time point – consistent with the non-linear best-model fits.

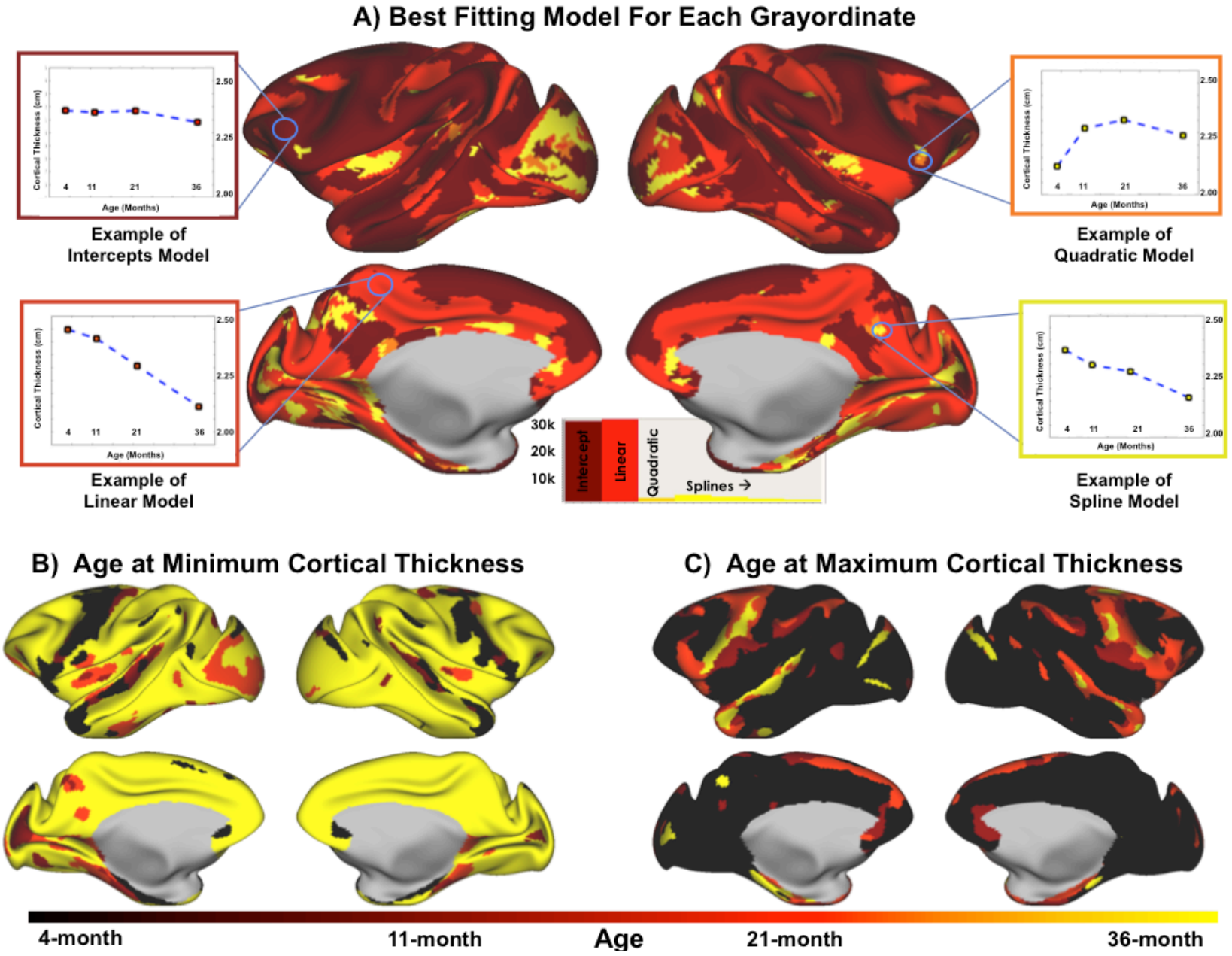
A) Best Fitting Model For Each Grayordinate
Cortical Thickness (cm)
2.50
2.25
2.00
4
11
21
36
Age (Months)
Example of
Intercepts Model
Example of
Quadratic Model
Example of
Linear Model
Example of
Spline Model
30k
20k
10k
Intercept
Linear
Quadratic
Splines →
B) Age at Minimum Cortical Thickness
C) Age at Maximum Cortical Thickness
4-month
11-month
Age
21-month
36-month

Figure 3.3: Best-fitting models are defined for each grayordinate using the chi-squared difference test comparing simple to more complex models. The best-fitting models are mapped onto the brain (A). A graph of mean cortical thickness for specific clusters where an intercepts-only (dark red), a linear (orange) a quadratic (light orange) or a spline (yellow) model best fit, to show that the model fits represent actual development. (B) Shows the age at which the cortical thickness was thinnest. Regions where it is yellow for example, indicate cortical thickness was thinnest at 36-months of age. (C) Similarly, this shows the age at which cortical thickness was the thickest (max). Similarly, dark colors indicate that the max thickness was at 4-months of age. In cases where the thickness was the max at 4-months (dark red) and min at 36-months (yellow), a gradual thinning over time can be inferred. Interesting patterns emerge where it is orange, indicating a change in direction of thickness that happened over time.

Having characterized the unconditional model, allowed us to view the estimated mean cortical thickness of each grayordinate across the four time-points. The estimated mean cortical thickness decreased in the majority of the cortex across time (Figure 3.4). However, in some regions, the estimated mean cortical thickness increased from 4 to 36-months of age (Figure 3.4). Cortical thickness changed anywhere between -20 and 20 percent depending on the region (Figure 3.4E).

When investigating the percent change between each time point, the majority of change occurred between the 4 and 11-month time point (Figure 3.4F), with the least amount of change occurring between 11 and 21 months of age (Figure 3.4G). The rate of cortical thickness development was not uniform across the brain. For example, while cortical thickness decreased ~15% in insular regions between the 4 and 11-month time

points, it increased from 21 to 36-months of age (Figure 3.4F & Figure 3.4H). This can be seen even more clearly in the supplemental video 1 showing the estimated mean cortical thickness development (Supp. Mov. 1) and Supplemental Figure 3.2 showing both hemispheres (Supp. Fig.3.2).

These interesting patterns in change across time were reflected in all three components of the current data representation. For example, the non-linear changes across the time points in mean cortical thickness (Figure 3.4) of the insular region was also reflected in the best fitting models diagram (Figure 3.3A) and the representation of having the minimum cortical thickness at the 11 and 21-month time points (Figure 3.3B). Similarly, noteworthy changes can be observed in the ventrolateral prefrontal/motor cortex, where the best fitting model was either a spline or a quadratic (Figure 3.3A). This trajectory is also reflected in the age at max thickness, which was around 21-months of age (Figure 3.3C). And further in the percent change across time, which showed an increased change in cortical thickness during the early months (Figure 3.4F-G) and a decreased percent change in thickness during the later months (Figure 3.4H). These are just some examples of the remarkable changes that occur across development that can be characterized by these types of analyses. Future research can use these observations to help guide developmental trajectory interpretations.

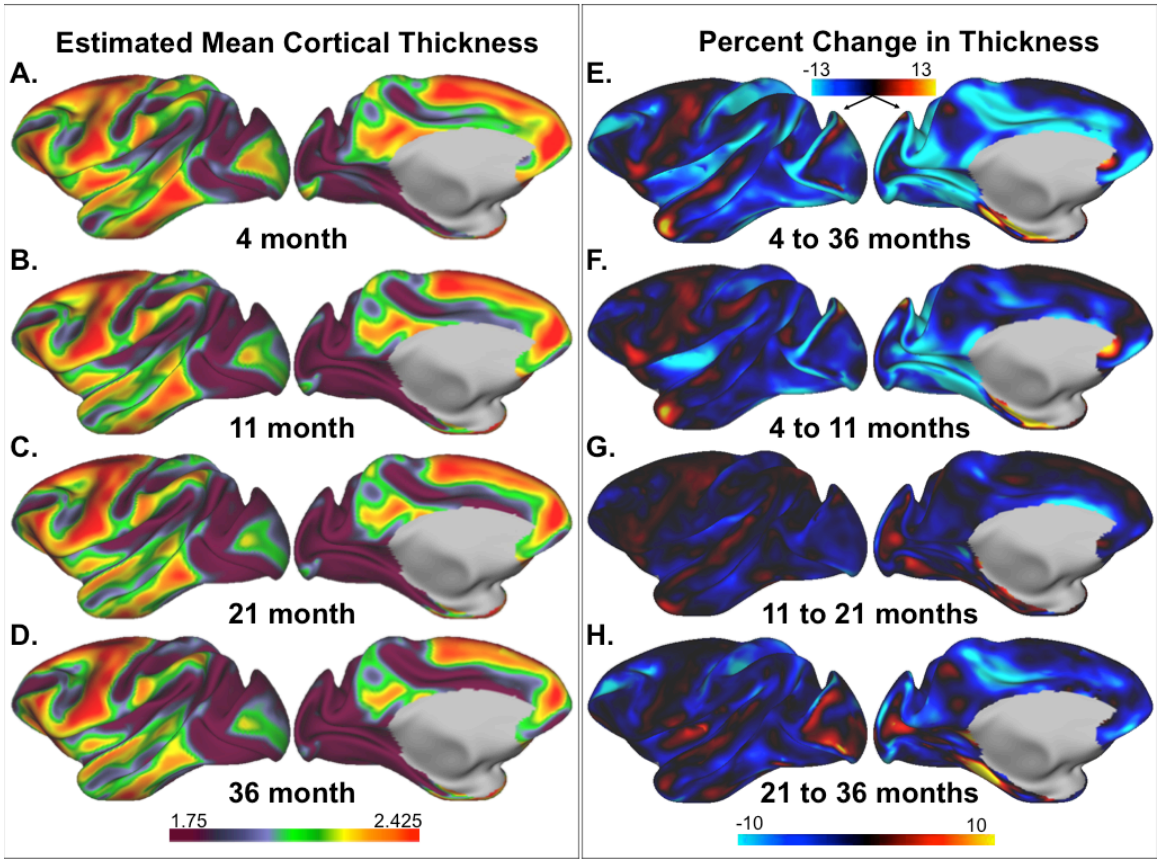

Figure 3.4 Cortical thickness development. The estimated mean thickness for the different age groups (A-D) and percent change in thickness between 4 and 36-months (E) and more gradual stages in change from 4 to 11 months (F), 11 to 21-months (G), and 21 to 36-months (H).

3.3.2 *How maternal IL-6 related to cortical thickness development.*

Having established the unconditional models describing typical cortical thickness development, next the predictors (Maternal Diet, Maternal IL-6 and Offspring Sex) of interest were introduced to identify how these related to the unconditional developmental trajectories. Maternal diet, IL-6 and offspring sex all had independent and variable relationships to the different components (i.e. intercept, slope, quadratic) of the

developmental trajectories, as seen through the overall estimates and significant clusters on the brain.

The maternal Western-style diet (WSD) was associated with both increased and decreased cortical thickness at the starting point (intercept) of a number of regions (Figure 3.5A & Figure 3.5C [green clusters]). Bilateral clusters where the WSD was associated with decreased (blue arrows) cortical thickness early in life (intercept/4-month time point) emerged in the posterior insula and at the pole of the temporal cortex. Similarly, WSD was associated with bilateral increased (yellow arrows) cortical thickness in the dorsolateral premotor/prefrontal cortex (Figure 3.5C). Intriguingly, a visual impression of the cluster results highlighted that the clusters tended to often fall on the edge of areas that were described by a different growth curve. These areas were often near a "focal point" in the brain, which the change in thickness seemed to gravitate towards (Supp. Mov. 1). For example, the insular cluster was located on the edge of where the best-fit model indicated a non-linear change. Similarly, this cluster and others were in surrounding areas where mean cortical thickness was thickest or thinnest (Figure 3.4; Supp. Mov. 1) with a gradual change in thickness happening towards these focal points over time.

In regards to the relationship with the growth rate (slope), several clusters showed increased or decreased relationships with WSD (Figure 3.5B & Figure 3.5C [pink clusters]). Some noteworthy bilateral clusters associated with slope showed a decreased (blue arrows) rate of cortical thinning in the posterior cingulate gyrus (Figure 3.5C). Interestingly, there was also an overlapping slope cluster in the right posterior insula indicating that WSD was associated with a decreased initial cortical thickness (intercept)

and an increased rate of cortical thinning (slope) (similar to the study 1 results). As there were so few regions that were best characterized by a quadratic functional form (Figure 3.4A & Supp. Fig. 3.3), no notable bilateral clusters stood out for this measure (Figure 3.5C [white clusters]).

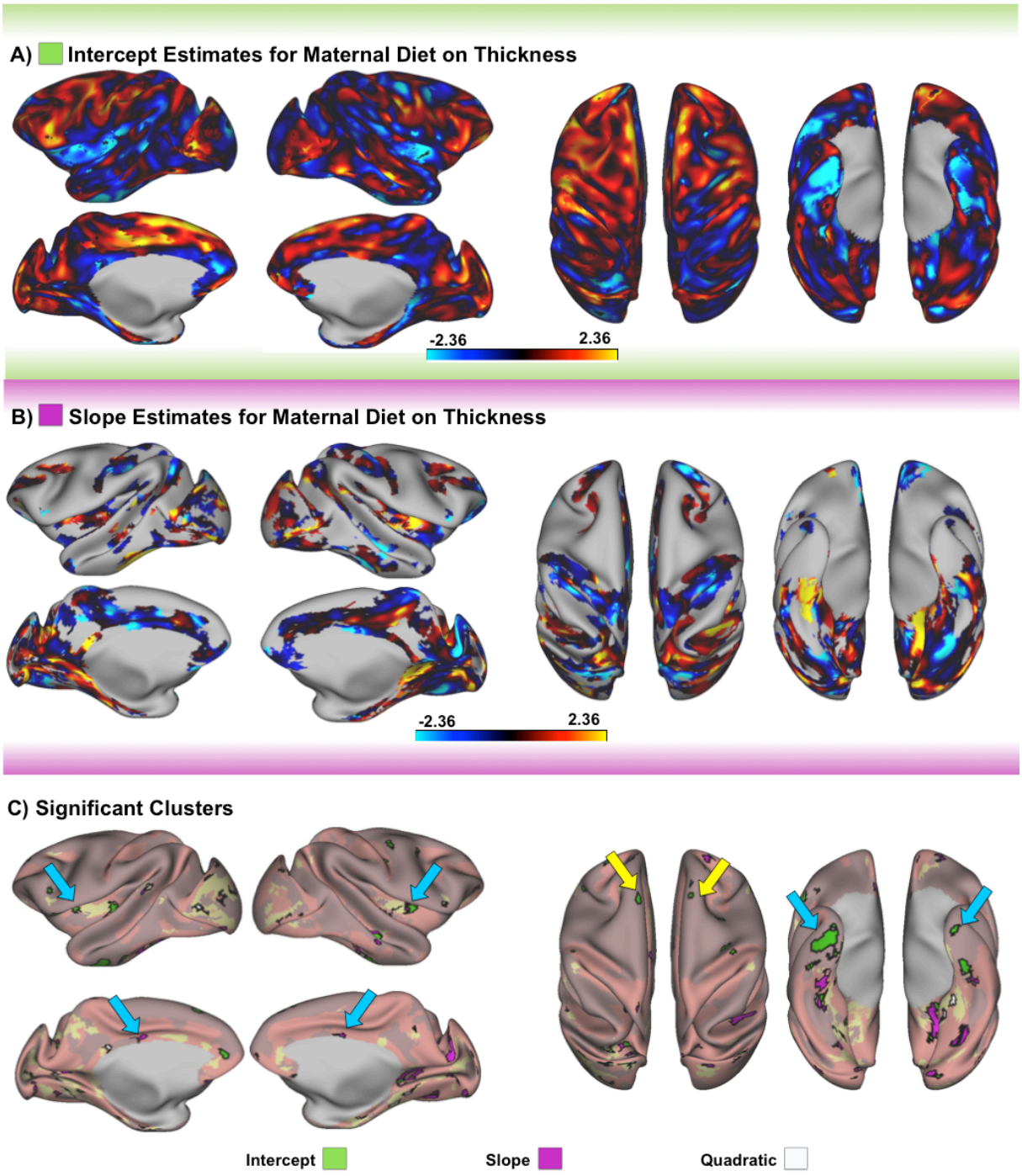

Figure 3.5: The influence of diet on cortical thickness development. (A) indicates the estimates of how diet relates to the intercepts of the models (B) shows the estimates of how

diet relates to the slope parameter, and (C) highlights the significant clusters from this analysis. Green clusters are clusters where diet had a significant relationship with the intercept, and pink clusters show the significant slope clusters. White clusters indicate the quadratic, however since there were so few best-fitting quadratic models, the estimates are reported in the supplemental materials. Arrows highlight some interesting bilateral clusters where a WSD was associated with decreased (blue arrow) or increased (yellow arrow) intercept (green cluster) or slope (pink cluster). Direction of association (highlighted by color of arrows) can be identified by the color of the estimates (A&B).

3.3.3 How maternal diet related to cortical thickness development.

Although IL-6 exhibited different patterns of association than did diet, it also related to increased and decreased starting points (intercept) and growth rate (slope) in cortical thickness (Figure 3.6A & Figure 3.6C [green & pink clusters]). Higher maternal IL-6 was associated with increased bilateral starting (4-month) cortical thickness in the pole of the temporal cortex (Figure 3.6C [green clusters; yellow arrows]). This result is the opposite of the temporal pole finding with WSD (Figure 3.5C [green clusters; blue arrows]). Nonetheless, increased IL-6 was also associated with decreased starting insular cortical thickness. However, this cluster fell in the anterior as opposed to the posterior insula as was seen with the WSD. However, these clusters still followed the interpreted trend of falling on the edge of the visually hypothesized focal point at which regions seemed to have the thickest or thinnest mean cortical thickness (Figure 3.4).

IL-6 slope showed decreased bilateral clusters in the medial parietal cortex (Figure 3.6C; blue arrows) and increased rate of growth in the inferior temporal cortex (Figure 3.6C; yellow arrows). Similar to the WSD findings, no meaningful bilateral

clusters stood out in relation to the quadratic term (Figure 3.6C [white clusters] & Supp. Fig. 3.3).

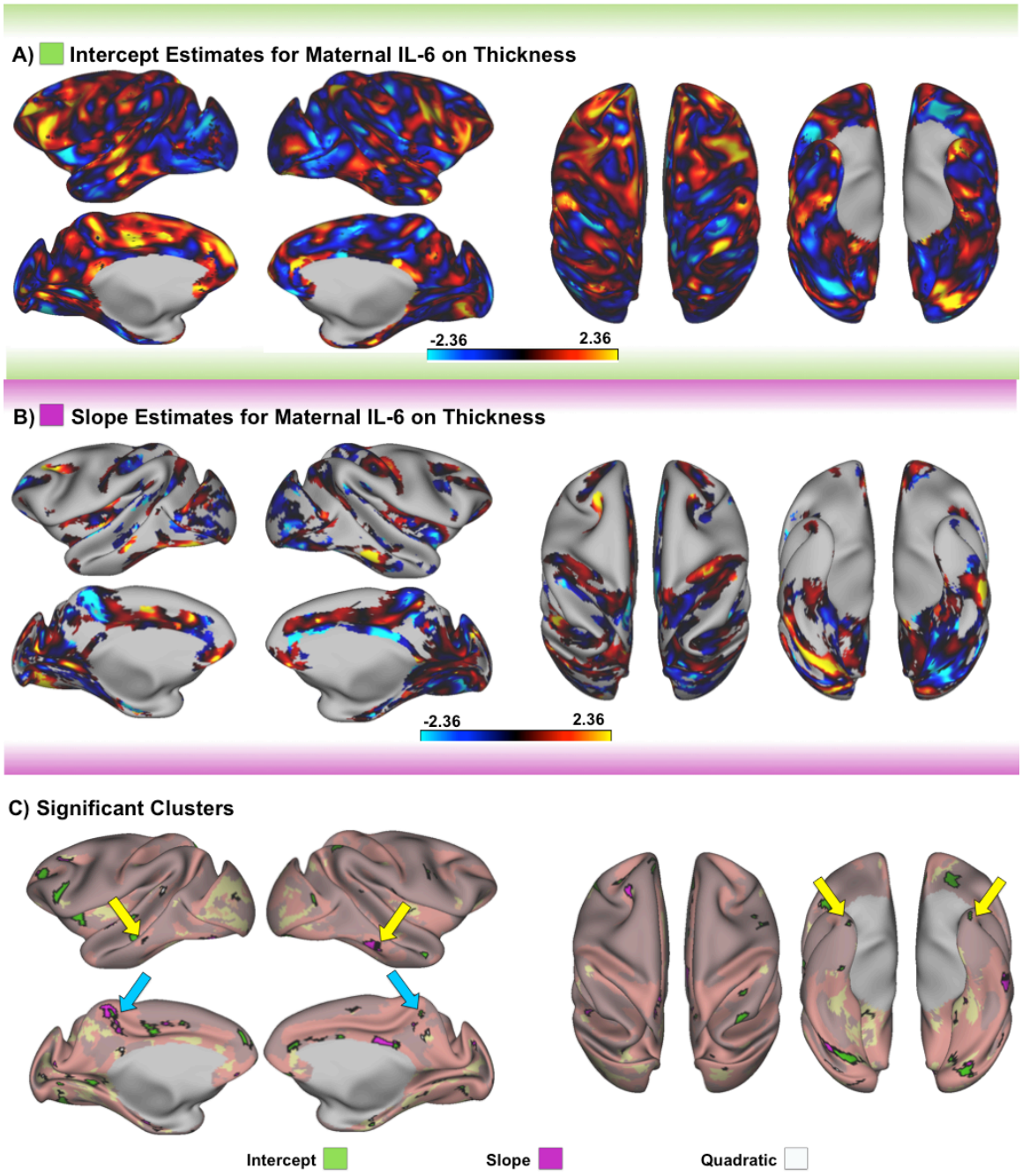

Figure 3.6: The influence of maternal IL-6 on cortical thickness development. (A) Indicates the estimates of how IL-6 relates to the intercepts of the models (B) shows the estimates of how IL-6 relates to the slope parameter, and (C) highlights the significant clusters from this analysis. Green clusters are clusters where IL-6 had a significant relationship with the intercept, and pink clusters show the significant slope clusters. White clusters indicate the quadratic, however since there were so few best-fitting quadratic models, the estimates are reported in the supplemental materials. Arrows highlight some interesting bilateral clusters where higher concentrations of IL-6 were associated with decreased (blue arrow) or increased (yellow arrow) intercept (green cluster) or slope (pink cluster). Direction of association (highlighted by color of arrows) can be identified by the color of the estimates (A&B).

3.3.4 How offspring sex related to cortical thickness development.

Additional associations with offspring sex were seen relating to the 4-month starting point (intercept) and the rate of cortical thickness growth (slope) across the four time-points (Figure 3.7). Due to the small sample size, and number of comparisons already run, no sex*diet or sex*IL-6 interactions were added to the model, so sex was only treated as an independent predictor in the model alongside IL-6 and Diet. Clusters associated with sex differences fell predominantly within the visual, default mode and somatomotor networks (these networks have been previously described in NHPs (Bezgin et al. 2012; Grayson et al. 2016) (Figure 3.7A&C). Males were associated with increased bilateral starting (intercept) cortical thickness in the dorsal part of the visual anterior cortex, as well as the inferior parietal cortex (Figure 3.7A&C; [green clusters; yellow

arrows]). However, males also showed decreased starting cortical thickness in the orbitomedial prefrontal cortex (Figure 3.7A&C; [green clusters; blue arrows]).

Regarding the rate of change, males exhibited increases in the superior parietal cortex and the primary somatosensory cortex (Figure 3.7B&C; [pink clusters; yellow arrows]). Finally, there was an interesting relationship between sex and the shape of development (quadratic). Males exhibited bilateral decreased quadratic clusters in the hippocampus (Figure 3.7C& Supp. Fig. 3.3; [white clusters; blue arrows]). These clusters also followed the previously described trend of falling on the edge of regions that had either the thickest or thinnest cortical thickness, as can be observed in the superior parietal/primary somatosensory cortex clusters and the orbitomedial prefrontal cortex clusters for example.

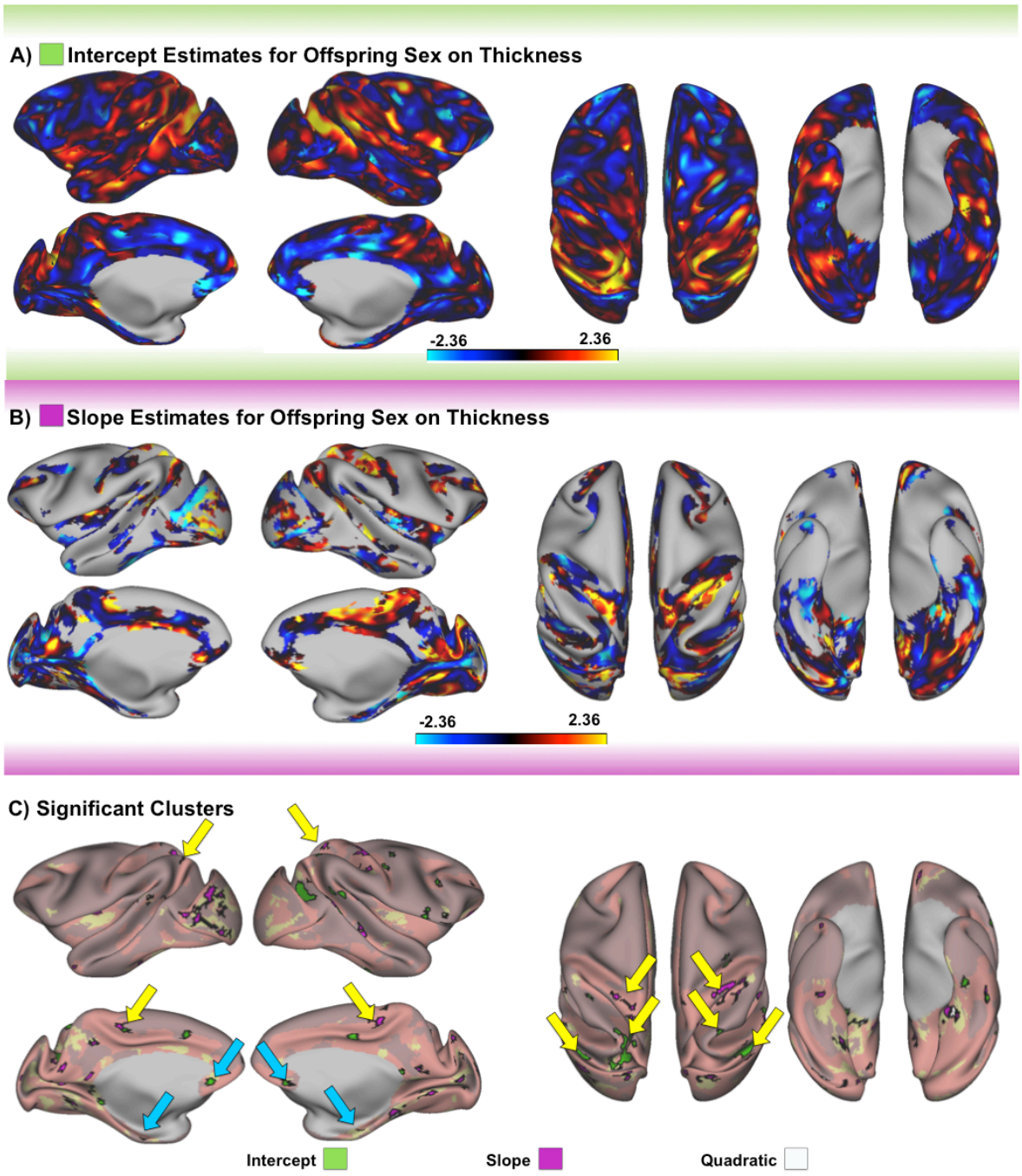

Figure 3.7: The influence of offspring sex on cortical thickness development. (A) Indicates the estimates of how sex relates to the intercepts of the models (B) shows the estimates of

how sex relates to the slope parameter, and (C) highlights the significant clusters from this analysis. Green clusters are clusters where sex had a significant relationship with the intercept, and pink clusters show the significant slope clusters. White clusters indicate the quadratic, however since there were so few best-fitting quadratic models, the estimates are reported in the supplemental materials. Arrows highlight some interesting bilateral clusters where males were associated with decreased (blue arrow) or increased (yellow arrow) intercept (green cluster) or slope (pink cluster). Direction of association (highlighted by color of arrows) can be identified by the color of the estimates (A&B).

3.3.5 Cluster surface areas in the light of functional networks.

After establishing a number of significant clusters that were associated with the predictors and cortical thickness development, the total surface area of all of the clusters was calculated and compared across the predictors. The comparison of total surface area between predictors was not statistically tested, but merely the totals were shown to help visually depict potential trends in these results. Rather than calculate the total surface across the entire brain, the surface area of clusters was calculated based on which functional network they fell into, highlight potentially interesting trends that could be further investigated in future studies. Networks and ROIs used for this have been previously described (Bezgin et al. 2012; Grayson et al. 2016). (

Figure 3.8).

These and following steps were solely conducted to visually depict potential trends coming out of the results from the current analyses, that could be further explored in future research. They do not indicate statistical testing or imply actual differences

between the different predictors or networks, but only show the total calculated surface area of the significant clusters that came out of the actual analyses. There was an optical trend towards more (not statistically tested) surface area of clusters falling in the visual and default mode network for diet and sex compared to IL-6, with more (not statistically tested) surface area of significant IL-6 clusters falling into Limbic regions (

Figure 3.8). The fact that the default and visual regions show similar trends is consistent with prior work by Power et al, highlighting that these systems tend to ‘hang’ together with regard to network characteristics (Power et al. 2011). While merely illustrative, this

comparison yields a useful heuristic for interpretation and potential hypothesis for further study.

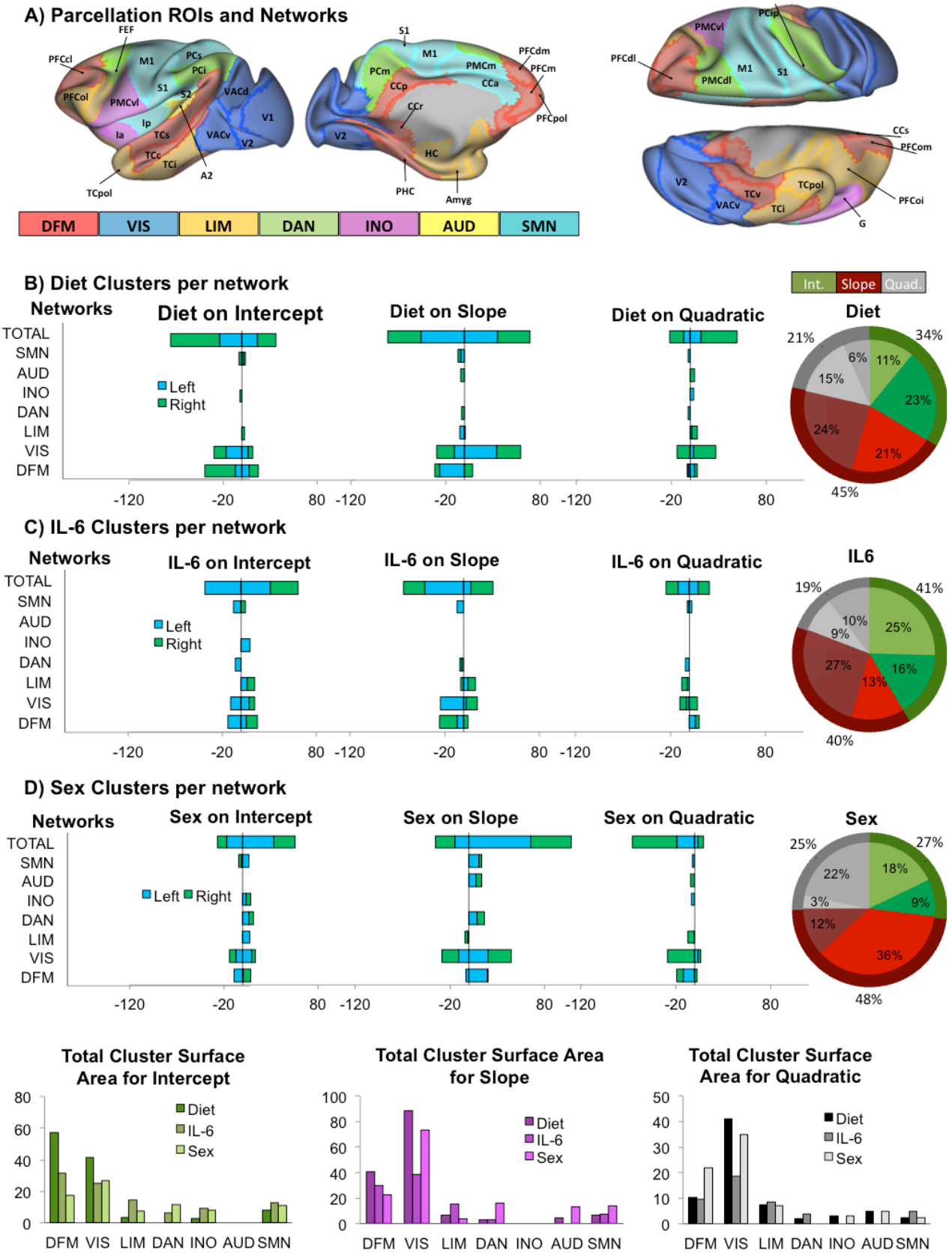

Figure 3.8: Summary results describing the cluster surface area for each predictor. (A) Shows

the functional networks and ROIs (Bezgin et al. 2012; Grayson et al. 2016). (B-D) highlight the surface area of the significant clusters for diet (B) IL-6 (C) and Sex (D). First, they show the significant clusters for the intercept, and where, in relation to the parcellation, these clusters fell, as indicated by the network they are in. The positive direction indicates that the estimates of that cluster were positive (e.g. WSD was associated with thicker cortical thickness at the intercept in the default mode network). This is also shown for the relationship to the slope and intercept. Finally, the pie charts indicate the percent of the surface area of the clusters related to the intercept (green), slope (red) or quadratic (grey), with lighter colors indicating a positive and darker a negative association. Finally, the last panel shows the total surface area (ignoring direction and hemisphere) comparing these across the different predictors.

3.3.6 Mean total brain cortical thickness was not specific enough to relate to the predictors of interest.

Finally, to show that these types of analyses are region-specific and do not just reflect global changes across the brain, mean whole-brain cortical thickness development was modeled in relation to maternal diet, IL-6 and offspring sex. Similar to the individual grayordinate models, first development of average total brain cortical thickness was assessed to determine the unconditional model, before introducing the predictors to establish the conditional model (Figure 3.9, Supp. Table 3.1). A spline model freeing the 11-month time point best described the unconditional mean cortical thickness development ($\chi2$ (5) = 9.20, p = 0.101, CFI = 0.81, TLI = 0.77, RMSEA = 0.13). Introducing the predictors (Maternal Diet, Maternal IL-6 and Offspring Sex) to the model improved the model fit ($\chi2$ (11) = 12.64, p = 0.317, CFI = 0.86, TLI = 0.77, RMSEA =

0.06) but failed to show any significant relationships between the variables IL-6 (Intercept: B=0.024, p=0.281, Slope: B=0.008, p=0.515), diet (Intercept: B=-0.005, p=0.775, Slope: B=0.008, p=0.376), or sex (Intercept: B=0.010, p=0.513, Slope: B=-0.015, p=0.095). These findings are depicted in Figure 3.9 and Supplemental Table 3.1.

As hypothesized, using mean cortical thickness was too crude of a measure and did not capture the complicated nature of how maternal IL-6, diet and offspring sex relate to cortical thickness development. A grayordinate level analysis would allow for specific bidirectional effects depending on the region to surface as opposed to this initial broad analysis.

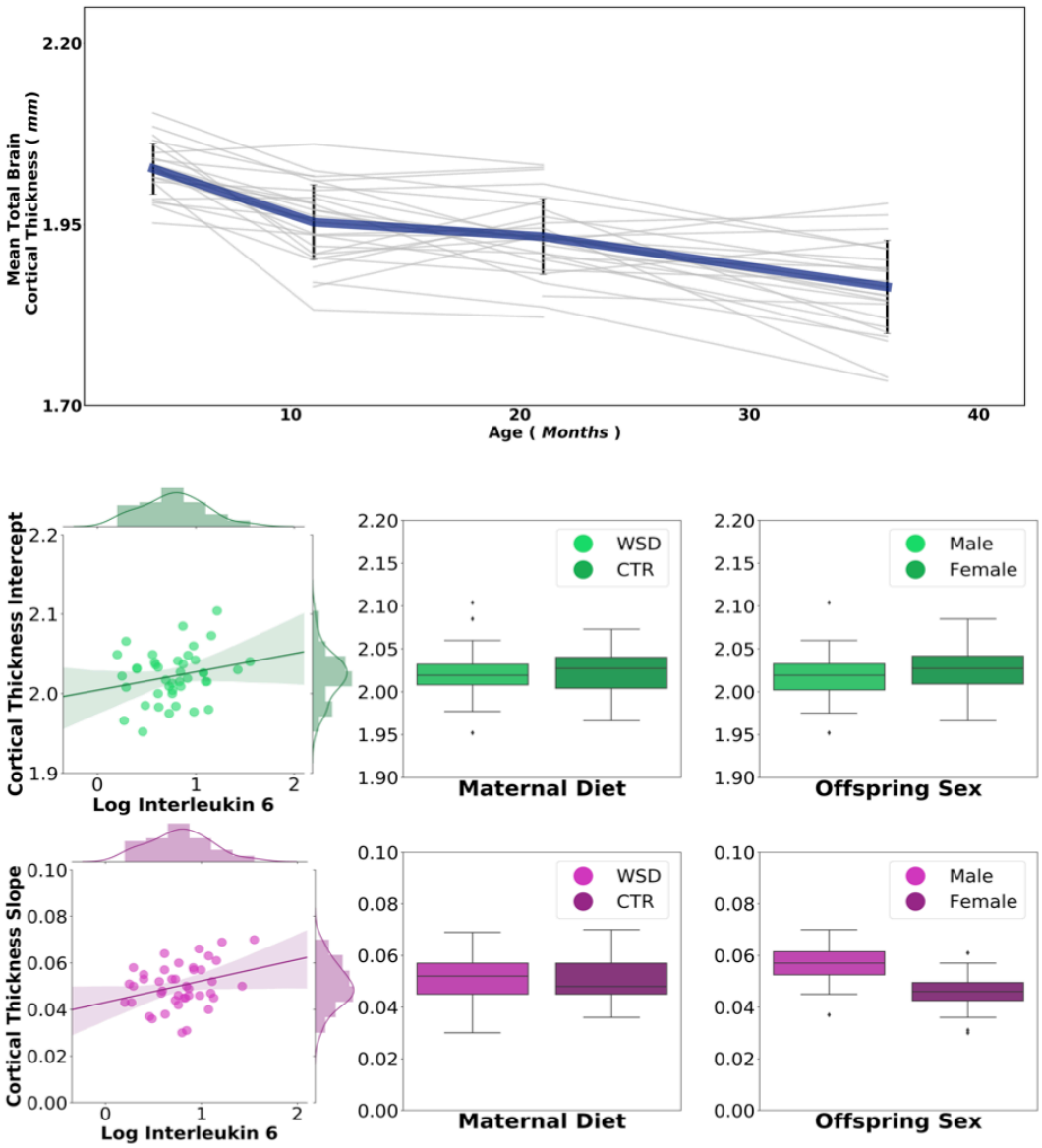

Figure 3.9: Mean total brain cortical thickness. Here total mean cortical thickness development is depicted to show that the relationships observed across the brain are specific to regions and directionality. Running an analysis on total mean cortical thickness, as is often done in the field, misses these more specified findings observed.

3.4 Discussion of Study 2

3.4.1 Overview of findings

Study 2 comprises various noteworthy insights into typical macaque cortical thickness development and its relation to the maternal inflammatory and dietary environment, as well as sex-specific differentiations. Specific growth models were needed to describe developmental trajectories depending on the region of the brain. These models ranged from describing either very little change across time (intercepts only model), continual thinning or thickening (Slope models) or changes in direction or rate of thinning or thickening (quadratic, or spline models) of cortical thickness across the 4, 11, 21 and 36-month-of-age time points. Furthermore, maternal and offspring variables may be associated with potential shifts in developmental trajectories either slowing or speeding up the rate of change or relating to even earlier shifts in development reflected by intercept differences. These relationships to developmental trajectories were unique to each predictor, and also distinctive to specific regions, as seen by the bi-directional beta weight estimates that occurred across the brain and functional forms for variables of interest. Finally, a potential new discovery was visually observed in which significant clusters fell on the edge of regions that had either the thinnest of thickest mean cortical thickness, to begin with. These clusters were observed in regions of change, adjacent to the "focal-point" towards which cortical thickness would change across time in a gradient. This is suggestive of the pattern of development.

3.4.2 Characterizing the best fitting model per grayordinate is a unique method and highlights some interesting patterns regarding the shape of development in a number of regions.

This study design enabled a unique method in characterizing development using the best fitting model per grayordinate. Notable developmental patterns were characterized in several regions through these analyses. For example, the distinct cortical thickness development of the posterior and anterior insula (defined as Ip & Ia in Figure 3.8A) was of interest. The development of these regions was best described with spline models in the central parts of the posterior insula, intercepts only models towards the edge of the anterior insula, and linear models going deeper into the anterior insula (Figure 3.4A). In Figure 3.4B & Figure 3.4C, the maximum cortical thickness starts at 4-months of age (Figure 3.4C dark color) but not all of these grayordinates end up having the minimum cortical thickness at 36-months of age (Figure 3.4B; yellow color). In areas of the insula, where the best fitting model was a spline (Figure 3.3A), the minimum thickness is around 21 or 11 months of age (Figure 3.4B) indicating a change in direction. Additionally, the percent change over time (Figure 3.4) also reflects this trajectory. In general, a decrease in thickness in both the posterior and anterior insula from 4 to 36-months-of-age was observed (Figure 3.4E). However, separating this change between different time points reflects why the best-fitting model was a spline in some areas but a linear or intercepts-only model in others. Initially, from 4-11 months there is a major decrease in thickness in the posterior (predominantly) and parts of the anterior insula (Figure 3.4F). However, from 11-36 (Figure 3.4G&H) there

are increases in thickness in the posterior but not most of the anterior insula. This is once again nicely reflected in the best-fitting models as spline models best describe the central part of the posterior insula development, but then towards the anterior part a linear or intercepts only model best describes this change (Figure 3.3A). Aspects of this developmental characterization may also be important for environmental effects, as maternal diet and IL-6 showed significant clusters around these regions, indicating they may have influenced this type of trajectory.

3.4.3 *Cluster detection seemed to provide in some cases misleading effects.*

As a result of these analyses, we observed an interesting phenomenon. When visually inspecting the typical cortical thickness development across time, multiple focal points could be observed in which the surrounding cortical thickness would change in gradients over time towards these regions. Figure 3.10 highlights one of these regions in the insula.

Surprisingly, a number of the clusters surrounded these focal points rather than falling within the center of the region as one might expect. While at first unexpected, after exploring the data, we speculate this phenomenon could be understood by analogy to glacier melt and accumulation over the years. Glaciers have accumulation and ablation zones, which are known as the edge of the glacier towards the bottom (ablation zone) or the top (accumulation zone) of the glacier. Between these is the equilibrium line-- as one moves further away from the equilibrium line towards the edge, much more rapid and variable accumulation or melting/evaporation of snow/ice is seen over the seasons and years (Anderson et al. 2006).

Analogously, this cluster phenomenon in the brain could be seen in the same light, as the brain is developing, more changes will be experienced on the edge (ablation zone) of the focal point (equilibrium line) of the ROI, explaining why the most differences in predictors were found in these regions. This is illustrated in (Figure 3.10).

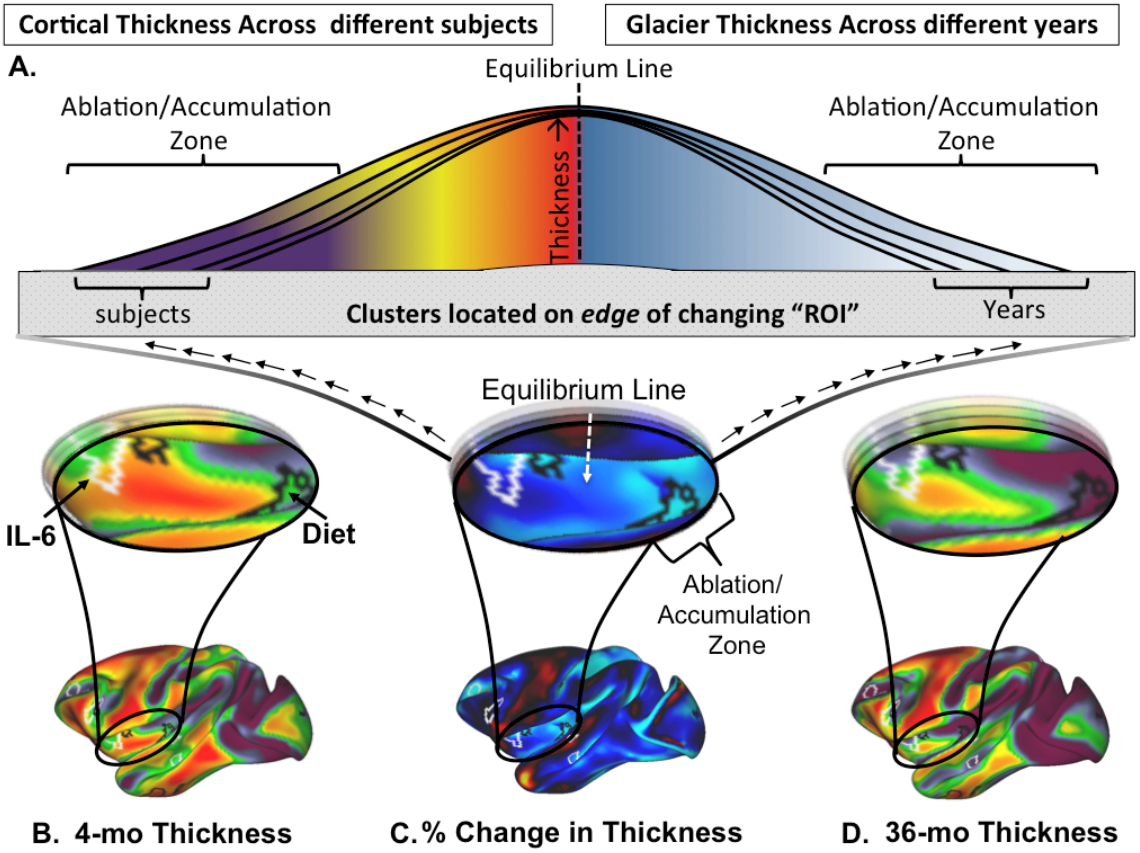

Figure 3.10: Proposed cluster phenomenon analogy schematic. Impressionistically many clusters fall on the edge of focal points where max or min thickness is, rather than at the center. We describe this phenomenon by analogy to glacier melt. Rather than seeing the most change in melting in the center, this occurs on the edges (i.e. the ablation zone). Typical macaque cortical thickness development highlights similarities and differences to the human literature.

These results successfully characterized development, and also mirrored broad growth trends observed in the human literature, lending to the translational value of using a macaque model. Visually inspecting the typical macaque change in thickness overtime highlighted a number of similar patterns to the human literature. For example, the increases observed in thickness of the motor cortex, the temporal pole, the parahippocampus, and some visual regions are also nicely reflected in human literature showing either a comparatively lower rate of thinning or even increased thickening relative to other regions in the brain (Li et al. 2015; Amlien et al. 2016; Walhovd et al. 2016; Tamnes et al. 2017). Furthermore, regions considered to have the most change in cortical thinning over time such as the medial and inferior parietal cortex, the centrolateral/pole of the prefrontal cortex, and the insula all also showed to the most parts similar characteristics to the human literature (Li et al. 2015; Amlien et al. 2016; Walhovd et al. 2016; Tamnes et al. 2017). The insula findings were less conclusive across these four studies, as only Amlien et al., 2016 showed this trend, with the other studies either not showing this data or having mixed trajectories. As the time frame was not the same across these studies, this could relate to some of the disparities. For example, these studies ranged from 0-2 years ((Li et al. 2015), or 4-10+ years of age, which is not directly comparable to the current study.

As few studies cover a similar timeframe as the current study (roughly 1 year through early puberty in human time) direct comparisons especially with different trajectories are difficult. However, a recent study that quantified typical cortical thickness development between the ages of 1 and 6, used a similar approach and found similar findings (Remer et al. 2017). When ordering the percent change in thickness of the 68 (34

per hemisphere) regions they looked at, the regions with the most negative change (decreased thickness) overlapped for the most part with the direction and magnitude of change observed in the current study. Additionally, the regions with the most positive (or least negative) also overlapped with these patterns of change. Furthermore, while this study only used linear, logarithmic and cubic functional forms, there was some overlap in these as well. Naturally, this was not complete, as this study used intercepts-only, slope, quadratic and slope terms, however, in regions they used quadratic or logarithmic functions, there was overlap with the quadratic and spline functions in similar regions (Remer et al. 2017). It would be interesting to see if these trajectories would match up even more if they used similar growth trajectories and an even more similar time window to the current study. This would give us some similarities to typical developmental comparisons, but what about environmental associations with this development?

3.4.4 Diet and inflammation affect regional trajectories in cortical thickness.

Our diet, inflammation and sex findings gave us some interesting insights into how these might relate to typical development and previous human literature. To the best of our knowledge, there has been no research to date investigating the influence of a maternal Western-style diet on cortical thickness development. This likely stems from the fact that it is hard to dissociate diet from obesity and inflammation in a human cohort and rodent models make it hard to study the complex nature of cortical thickness development across multiple time points. Even when looking at more generally related measures such as maternal obesity or inflammation, very little research exists (Gumusoglu and Stevens 2019; Pulli et al. 2019). Multiple studies have linked maternal obesity and inflammatory responses to alterations in the offspring brain (Reviews:

Bergdolt & Dunaevsky, 2019; Guma, Plitman, & Chakravarty, 2019; Gumusoglu & Stevens, 2019; Pulli et al., 2019; Willette et al., 2011). While none of these have investigated cortical thickness, these findings have shown that maternal inflammation can relate to functional networks, the connectivity of specific regions, as well as changes in structural volumes. On a network level, IL-6 has been associated with within network connectivity of the subcortical, dorsal attention, salience, cerebellar, ventral attention, visual, cingulo-opercular and frontoparietal networks, and between network connectivity of the subcortical-cerebellar, visual-dorsal attention and the salience-cingulo-opercular networks (Rudolph et al., 2018). Regarding the connectivity of specific ROIs prior research has related inflammatory markers to increased connectivity of the left and right insula, the dorsal anterior cingulate, and the right and left amygdala (Graham et al., 2017; Spann, Monk, Scheinost, & Peterson, 2018). Furthermore, these studies also showed decreased connectivity of the dorsal anterior cingulate as well as the left and right amygdala (Graham et al., 2017; Spann et al., 2018). Finally, inflammatory markers were also related to increased right amygdala, and ventricular volumes as well as the rate of left amygdala volume growth (Ellman et al., 2010; Graham et al., 2017; Ramirez et al., 2019). With an additional relationship indicating decreased entorhinal cortex, posterior cingulate and left amygdala volumes (Ellman et al., 2010; Ramirez et al., 2019). While these measures do not directly relate to cortical thickness, they do highlight some of the clusters found regarding the insula, the cingulate and some of the networks in which the clusters fall. Future research will need to investigate these relationships further, however, the current findings show regions that could be targeted for these types of studies.

3.4.5 Sex-specific findings also relate to sex-specific results in the literature.

Sex differences in cortical thickness development have been heavily studied (Raznahan et al. 2011; Lyall et al. 2015; Vijayakumar et al. 2016; Gennatas et al. 2017). Sex differences observed in this study match up to current literature in humans (Amlien et al. 2016; Gennatas et al. 2017). The current studies macaque timeline of 4 to 36-months of age, roughly translates to 1 year through early puberty in humans, generally speaking. However, individual processes may be expedited or delayed depending on the developmental species dependent function and anatomy. For example, interspecies cortical expansion is lower in the occipital and temporal regions between macaque and human development, with the interspecies expansion maps correlating more strongly during early (4-10yrs) than late (17-30yrs) development (Amlien et al. 2016). The current data showed that males predominantly had thicker occipital cortical thickness starting points (intercept) but then in general increased rate of cortical thinning over time (slope). This occipital trend heuristically matches up with developmental findings showing increased male thickness in early ages (up until around 15 years), with decreased cortical thickness in males later in life (up until early adulthood) (Gennatas et al. 2017). Parietal cortices were also in general thicker in males than females, with decreased frontal thickness in males compared to females (Gennatas et al. 2017). It is important to note, that the macaque and human studies do not match in terms of homologous developmental timelines. This is a limitation as a result of no studies existing in the human literature that investigate sex differences in cortical thickness from 1 year to early puberty. Despite this limitation, it is reassuring to see that the general trends observed in the human literature match up to the most part with the current findings.

3.4.6 Limitations

While we believe these findings are informative and valuable, some considerations regarding what was reported need to be taken into consideration when interpreting these results. The sample size of this study was much smaller than the typical sample sizes observed in human literature. However, only a small number of longitudinal infant monkey MRI studies exist because these data are exceptionally rare and hard to attain with only seven primate research centers funded by the NIH existing in the United States. Nonetheless, running these types of growth models is still difficult with small sample sizes, as including multiple covariates to the model can cause the model to not converge or produce other statistical warnings. For this reason, only hypothesized variables of interest; maternal diet, maternal IL-6, and offspring sex were chosen to include the analysis, as including other factors, may have decreased the usable models. Notably, there were no significant differences between the sex (male & female) and diet (WSD & CTR) subjects for potential covariates such as post-weaning diet (diet p=0.68; sex p=0.21) or maternal percent body fat (diet p=0.98; sex p=0.33). Regardless, these factors and the inclusion of other inflammatory cytokines or glucose/insulin levels would be important to explore in future studies as they may all independently relate to different facets of neurodevelopment. With the variables considered in this study and the use of the Mplus statistical software, this study was able to only use statistically trustworthy models by filtering out models that contained warning messages in the output. This is often missed when using other software, as issues can still exist in a model that ran successfully. Hence it is good practice to look at the model fit parameters and also identify warning issues such as instances of having a negative residual variance, a greater

than 1 correlation or linear dependencies between variables to know you are running a trustworthy model. Of note, a considerable portion of the subjects did not have data for all time points as a result of the longitudinal design and difficult to attain species. However, this is common in longitudinal designs and the use of the full information maximum likelihood estimator has been addressed extensively in prior literature (Collins et al. 2001; Enders 2001; Graham 2003; Raykov 2005; Buhi 2008; Jeličić et al. 2009; Schlomer et al. 2010; Larsen 2011; Peyre et al. 2011; Gustavson et al. 2012). Finally, in some cases, findings are reported in the light of which functional network they fall into. The author is aware that differences in cortical thickness do not necessarily mandate differences in functional connectivity, however, this was merely done to identify regions that future studies could investigate these relationships in. It would be interesting to see in future studies if these clusters could be used to relate to offspring functional connectivity and behavioral outcomes.

3.4.7 Conclusions

Findings from this report improve our understanding of typical macaque cortical development and how maternal inflammatory and dietary factors may relate to these trajectories. These results help show the validity of using a macaque model to study cortical development and capitalize on the importance of a controlled experimental design when studying maternal factors such as diet. Not only do the developmental trajectories make sense, and mimic typical human development, but the current experimental findings also were consistent showing bilateral clusters in expected regions. While at first surprising, the cluster results in combination with developmental trajectories helped shed light on an interesting pattern suggesting that these clusters are

determined on the edge of change in thickness over time towards a focal point. While other risk factors undoubtedly contribute to aspects of cortical thickness development, these findings highlight some interesting regions and relationships that could be further investigated in future studies. The current findings come at a critical time with the vast increases in obesity and stress rates, in combination with increased consumption of a Western-style diet.

3.5 Supplemental Materials of Study 2

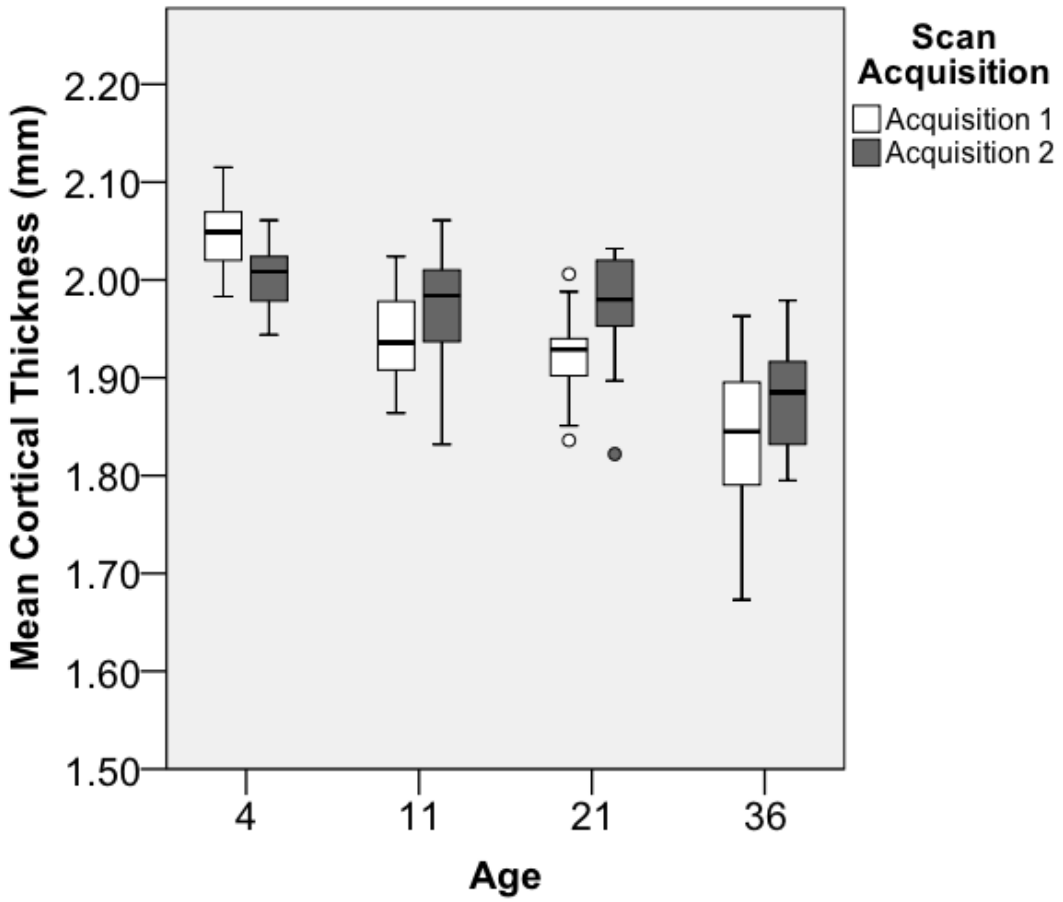

Supplemental Figure 3.5: Comparing the scan acquisition across age, to show they were not significantly different.

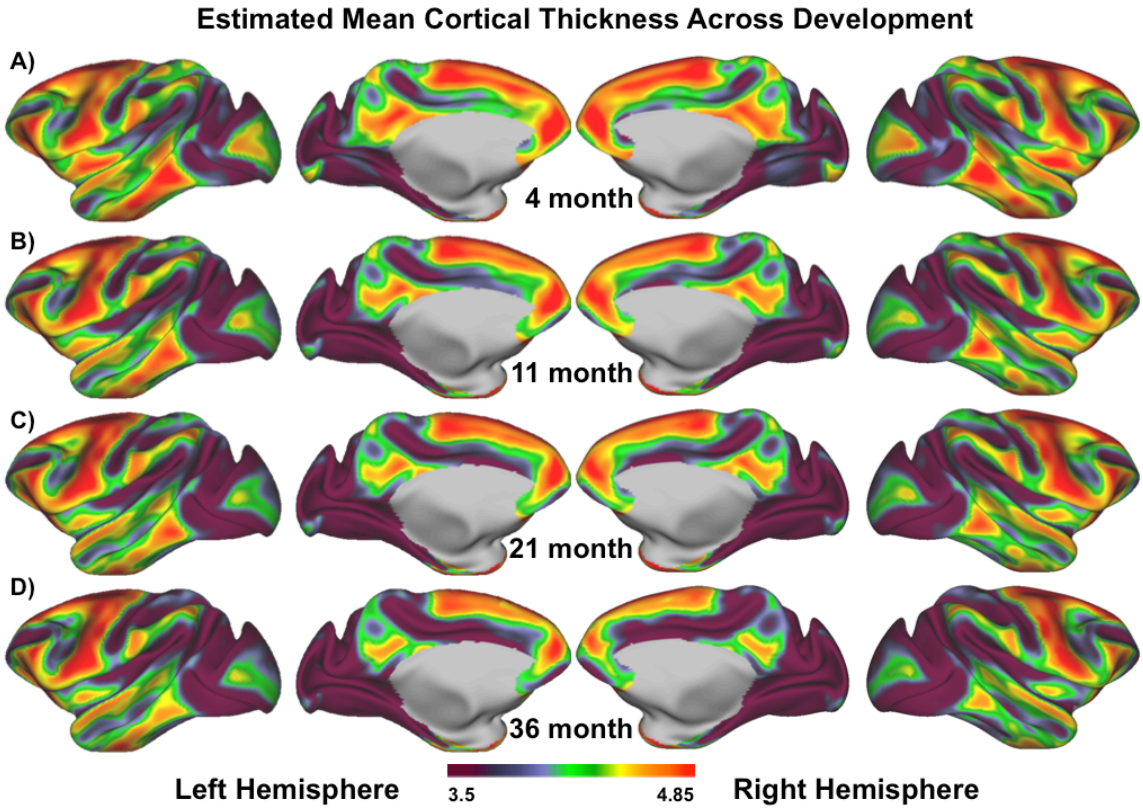

Supplemental Figure 3.6 Both hemispheres of mean cortical thickness

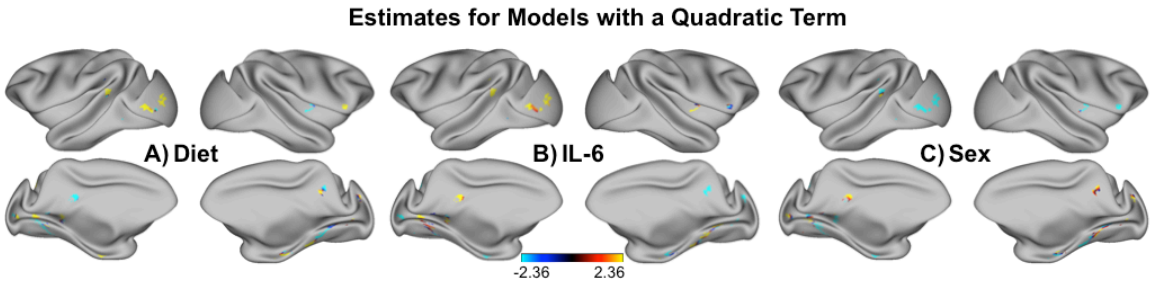

Supplemental Figure 3.7: Shows the estimates for the quadratic term for maternal diet (A), maternal IL-6 (B) and offspring sex (C). As the majority of grayordinates were not described by a best-fitting quadratic trajectory (Figure 3.3), only a few regions contain this quadratic estimate.

Supplemental Table 3.1: Model statistics for average total brain cortical thickness

	Unconditional Model		Conditional Model	
Parameter	Estimate	S.E.	Estimate	S.E.
Intercept Mean	*** 2.019	0.007	***2.001	0.020
Intercept Variance	***0.002	<0.001	**0.001	<0.001
Slope Mean	***0.051	0.005	***0.047	0.012
Slope Variance	<0.001	<0.001	<0.001	<0.001
Intercept & Slope Covariance	<0.001	<0.001	<0.001	<0.001
Predictors of Intercept				
Interleukin-6	N/A	N/A	0.024	0.022
Maternal Diet	N/A	N/A	-0.005	0.017
Offspring Sex	N/A	N/A	0.010	0.016
Predictors of Slope				
Interleukin-6	N/A	N/A	0.008	0.012
Maternal Diet	N/A	N/A	0.008	0.009
Offspring Sex	N/A	N/A	ł -0.015	0.009

Note: ł= p <.10; *p<.05; **p<.01;***p<.001. N/A *indicates covariates not included in the final model*

Chapter 4: Study 3: A Cross-Species Translational Study: Predicting human maternal IL-6 from monkey offspring functional brain connectivity.

4.1 Introduction of Study 3

Study 2 investigated differences in offspring cortical thickness in relation to the maternal environment. Results from the cortical thickness associations were ultimately displayed on top of a functional parcellation to identify heuristic trends in terms of what functional networks overlapped with the cortical thickness clusters of study 2. While these observations did not contribute conclusive information about functional relationships to the maternal environment, they did highlight that functional networks may be of interest when studying maternal-offspring brain development relationships. Hence, study 3 investigated how offspring functional connectivity can be used to make inferences about the maternal environment, and also asks if these results can be translated across species.

A growing number of animal and human studies have linked maternal inflammation to adverse offspring outcomes (Estes and McAllister 2016; Careaga et al. 2017; Bergdolt and Dunaevsky 2019; Dunn et al. 2019; Guma et al. 2019; Gumusoglu and Stevens 2019). These studies are centered on the idea that maternal inflammation interferes with developmental programming during a critical period of in-utero development, a period during which the fetus is especially vulnerable (Entringer 2007; Bale et al. 2010; Kwon and Kim 2017; DeCapo et al. 2019). During this period, external stimuli such as maternal inflammation and nutrition, for example, may influence brain development and subsequent developmental trajectories. These findings are supported by

increasing evidence linking maternal inflammation to neurodevelopmental disorders such as attention deficit hyperactivity disorder (ADHD) (Dunn et al. 2019), autism spectrum disorder (ASD)(Parker-Athill and Tan 2010; Careaga et al. 2017; Guma et al. 2019) and schizophrenia (SCZ) (Estes and McAllister 2016; Scola and Duong 2017; Guma et al. 2019). Animal and human studies suggest that maternal inflammation interferes with specific behavioral and/neuronal characteristics, represented in these disorders (Graham et al. 2018; Rasmussen et al. 2018; Rudolph et al. 2018; Thompson, Gustafsson, DeCapo, et al. 2018; Ramirez et al. 2019).

While human and animal studies have made a number of valuable discoveries regarding the relationship between maternal inflammation and offspring brain development, no studies address this relationship in a truly translational manner. Human studies are often conducted under experimental settings that are difficult to control, while most animal models (especially rodents), often do not capture the complexity of human behavior, brain structure, and function. Non-human primates (NHP) offer a unique middle ground between the benefits imbued by the more traditional animal models, and the unique similarities to humans regarding brain structure and function (Orban et al. 2004; Hutchison and Everling 2012; Gottlieb and Capitanio 2013; Miranda-Dominguez, Mills, Carpenter, et al. 2014; Miranda-Dominguez, Mills, Grayson, et al. 2014; Grayson et al. 2016; Casimo et al. 2017; Xu et al. 2018; Xu, Nenning, et al. 2019; Xu, Sturgeon, Ramirez, Froudist-Walsh, Margulies, Schroeder, Fair, et al. 2019b). In particular with regards to neurodevelopment, it is advantageous that NHPs have a similar gestational period to humans (Sullivan and Kievit 2016). Having a way to study and directly compare humans to animal model research, and vice versa would be tremendously

beneficial for dissociating the similarities and differences across these studies. Non-invasive MRI now provides an avenue to this end.

MRI is a useful non-invasive tool that allows the characterization of resting-state brain function in animal and human models. Moreover, MRI studies conducted in rodent, NHPs, and humans reveal that core features in functional connectivity are maintained in large-scale network topology (Miranda-Dominguez, Mills, Grayson, et al. 2014; Stafford et al. 2014; Grayson et al. 2016; Xu, Nenning, et al. 2019). As a result of these studies brain surfaces can be aligned and deformed across species using well-documented cross-species landmarks, joint embedding methods and Multimodal Surface Matching (MSM) (Van Essen 2005; Miranda-Dominguez, Mills, Grayson, et al. 2014; Robinson et al. 2014; Nenning et al. 2017; Xu, Nenning, et al. 2019). These methodological advancements make it feasible to map pre-defined cortical parcellations in NHPs to humans allowing for the comparisons across-species in the same space.

Previous findings in humans have shown that infant resting-state functional network connectivity can be used to make inferences about levels of maternal interleukin-6, a pro-inflammatory cytokine. The present study used these large-scale functional networks in combination with machine learning techniques to make inferences about the maternal environment. Between and within-network connectivity patterns were shown to be most predictive of maternal IL-6 by training a model in a subset of subjects and testing it on the remaining subjects for accuracy.

Here study 3 aims to 1) replicate these findings in a non-human primate model and 2) cross-validate these findings across species in a human cohort using a macaque-to-human registered network parcellation. These findings will help bridge the gap in

translational research by using insights gained in one species to predict the outcome of another species.

4.2 Materials and Methods of Study 3

4.2.1 Study Overview

The current study utilized subjects from two distinct populations 1) Japanese Macaques (same as in Study 1 and 2) and 2) Human infants collected by the Buss Laboratory at the University of California Irvine. Both data sets obtained infant resting-state functional connectivity MRI's and collected maternal interleukin-6 (IL-6) data during pregnancy.

4.2.2 Subjects

Japanese Macaques: To ease readability and coherence, some methods are restated from study 1 & 2 although the animals are the same. The first population consisted of 4-month old Japanese Macaque Infants from a thoroughly validated NHP model investigating how a maternal Western-style diet (WSD) *(TAD Primate Diet no. 5LOP, Test Diet, Purina Mills)* or control diet (CTR) *(Monkey Diet no. 5000; Purina Mills)* may relate to changes in offspring brain and behavioral development (McCurdy et al. 2009; Sullivan et al. 2010, 2012, 2017; Comstock et al. 2013; Thompson et al. 2017; Ramirez et al. 2019). Offspring lived with their mothers until weaning (~8-months) and were peer social housed with 6-10 juvenile and 1-2 unrelated female adults. Rearing and diet characteristics have been described in more detail in a previous report (Thompson et al. 2017). A total of 32 (Female n=14; CTR n =17) 4-month old Japanese macaques were included in this study. Procedures and methods for this study have been approved by the Oregon National Primate Research Center (ONPRC) Institutional Animal Care and Use

Committee and follow the guidelines on ethical use of animals implemented by the National Institutes of Health (NIH).

Human Infants: The infant subject cohort (Subjects included: N = 90; M = 26.33 ± 12.69 days; Female n=45) consisted of an ongoing established longitudinal study by Dr. Claudia Buss' Laboratory at University of California Irvine in which mothers were recruited during their first trimester of pregnancy. Details on this cohort have previously been published (Graham et al. 2018, 2019; Rasmussen et al. 2018; Rudolph et al. 2018; Thomas et al. 2019). In brief, mothers were excluded in cases of, maternal use of psychotropic medication, corticosteroids, and alcohol or drug use during pregnancy. Further exclusionary criteria were based on having a known genetic, congenital, or neurologic disorder in the fetus (e.g. fragile X or Down syndrome) or having been birthed prior to 34 weeks of gestation. All procedures and methods were approved by the Institutional Review Board at the University of California, Irvine and Oregon Health & Science University, and were in compliance with NIH ethical regulations and standards.

4.2.3 Maternal IL-6 collection

Japanese Macaques: During the third trimester of pregnancy, maternal plasma IL-6 concentrations were collected. A 1.23 pg/mL threshold was used for the lower limit of quantification (LLOQ) and excluded subjects under this threshold which resulted in 32 (Female n = 14; CTR n = 17) subject. IL-6 levels were normalized, and box cox transformed (using the Boxcox function in MATLAB). Plasma IL-6 collection methods have been described in more detail in a prior publication (Thompson, Gustafsson, Decapo, & Takahashi, 2018).

Human Infants: Maternal IL-6 came from three blood samples collected during early, middle and late pregnancy, and averaged for this study. Blood was collected in serum tubes (BD Vacutainer) and allowed to clot at room temperature for 30 minutes. Samples were then centrifuged at 4 °C at 1,500 g and stored at -80 °C. A commercial ELISA (eBioscience) was used to determine IL-6 concentrations, with a sensitivity of 0.03 pg/ml.

4.2.4 MRI acquisition

Macaque acquisition: As described in the prior studies, a Siemens TIM Trio 3.0 Tesla Scanner with a monkey-adapted 15-channel knee coil was used to acquire the MRI scans. Scan occurred at 4-months (M = 133.78 ± 4.96 days). A single dose of ketamine (10-15mg/kg) was administered for intubation, after which macaques were maintained on <1.5% isoflurane anesthesia and monitored on heart rate, respiration, and peripheral oxygen saturation. The structural scan acquisition protocol was adjusted partway through the study. A total of N= 20 subjects were scanned using scan acquisition #1 with the rest (N=12) having acquisition #2. Naturally this is considered a limitation, however, as only the structural scans were updated, the author believes this related to negligible differences in the resting-state functional outputs. For both acquisitions four T1-weighted anatomical images were acquired (Acquisition #1: TE= 3.86 ms, TR= 2500 ms, TI= 1100 ms, flip angle= 12°, 0.5 mm isotropic voxel & Acquisition #2: TE= 3.33 ms, TR= 2600 ms, TI= 900 ms, flip angle= 8°, 0.5 mm isotropic voxel). One T2-weighted anatomical image was acquired for both acquisitions (Acquisition #1: TE= 95 ms, TR= 10240 ms, flip angle= 150°, 0.5 mm isotropic voxel & Acquisition #2: TE= 407 ms, TR= 3200 ms, 0.5 mm isotropic voxel). A 30-minute resting-state blood oxygen level-dependent (BOLD) scan

was acquired 45-minutes after the initial ketamine injection, and utilized a gradient echoplanar imaging (EPI) sequence (TR = 2070 ms, TE = 25 ms, FA = 90°, 1.5 mm^3 voxels, 32 slices with interleaved acquisition, FOV = 96 × 96 mm). Field maps (TR = 450 ms, TE = 5.19 ms/7.65 ms, FA = 60°, 1.25 × 1.25 × 2 mm^3 voxels, 40 slices, FOV = 120 × 120 mm) for acquisition #1 and a reverse EPI sequence for the acquisition #2 scans were used for distortion correction when preprocessing the data.

Human acquisition: Human infant scans were acquired ~4 weeks after birth (M = 3.79 weeks, s.d. = 1.84) on a 3.0 Tesla Siemens TIM Trio scanner. Subjects were swaddled and scan noise was reduced via fitted ear protection to allow for infants to sleep for the duration of the scan. Respiration and waking periods were monitored throughout. A T1-weighted (MPRAGE TR=2,400 ms, inversion time = 1,200 ms, echo time = 3.16 ms, flip angle = 8°, resolution = 1 × 1 × 1 mm, 6.18 min) and T2-weighted (TR = 3,200 ms, echo time = 255 ms, resolution = 1 × 1 × 1 mm, 4.18 min) structural scans were acquired. Resting-state functional scans were collected using an EPI gradient sequence sensitive to BOLD contrast (TR = 2,000 ms, TE = 30 ms, FOV = 220 × 220 × 160 mm, flip angle = 77°, ~195 volumes). Axial slices (4-mm) were collected with a 1-mm ascending-interleaved skip, dropping the first 4 frames.

4.2.5 MRI preprocessing

Macaque preprocessing: A macaque specific modified version of the Human Connectome Project (HCP) preprocessing pipeline (Glasser et al. 2013) was used for processing these data. These procedures have previously been used and described (Xu et al. 2018; Ramirez et al. 2019; Xu, Sturgeon, Ramirez, Froudist-Walsh, Margulies, Schroeder, Fair, et al. 2019b). The Structural aspects of this pipeline have been described

in the Methods sections of Study 1 and 2 (p.33 & p.70), so only functional procedures are explained here.

For functional data, the pipeline used a 6-degrees of freedom linear registration to register the EPI data to the first volume, while correcting for field distortions using FSL's TOPUP (Acquisition #1) or Fieldmap phase and magnitude (Acquisition #2) images. The average EPI volume was registered to the T1w volume, and the combined registration matrices of each step are applied for each frame in a single transform (i.e. only one interpolation).

Time-courses were constrained by the gray matter segmentations and mapped into the yerkes19 standard space of 56522 surface anchor points (grayordinates). This procedure accounts for partial voluming as it limits the influence of volumetric voxels overlapping in gray and non-gray matter voxels (e.g. pial surface, white matter, vessels, ventricles).

For motion censoring, the absolute value of the backward-difference for all translation and rotation measures, using a brain radius of 30 mm was summed for a measure of overall framewise displacement (FD). Volumes FD>0.2 mm were excluded as well as frames that had less than five contiguous frames below this threshold. These motion correction procedures have been previously validated in the field (Fair et al. 2012; Power et al. 2012, 2014).

Trained raters conducted a rigorous quality control assessment on processed MRI outputs. A scale of 1(good) to 3 (bad) was used to assess the quality of outputs based on images registration, surface delineations, ringing artifacts, abnormal warping of the brain, excessive blurriness, etc.

Human preprocessing: A similar procedure to the macaques was devised for processing of the data. Similarly, the HCP pipeline was modified for the use of human infant scans. A modified version of the HCP pipeline has been previously described in the literature (Marek et al. 2019). A major difference in processing procedure is the use of registering the subject data to the MNI Infant Atlas. Similarly, the final standard space for surface anchor points was 91,282 as opposed to 56,522 in the macaques. However, in general, the preprocessing procedures for the macaques did not differ significantly from the human infants.

4.2.6 Deformation of macaque parcellations to human space

One of the major innovations utilized in this study was the ability to utilize the deformation of the macaque parcellations in human space. This method was recently published in bioRxiv (Xu, Nenning, et al. 2019) and uses a functional-based method joint-embedding to align cortical surfaces across species. Joint-embedding extracts like dimensions of functional organization that are common across these two species which determines a mutual coordinate space. This approach is an extension of a previously characterized embedding approach "connectopies" (Langs et al. 2010; Margulies et al. 2016; Nenning et al. 2017; Haak et al. 2018), but instead of calculating spectral embeddings for each species, here the embedding is applied to a joint similarity matrix (Xu, Nenning, et al. 2019). Functional connectivity shared between species is represented as components. The top 200 components (referred to as gradients) matched for both species represent a feature in the embedding axis of the joint-embedding space. Multimodal Surface Matching (MSM) was used to register the surfaces between the two

species using the top 15 gradients as functional mesh features (Robinson et al. 2014; Nenning et al. 2017). This surface deformation was then applied to the previously validated macaque functional network parcellations (Bezgin et al. 2012; Grayson et al. 2016) to register this parcellation into human space. This enabled us to investigate the connectivity of each of the 82 regions of interest (ROIs) in macaque and human space alike. Functional connectivity matrices can then be made for the macaques and humans for use in the cross-species cross-validation analysis (Figure 4.1).

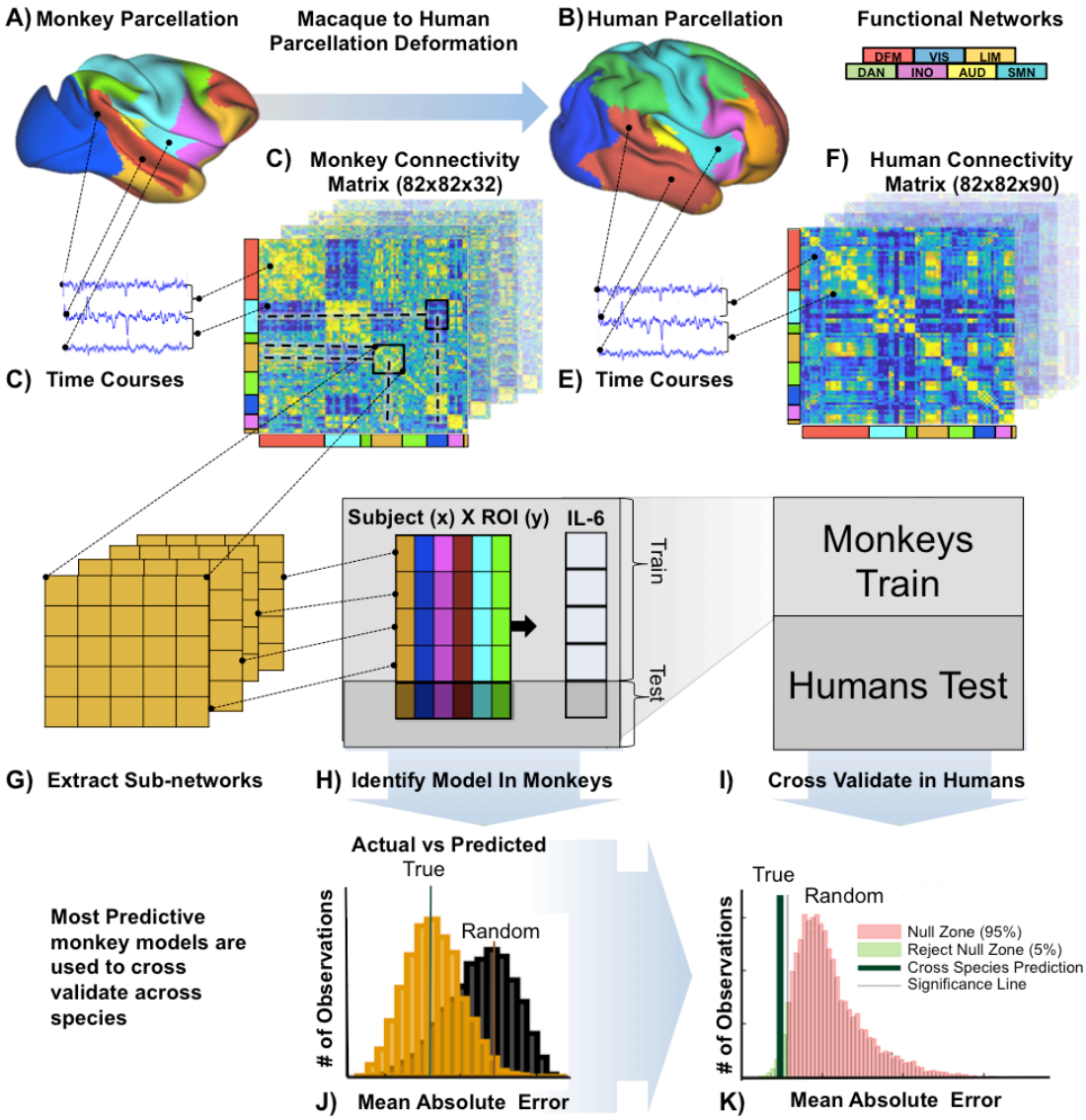

Figure 4.1: Methods overview. Macaque parcellation (A) is deformed to human space (B). Time courses (C) can be extracted from the macaques to make a connectivity matrix (D). Similarly, for humans (E-F). Sub-networks can bet extracted from these matrices (G) and within and between network connectivity is used to make inferences about subject levels of maternal IL-6 using partial least squares regression in the monkeys. This is done using the top 75% of subjects to train the model, and then test it in the remaining 25%, and comparing

how well this model does to a null curve. Best models are extracted (J) and used for the next translational step. Instead of cross-validating models in the monkeys, now the entire monkey data set was used for training, and tested it in the humans, to make inferences across species (I). With this, it can be identified if the monkey model significantly predicted human maternal IL-6 concentrations (K).

4.2.7 General analysis overview

This study used partial least squared regression (PLSR) to 1) use macaque connectivity to make inferences about macaque maternal IL-6 concentrations and 2) use the most predictive macaque models to train the data in macaques and cross-validate them in the humans as a test set to see if macaque models translate across species. PLSR procedures were conducted in MATLAB 2019 and have previously been described using human subjects (Rudolph et al. 2018). In brief, PLSR is a multivariate machine learning method that reduces multiple correlated features into uncorrelated orthogonal components. PLSR uses singular value decomposition (SVD) to maximize the covariance (prediction) between the outcome variable (y) it is trying to predict (i.e. maternal IL-6) and the predictor (x) variables (i.e. connections) by limiting the covariance between the predictor (x) variables (Abdi and Williams 2013). The predictor (x) consists of a structure containing the number of connections (columns)-by- the number of participants (rows) within a given between- or within-network functional matrix. The outcome of interest (y) is a one-dimensional vector with the mean IL-6 concentration for each participant. This study ran the prediction across a number of components and percent holdout to identify the model parameters that gave the most consistent and reliable across different states to then later use for the cross-species test. A step-by-step overview of how we combined

resting-state functional connectivity MRI (rs-fcMRI), random resampling, PLSR, and the cross-species validation can be seen in Figure 4.1.

4.2.8 Using partial least squares regression in NHPs to make inferences about maternal IL-6.

The functional time-courses representing regional activation for each of the 82 ROIs defined by the parcellation were used. These were cross-correlated to determine a functional connectivity matrix for each subject (ROI x ROI x Subject). Individual sub-networks were extracted for each of the seven networks of the parcellation assessing 1) within and 2) between network connectivity. The connectivity between ROIs for a given within- or between-network matrix were used as features in the PLSR to estimate mean maternal IL-6. This study used a repeated (k-10,000) hold-out resampling procedure where the data are partitioned into multiple training (75% of subjects) and test (25%) sets. For each of the iterations (k), the absolute error between the actual maternal IL-6 concentration and the predicted concentration from the training set were calculated. This resulted in a distribution of absolute errors, which can be tested for significance against a null distribution acquired by randomly shuffling the actual IL-6 values for each of the iterations.

4.2.9 Translating top models across species to make inferences about human maternal IL-6 using macaque derived models.

After running the analysis on the macaques to determine the parameters to use for the cross-species validation, and also determine which between- and within- network models to use for the prediction, the current study aimed to translate across species, by training the data in all of the macaque data (100%) k=1, and then testing it in the human

data. The test prediction absolute error is then compared to a null distribution derived by shuffling the human maternal IL-6 variables and running this prediction 10,000 times to identify chance. If the actual prediction falls is below chance, the null hypothesis can be rejected concluding that the cross-species prediction has a high probability of being accurate.

4.3 Results of Study 3

4.3.1 Estimating mean macaque maternal IL-6 concentrations from offspring functional connectivity

The current study identified significant relationships between macaque offspring functional connectivity and third trimester maternal IL-6 concentrations using seven previously validated functional networks (Bezgin et al. 2012; Grayson et al. 2016). Offspring-maternal associations were estimated from 1) within and 2) between network connectivity models.

The most likely models linked to maternal IL-6 were selected if they passed statistical significance and a medium effect size threshold. This identified a number of within and between network-IL-6 associations (number of observations) in the INO (2), AUD (2), LIM (2) and DAN (1) networks. The AUD-DAN network connectivity was the most predictive of maternal IL-6 (Cohen's d=1.59), followed by, AUD-INO (Cohen's d=1.08), AUD-AUD (Cohen's d=0.73), INO- LIM (Cohen's d=0.70), and DAN-LIM (Cohen's d=0.53) networks (Figure 4.2). Interestingly, these findings nicely replicate the prior findings in humans, which predominantly highlighted the salience, subcortical and dorsal attention networks in human infants (Rudolph et al., 2018).

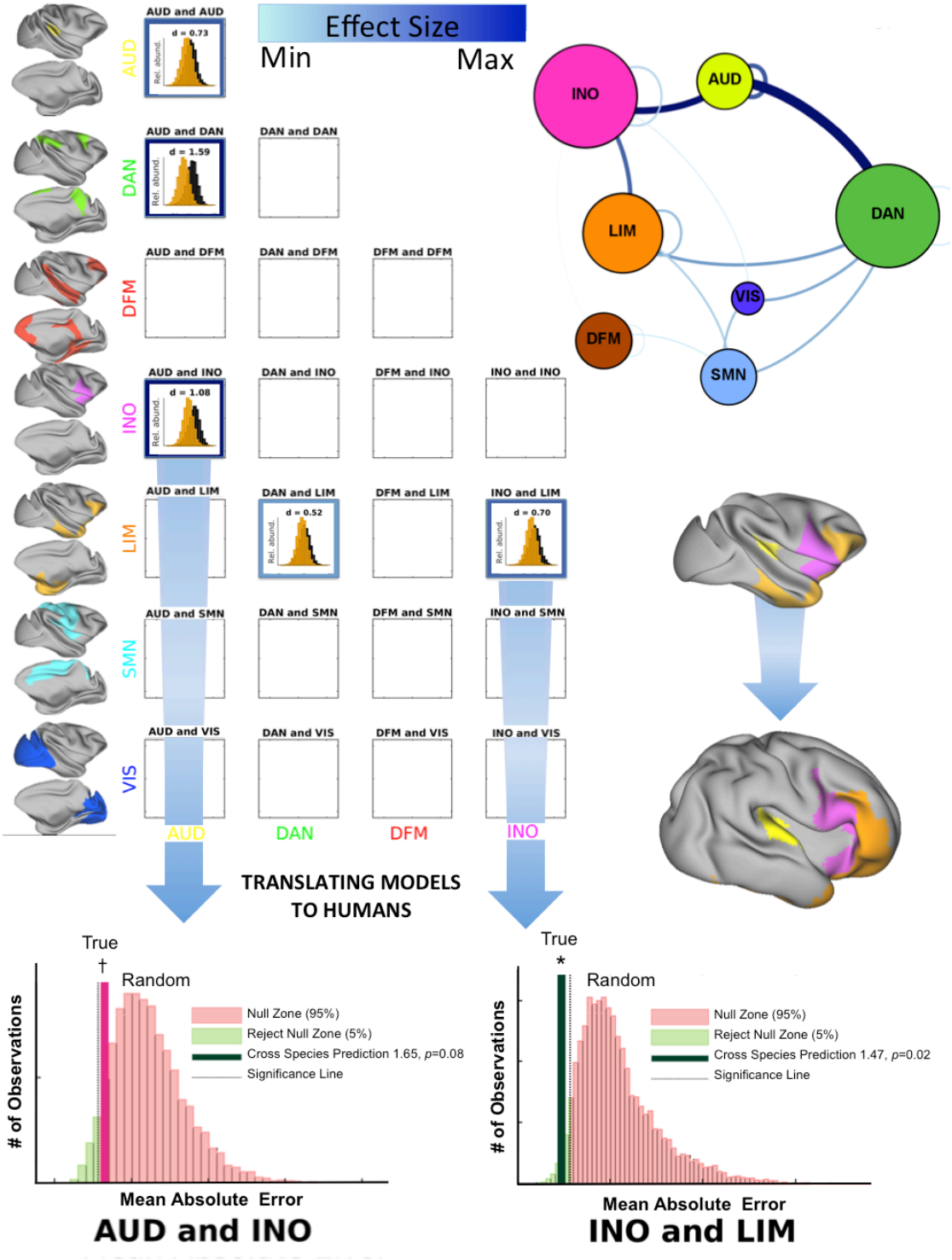

Figure 4.2 Macaque connectivity predicts maternal IL-6 and top macaque models translate to humans. The topmost predictive models in the macaque replication show

within and between connectivity. The effect size of this prediction is seen in the color around the boxes, but also in the bubbles. The bigger the bubble, the bigger the association with maternal IL-6. When testing these models in humans, only the INO and LIM model significantly predicted across-species, with a trend (p=0.08) in the AUD-INO model.

4.3.2 Most predictive models in macaques can be used to make inferences about the human maternal IL-6.

Out of the five most predictive models determined in the monkeys, one model, the INO-LIM network connectivity translated across species and was significantly associated with human maternal IL-6 (Mean Absolute Error = 1.47, p=0.02). Additionally, the second most predictive model the AUD-INO network trended towards predicting across species (Mean Absolute Error = 1.65, p=0.08). The other models AUD-DAN, AUD-AUD, DAN-LIM did not significantly translate across species.

4.4 Discussion of Study 3

4.4.1 Overview of findings

This study determined the best models in macaques which were later tested in the human population. Five within- or between-network models were above the chosen threshold of a medium effect size (Cohen's > 0.5). After successfully deforming the macaque parcellation to align to human space the best models determined in the monkey population could be used to make predictions about human infant maternal IL-6. Remarkably, one (INO-LIM) of the top five models determined in the macaques successfully translated across species above chance, with another (AUD-INO) trending towards significance. These findings highlight that there is some information that

translates across species, which can be used to make inferences in humans from macaque-derived models. This is an important first step towards making translational research across species more reliable and applicable.

4.4.2 Top predictive models in macaques nicely replicate aspects of previous findings in humans.

The top five within/between-network functional connectivity models in the macaque prediction replicated aspects of the previous findings in humans. These networks were the AUD-DAN, AUD-INO, AUD-AUD, INO- LIM, and DAN-LIM networks in the present study. These findings nicely replicate aspects of previous work which showed that the subcortical, salience and dorsal attention networks had the strongest relationship to maternal IL-6 (Rudolph et al. 2018). As these studies used different parcellation schemes containing different networks, it is hard to make direct comparisons. However, it is still promising to see that the networks contributing the most predictive association in monkeys such as the dorsal attention, the insular-opercular and the limbic networks all contained regions within these networks that overlapped nicely with the top models in the human study. Even though the dorsal attention network did not directly translate across species, it was still promising to see that this network was prominent in both the human and macaque findings.

4.4.3 The top cross-species translational model (INO-LIM) makes conceptual sense based on prior findings in the literature.

Of the networks that did translate from macaques to humans, the insular-opercular with limbic (INO-LIM) network connectivity was the most likely candidate to link brain connectivity with maternal IL-6 across species. This is a promising finding since prior

work in humans showed a relationship between maternal IL-6 to infant amygdala volumes and functional connectivity from the amygdala to the anterior insula and the fusiform gyrus (Graham et al. 2018). This is relevant, as both the amygdala (LIM) and the insula (INO) were part of the most predictive cross-species models. Additionally, in macaques, study 1 indirectly linked maternal IL-6 to anxiety-like behavior via amygdala volumes (Ramirez et al. 2019). Remarkably, it has been shown in humans that amygdala-insula connectivity could be linked to future infant fear development from 6-24 months of age. Furthermore, these relationships may even last into adulthood as recent work has also related the resting-state functional connectivity of the insular-opercular network to anxious personality traits in young adult humans (Markett et al. 2016).

4.4.4 Parcellations and networks

This study utilized the Bezgin Regional Map parcellation (Bezgin et al. 2012) which contained monkey specific ROIs, as well as functional networks defined in monkeys (Grayson et al. 2016). This parcellation contained seven functional networks, which were used to translate across species. While not all of the top models translated across species, it is important to note that more functional networks have been defined in the human population as opposed to monkeys. For example, the Power 264 parcellation (Power et al. 2011) used in the Rudolph et al., paper (Rudolph et al. 2018) to make similar predictions in humans contained ten networks and 264 ROIs as opposed to the 7 networks and 82 ROIs in macaques. Naturally, there will be some discrepancy in the strength of the monkey networks mapped onto the humans, even if the ROIs were matched correctly. Hence, these findings are very promising as two of the five top networks trended or significantly translated across species. Future research should run a

similar study, but instead of using the macaque parcellation registered to human space, it should use the human parcellation deformed to monkeys to see if these findings are robust enough in both scenarios.

4.4.5 Understanding why only some networks translated across species.

Regardless, it is important to understand why only the INO-LIM model significantly predicted across species. Initially, it was unclear why the most predictive model in macaques (AUD-DAN) did not translate across species. However, prior findings from making the deformations, that investigated how similar the functional relationships between species were depending on the region may help explain this discrepancy in the current findings (Xu, Nenning, et al. 2019).

Xu et al., define the cross-species Functional Homology Index (FHI), which identifies the cross-species functional similarity and network hierarchy. FHI uses pairs of coordinates matching between species identified from the Multimodal Surface Matching (MSM) and calculates the maximum similarity of functional gradients across the species using a searchlight radius of 12 mm along the surface. The maximal similarity identifies the probability that the functional gradients of each vertex in one species relate to the other. Hence the macaque-to-human functional homology index reveals the level of common functional organization across both species (Xu, Nenning, et al. 2019).

The FHI of regions in the most predictive monkey models, may help explain why the most predictive (AUD-DAN) model in the monkeys did not translate across species. For example, a major portion of ROIs in the monkey DAN network such as the frontal eye field (FEF), the dorsal lateral premotor cortex (dlPMC) and the medial parietal cortex (PCm) all fall within the lower percentile (Below 30%) FHI ranking compared to other

regions in the brain. In contrast, regions of the LIM, INO and AUD networks fell within the higher percentiles (Above 60%) of FHI (Xu, Nenning, et al. 2019). Even though the AUD-DAN network was the most predictive in monkeys, the lower cross-species functional homology index of regions in the DAN network most likely limited this effect from translating across species. Similarly, there was no significant cross-species translation in the DAN-LIM and AUD-AUD networks, which could either be a result of the low FHI in the DAN or maybe the prediction of these models was just not robust enough to translate across. This may elucidate why only the INO-LIM and AUD-INO models translated or came close to translating across-species. These findings highlight the strength of this model and the importance of investigating the similarities and differences across these species when running these types of analyses.

4.4.6 Limitations

While these findings are robust and shed light on the benefits of translating across different species, some considerations need to be taken into account when interpreting these findings. Using machine-learning methods with small sample sizes, as was done in the macaques, can sometimes run into issues with over-fitting, outliers or noise. While this may bring some caution to the initial findings within the macaques to identify the best fitting models, we believe that cross-validating these findings in humans in a completely new data set, and even across a different species shows that the current findings may be robust enough to avoid the over-fitting issue. Additionally, it is important to note that the size of the macaque population (N=32) is very large relative to other non-human primate studies to date. Acquiring this type of data, especially in infants, is tremendously difficult as a result of only seven NIH funded primate centers

existing in the USA. One limitation of using NHP is the increased demand to scan them under anesthesia. While this does dampen the signal, previous work from awake and anaesthetized macaques has shown you can identify robust and stable networks in both states (Xu et al. 2018; Xu, Nenning, et al. 2019; Xu, Sturgeon, Ramirez, Froudist-Walsh, Margulies, Schroeder, Fair, et al. 2019b). Additionally, this state also makes for a better comparison to the human infants used in this study, as they were collected during infant sleep. Finally, as this study used networks defined in the macaque population, and translated these to humans, it is important to note, that these networks may not directly translate across, and cause noise in regions where these networks are not correctly identified across species. However, as seen in figure 1, the networks in the human and macaque connectivity matrices, look relatively comparable justifying this approach. Future studies should however also use a human parcellation deformed to macaque space and repeat these analyses.

4.4.7 Conclusions and Future Directions

In general, these findings pose a tremendous potential, as they show the possibility to translate findings established in one species to make predictions in another. Not only could estimations about macaque maternal IL-6 be made from macaque brain connectivity, but these models could also be used to make inferences about the human maternal IL-6 concentrations. These types of studies open up the possibility for future studies to utilize the benefits of an animal model and test these manipulations in the human population. While these findings are still preliminary, they still lend promise for similar methodologies to be used in future translational studies.

Chapter 5: Discussion and Future Directions

5.1 Overview

This dissertation presents work from three research studies that investigate a link between select aspects of the maternal environment, and how they may relate to offspring brain characteristics after birth. The goal of these projects was to better understand the importance of in-utero brain development and highlight risk factors such as maternal inflammation and maternal diet that may alter subsequent structural and functional brain characteristics in offspring. This was achieved in threefold: 1) investigating how the maternal pro-inflammatory cytokine interleukin-6 (IL-6) relates to offspring amygdala volume development and anxiety-like behavior (study 1); 2) Studying typical macaque cortical thickness development and how growth trajectories of specific regions in the cortex may be linked to maternal IL-6, diet and offspring sex (study 2); and 3) Examine the relationship between offspring rs-fcMRI and maternal IL-6 using a translational cross-species cross-validation method (study 3).

5.1.1 Overview of findings from study 1

Findings from this study have helped us better understand how maternal IL-6 may influence offspring amygdala volume development. While studies in the human literature have associated maternal IL-6 with amygdala volume size in infancy (Graham et al. 2018), no studies have investigated this link in NHPs and more importantly across development from infancy to early puberty. The current work showed that maternal IL-6 concentrations during the third trimester were associated with initial decreased amygdala volumes at 4-months-of-age (intercept), but remarkably an increased rate of growth from

4 to 36-months of age (slope). Interestingly, there was a significant indirect association between early (4-month) amygdala volumes and anxiety-like behavior at 11-months-of-age. Higher levels of maternal IL-6 were associated with increased anxiety-like behavior, via the decreased 4-month amygdala volumes. These findings highlight the importance of using a longitudinal design to study these relationships, as there was a change in the developmental trajectory. This is significant, as the interpretation of the current findings would be different if investigating only one time-point (e.g. 4-months or 36-months). These findings indicate a meaningful connection between the maternal inflammatory state during pregnancy, changes in brain development and potential manifestations in offspring behavioral differences.

5.1.2 Overview of findings from study 2

The findings from study 2 further expand on the maternal-to-offspring brain relationships by investigating maternal IL-6, diet and offspring sex in the light of cortical thickness development across time. Study 2 first characterize typical Japanese macaque cortical thickness and then identify how maternal and offspring factors may associate with specific developmental trajectories of different regions of the brain.

Study 2 showed that unconditional latent growth curve models could be used to identify the best fitting growth curve and functional forms for each cortical surface vertex (grayordinate). This highlighted differential region-specific patterns in typical cortical thickness development. These patterns were further accentuated by showing a change in estimated mean cortical thickness across time, identifying unique developmental trends across the brain. Some regions would show negligible (intercepts-only) or gradual (slope) decreases/increases in thickness over time, while others would show more unique

presentations of change. These would be exhibited in trajectories such as changes in direction of growth (Quadratic), or rapid increases/decrease in development between one or two time points (spline).

The characterization of typical cortical thickness development was used to identify how maternal IL-6, diet (Western-style or control) and offspring sex related to the growth terms describing cortical thickness development. Findings indicated that the variables of interest were associated with unique, variable- and region-dependent, differences in starting and or growth trajectories of cortical thickness development. For example, increased levels of maternal IL-6 were associated with thicker starting cortical thickness in the temporal pole, while a maternal Western-style diet was associated with thinner starting cortical thickness in this region. Alternatively, both higher levels of maternal IL-6 and a maternal Western-style diet were associated with thinner starting (intercept) anterior insular thickness, but also showed patterns of increased rate-of-change (slope) overtime.

Lastly, these significant cluster findings exhibited a unique pattern of placement. Rather than finding that the predictor clusters predominantly landed in areas that showed the max or min mean thickness, it was observed that a majority of these clusters were on the edge of change, adjacent to these max or min focal points. We speculate (hypothesize) that this phenomenon is analogous to a glacier melting in nature over time, where the most change and external influence happens at the edge of the glacier (ablation zone) as opposed to the center (Anderson et al. 2006). While perhaps at first counterintuitive, in the light of this explanation these findings make sense when taking theories on how cortical thickness development occurs into account.

The mechanisms of how cortical thickness develops across time are not fully understood. In general, three developmental theories have been proposed to help explain how the cortex appears to be thinning or thickening over time These theories attribute 1) pruning, 2) myelination and 3) cortical morphology to cortical thinning over development (Natu et al. 2019). For example, an exciting recent study showed evidence that the cortex may in fact not be getting thinner, but instead only appear to get thinner as a result of increased myelination changing the intensity of the boundary between the white and gray matter of the cortex (Natu et al. 2019). In this scenario, as this systematic change in myelination occurs in a gradient forming a region across time, the variability in this process across subjects is going to be more prominent on the edges of change as opposed to areas there this change is not yet happening, or has already happened in an earlier developmental window. Hence, the different individual growth trajectories of multiple subjects all moving towards a similar end point will show more variability on these edges as opposed to the end point of development. Regarding the glacial analogy, the variability between subjects and where they are in the "myelination process" may be analogous to the variability in glacial melt across the years, as a result of this process happening systematically on the edge and moving closer to the center with time (cortical thinning).

Overall, the findings from this study are thought-provoking and noteworthy as they not only characterize typical cortical thickness development in a Japanese macaque model (unique to the field), but they also give us insights into how this development may be influenced by external factors such as maternal diet or IL-6. These findings help us identify target regions to explore in future directions in relation to functional connectivity and behavior. Furthermore, they also capitalize on the strength of using an animal model,

as running a controlled experiment using two diet groups across a critical developmental window (infancy to early puberty) would be tremendously difficult to achieve in a human cohort.

5.1.3 Overview of findings from study 3

Aims 1 and 2 helped established the benefits of using a NHP model to show that maternal environmental factors may relate to structural changes across time. Study 3 built on these findings to see if there were functional connectivity associations to the maternal environment (IL-6) in macaques (a replication of prior human literature (Rudolph et al. 2018)), but also translate these findings across-species. The results indicated that there was enough information in macaque functional connectivity networks to make significant inferences about the maternal IL-6 concentrations. The networks most significant in this association also showed sufficient overlap with networks previously shown to relate to maternal IL-6 in humans (Rudolph et al. 2018). Most predictive networks in macaques were the insular-opercular (INO), the limbic (LIM), the auditory (AUD), and the dorsal attention (DAN) networks. In humans, the most predictive networks were the salience (SAL), the subcortical (SUB) and the dorsal attention (DAN) networks. Not only did these findings reasonably replicate the findings from the human literature, but they also were able to translate in part across-species. When training the model in the macaque population, and testing it in the humans, the results indicated that the INO to LIM network connectivity translated across-species above a significance threshold of p=0.05. Human infant connectivity tested on the macaque model significantly predicted maternal IL-6 levels above chance.

For all three aims, brain characteristics were recorded using the non-invasive neuroimaging technique Magnetic Resonance Imaging (MRI). This tool was used because a core element of this dissertation was to not only replicate, but also translate findings from the non-human primate (NHPs) to human subjects. Using a non-invasive tool as such, allowed us to make these comparisons using similar methodologies in both species and still characterize brain structure and function. This was important, as finding similarities and differences between these two populations, and bridging these results across-species will open the door for future translational work overcoming common roadblocks by capitalizing on the benefits gained from using either species. For instance, it was important for us to characterize the maternal-to-offspring brain associations across developmental trajectories. In this case, using the accelerated developmental timeline of a NHP model allowed us to study trajectories without having to worry about human attrition or reducing the time of the experiment. These three aims all answer unique and relevant questions on their own. However, when taking these findings together, further inferences and conceptual viewpoints can be deduced.

5.2 The amygdala-prefrontal cortex feedback loop

A large collection of research indicates bi-directional connections between the amygdala and the prefrontal cortex (PFC). The majority of these findings highlight a top-down control from the PFC to the amygdala in order to regulate emotional arousal, regulation and decision making (Banks et al. 2007; Ameis et al. 2014; Buhle et al. 2014; Motzkin et al. 2015; Smith et al. 2016). However, an exciting recent paper by Tottenham and Gabard-Durnam sheds light on a developmental view of this circuitry (Tottenham and Gabard-Durnam 2017). They convincingly propose a developmental feedback loop,

where early environmental experiences help shape the amygdala, which in turn supports later medial prefrontal cortex (mPFC) development (Tottenham and Gabard-Durnam 2017). For instance, anatomical tracing studies in rodents highlight the directionality of this developmental relationship as amygdala → PFC connections emerge before PFC → Amygdala projections (Bouwmeester, Smits, et al. 2002; Bouwmeester, Wolterink, et al. 2002). These findings and many others highlighted by Tottenham and Gabard-Durnam indicate an amygdala - mPFC feedback loop, where the amygdala helps the mPFC develop, which in turn helps regulate the amygdala.

In this light, having a smaller amygdala may also be associated with atypical mPFC cortical thickness development. In chapter 3 of this dissertation, typical macaque cortical thickness development was characterized. Some regions of the brain typically became thinner over time, while others typically became thicker (Chapter 3, Fig. 4). Typical cortical development in the medial prefrontal cortex decreases in thickness over time (Figure 3.4 [percent change in thickness]). Accordingly, one might postulate, that having a thicker cortical thickness in this region could be associated with atypical cortical thickness development (i.e. a delayed developmental trajectory). Similarly, having a decreased rate of thinning between 4 and 36-months of age (slope) could also be associated with atypical development. Taking these ideas together, the findings from chapter 2 and chapter 3 fit nicely into this framework.

In chapter 2, higher levels of maternal IL-6 are associated with smaller starting (4-month/intercept) amygdala volumes. In chapter 3, increased levels of maternal IL-6 were associated with enlarged (atypical) cortical thickness at the intercept in the medial prefrontal cortex (Figure 3.6C). Visually, there was also a trend (but no significant

clusters) towards decreased cortical thinning (slope) in this same area. Expressly, the decrease amygdala volumes from the higher maternal IL-6 may have regulated the cortical thickness development in the medial prefrontal cortex.

Additionally, if the theory of the amygdala-mPFC feedback loop is true, this may also help explain why an increased rate of amygdala growth (slope) was associated with maternal IL-6. If the amygdala helps regulate mPFC development, and the mPFC regulates the amygdala, a less developed mPFC may also demonstrate less top-down control on the amygdala (increased growth rate). Furthermore, this may also explain some of the anxiety-like findings, as less top-down control may be linked to the increased emotion regulatory behaviors (Banks et al. 2007; Ameis et al. 2014; Buhle et al. 2014; Motzkin et al. 2015; Graham et al. 2016; Smith et al. 2016; Thomas et al. 2019). These findings are promising in highlighting conceptual support for the amygdala-medial-PFC feedback loop and may indicate an avenue of how these characteristics develop together. Higher levels of IL-6 may lead to decreased amygdala volumes (Chapter 2) which may regulate mPFC cortical thickness development (Chapter 3) which in turn may decrease the inhibition on amygdala development, resulting in higher rates of growth, and increased anxiety-like behavior (Chapter 2).

5.3 Larger scale feedback loops

It is important to note, that these findings may not be limited to just a two-region feedback loop and anxiety-like behavior. Furthermore, while the behaviors attained from the human intruder and novel object test are often classified as anxiety-like behaviors, others may interpret these as fear-induced behaviors, emotional regulatory behaviors, as well as containing components of impulse control (Kalin et al. 1991; Williamson et al.

2003; Sullivan et al. 2010; Raper et al. 2013). Complex behaviors such as anxiety-like behavior do not solely rely on the relationship between two regions, but instead, manifest as a result of multiple region interactions such as the connectivity of dispersed networks throughout the brain. For example, previous findings in humans implicated that infant amygdala connectivity to the anterior insula and the ventromedial PFC was related to later fear, sadness or cognitive development (Graham et al. 2016; Thomas et al. 2019). Interestingly, in chapter 3, we also observed a large significant cluster in the anterior insula relating to maternal IL-6 and Diet. Could early amygdala activity and development also regulate other cortical development?

Interestingly, the summary results of the cortical thickness study (

Figure 3.8), suggest that the potential amygdala - mPFC relationship may not be mPFC dependent. In support, IL-6 was associated with similar trends across other regions of the cortex. Hence, larger-scale feedback loops or downstream effects may exist that need to be investigated in future studies.

The cortical thickness results showing the surface area of all of the clusters significantly associated with maternal IL-6 shed light on these potentially intriguing trends (

Figure 3.8C). IL-6 also related to other significant clusters throughout the brain with a similar trend to the previously discussed mPFC findings (i.e. thicker starting but negative slope). Regardless of which functional network these clusters fell in (Total), IL-6 was mostly associated with thicker starting (intercept) and a slower rate of change (slope). This may

indicate that this amygdala PFC feedback loop may be even more widespread and regulate a broader spectrum of cortical development than just the PFC. The pie charts in chapter 3 Fig. 8 show that 25%, as opposed to 16% of the total cluster surface area from the IL-6 results, came from positive not negative intercept relationships (

Figure 3.8C). Interestingly, only 13%, as opposed to 27% of slope relationships, were positive. While these percentages were not statistically tested to indicate a meaningful difference, they may highlight a heuristic trend towards IL-6 predominantly slowing the rate of development rather than speeding it up. This directionality in percentages was not the case for the diet intercept (positive = 11%; negative= 23%) or slope (positive = 24%; negative= 21%) results. In this light, offspring sex had similar intercept (positive = 18%; negative= 9%) but opposite slope (positive = 36%; negative= 12%) organization compared to IL-6. These observations may highlight unique opposing or similar trends in the different predictors.

5.4 Differential outcomes of predictors (IL-6, Diet, Sex) and potential mechanisms

The similar directionality in offspring sex (positive = 18%; negative= 9%) and maternal IL-6 (positive = 18%; negative= 9%) intercept distributions are intriguing. There is evidence to believe that a tight link between offspring sex differentiation and maternal inflammation may be driving similar large-scale outcomes. For example, both maternal inflammation and offspring sex (maleness) are often associated as risk factors for neuropsychiatric disorders (McCarthy and Wright 2017; Dunn et al. 2019; Guma et al. 2019; McCarthy 2019). It has been proposed that these two risk factors may even be

interrelated (Lenz and McCarthy 2015; McCarthy 2019). Sensitive windows in fetal brain development determining sexual differentiation of the brain, overlap with sensitive periods during which inflammation increases the risk for atypical developmental outcomes (McCarthy 2019). This may explain why both sex and IL-6 initially relate to thicker cortical thickness trends, but these diverge as offspring deviate further from the maternal environment, ultimately showing opposing directionality in growth (slope) trends.

Along these lines, proportionally, IL-6 clusters were predominantly related to intercept findings (41%), while diet (45%) and sex (48%) clusters predominantly related to slope statistics. While these differences were minimal and not statistically validated, they still may implicate interesting hypotheses about the mechanism of these differences. The increased relationships to slope in the sex predictor make intuitive sense, as sex differences in brain size become larger during early development (Scott et al. 2016b). However, differences between maternal IL-6 and diet are harder to explain. Studies investigating the developmental origins of health and disease (DOHaD) have implicated that early epigenetic modifications may respond to the nutritional state of the fetal environment.

For example, an earlier study famously showed that exposure to malnutrition during early fetal development as a result of 1944 Dutch famine resulted in a higher risk for obesity later in life. It was theorized that in-utero epigenetic modifications predisposed the infant to “prepare” for an environment with low food availability. Similarly, the Western-Style diet (WSD) may have predisposed the infants for later developmental traits that differentiate them from the controls over time (slope effects). A

similar concept was shown in these macaques, where offspring of obese mothers that consumed a WSD had a significantly higher intake of palatable food (high in fat and sucrose content) compared to offspring of lean control diet mothers (Rivera, Kievit, et al. 2015). Hence, more slope effects may be related to diet, as these offspring may be taking in more food after birth, during these developmental trajectories, potentially altering their cortical thickness.

Finally, as discussed in chapter 1, the brain goes through a number of developmental processes through the first, second and third trimester of gestation. During early gestation (first), fundamental neurodevelopmental changes happen in fetal brain development. These range from processes such as neurulation, neurogenesis, and the beginning of immune and progenitor and neuronal cell migration (Semple et al. 2013; Selemon and Zecevic 2015; Guma et al. 2019). As some of these processes continue, colonization of immune cells, apoptosis and synaptogenesis begin in the 2nd trimester of gestation (Semple et al. 2013; Guma et al. 2019). Furthermore, during this transition, the blood-brain barrier starts to form, sex is determined, and neurogenesis continues in many midbrain and subcortical regions (Eggers and Sinclair 2012; Semple et al. 2013; Guma et al. 2019). Finally, transitioning to the third trimester, neurogenesis increases in the hippocampus and cortical regions as cortical layer organization occurs as well as synaptogenesis, gliogenesis, and apoptosis and myelination begin to take place (Knuesel et al. 2014; Estes and McAllister 2016; Guma et al. 2019).

As the placenta enables direct contact between maternal and fetal compartments, the maternal cytokines, chemokines and micronutrients may disrupt equilibrium levels if in excess and alter typical fetal brain development (Colucci et al. 2011; Reisinger et al.

2015; DeCapo et al. 2019; Guma et al. 2019). Microglia, play a regulatory role in the maintenance of synapses and pruning, for which they often considered critical in the light of developmental changes resulting from maternal immune activation (MIA) (Smolders et al. 2018). Prior research has indicated sex differences in microglia morphology and inflammatory cytokine and chemokine expression of the developing amygdala, hippocampus and cortex (Schwarz et al. 2012). These expression differences may help explain the amygdala findings from the current study, as IL-6, an inflammatory cytokine was linked to amygdala volume differences and indirectly to anxiety-like behavior (study 1).

Prior research from this cohort of monkeys has also linked maternal diet to differences in anxiety-like behavior and impairment to the serotonin (5HT) system in the raphe and prefrontal cortex (Sullivan et al. 2010; Thompson et al. 2017). Since the serotonin system in regions such as the substantia nigra, raphe, prefrontal cortex and the amygdala has also been shown to be sensitive to inflammatory cytokines, early-life stress and even sex differences, a mechanistic link to the serotonin system may help explain the IL-6, diet and sex difference findings from the current report. Microglia, related to inflammatory cytokines, offspring sex or diet may alter serotonin function and projections to other cortical and subcortical regions such as the amygdala or medial prefrontal cortex, which in turn may help regulate behavioral outcomes. As sex differentiation, the development of the blood brain barrier, gliogenesis, myelination and other neural developmental processes all happen at various stages in development, it may help explain how diet, inflammation and sex showed different and overlapping results in the current report.

There is overlap in the mechanisms of how diet and maternal IL-6 may influence fetal brain development. However, there are also independent mechanisms that may be driving these different results which could be dependent on the timing of these developmental processes (e.g. the development of the blood brain barrier or sex differentiation). Micronutrients from maternal food intake circulating in the fetal circulatory system can have independent influences on glial maturation, dendritic stability cell signaling and myelination, as well as altering inflammatory cytokine concentrations (DeCapo et al. 2019). The overlap in the IL-6 and diet findings may be a result of this nutrition to inflammation relationship. However, the association between maternal nutrition and inflammation also indicates that other inflammatory cytokines other than IL-6 may be linked to different independent changes in the brain. The current report looked at IL-6, diet and sex in the same model (i.e. investigating the outcome of one predictor while controlling for the others). Future research should investigate these relationships in the light of diet sex and inflammation interactions and also see how these relate to independent behavior and brain function.

5.5 Structure-function relationships

Without making direct comparisons, it is hard to make inferences about a relationship between the current structural and functional findings. Interestingly, IL-6 clusters visually showed higher total surface area coverage in the limbic (LIM) network compared to the other predictors, maternal diet and offspring sex (

Figure 3.8E). This was also the case for intercept clusters in the insula-opercular (INO) and somatomotor (SMN) networks. Maternal diet clusters, on the other hand,

showed more surface area coverage in the default mode (DMN) and visual (VIS) networks compared to the other predictors. These findings might shed some light on the functional findings found in chapter 4. When using functional connectivity to make predictions about maternal IL-6, only the LIM-INO network predicted across species. While it is important to note that the surface area coverage of all predictors was highest in the DMN and VIS compared to other networks, this may be an artifact of these networks having more surface area in general. A ratio of the cluster to total network surface area would potentially alter these interpretations.

Additionally, the prominent and bilateral clusters, significantly associated with maternal IL-6 and cortical thickness, also help support the notion of a meaningful structure-function relationship in these findings. Thicker temporal pole, increased rate of growth in the inferior temporal lobe, and the large clusters in the anterior insula and PFC all overlap with the most significant networks predicting maternal IL-6 (INO-LIM). These findings align with previous structure-function relationships described in this parcellation, where functionally inactivating the amygdala using chemogenetic tools (Designer receptors exclusively activated by designer drugs (DREADDs)) showed comparable changes to simulated structural lesions of the amygdala (Grayson et al. 2016). The current work showed that IL-6 is associated with decreased amygdala volume size (chapter 2), and also changes in cortical thickness (chapter 3) in regions of networks that functionally back predict maternal IL-6 (chapter 4). These findings, alongside the Grayson et al., results, indicate a highly probable link between the structural and functional findings from chapters 2, 3 and 4 of this dissertation.

5.6 Conclusions

The findings presented in this dissertation help characterize typical offspring brain development and how it may be altered by differences in the maternal in-uterine state. They highlight structural differences on a volumetric and cortical thickness scale, and also identify patterns in complex infant functional connectivity that may relate to the maternal environment. While the structural and functional results from the current studies were not directly compared, they open the door for future investigations to integrate these findings into one cohesive project. Regardless, the current results underline the essential importance of investigating these mother-offspring relationships on a longitudinal scale, as complex developmental feedback loops and trajectories can significantly alter the interpretation of your findings, depending on time point. It can be hypothesized that differences in structural volumes or thickness may share similarities in functional connectivity. However, future studies will need to investigate these links further. Running seed-based connectivity studies, using the significant clusters from the cortical thickness findings to make inferences about the maternal or later offspring behavioral environment would be of high interest. Similarly, it would be interesting to investigate if clusters related to the different predictors had similar patterns in the BOLD signal helping you identify a “maternal IL-6” or “maternal diet” network for instance. Similarly, the current study only investigated the pro-inflammatory cytokine IL-6 due to prior findings indicating it to be sufficient to independently induce offspring behavioral changes (Smith et al. 2007). However, it is well known that maternal immune activation entails many other pro- and anti-inflammatory cytokines which should be investigated in future studies. The current finding may lend as a starting point and a proof of concept, but a more in-depth analyses or replication using additional cytokines likely would be of great

benefit. Regardless, the current findings were helpful for future translational work, and indicated that functional brain networks in part are similar enough across the macaque and human population to make meaningful predictions in one population from inferences attained in the other. These methodologies are novel and open the door for exciting future translational work. Having the ability to optimize the advantages and disadvantages of different model types by studying relationships across-species in the same space may reveal a plethora of novel discoveries for years to come.

References

Abdi H, Williams LJ. 2013. Partial Least Squares Methods: Partial Least Squares Correlation and Partial Least Square Regression. Humana Press, Totowa, NJ. p. 549–579.

Aggrey S. 2002. Comparison of three nonlinear and spline regression models for describing chicken growth curves. Poult Sci. 81:1782–1788.

Alexander-Bloch AF, Reiss PT, Rapoport J, McAdams H, Giedd JN, Bullmore ET, Gogtay N. 2014. Abnormal Cortical Growth in Schizophrenia Targets Normative Modules of Synchronized Development. Biol Psychiatry. 76:438–446.

Alexander C, Rietschel ET. 2001. Bacterial lipopolysaccharides and innate immunity. J Endotoxin Res.

Amaral DG, Bauman MD, Mills Schumann C. 2003. The amygdala and autism: implications from non-human primate studies. Genes, Brain Behav. 2:295–302.

Ameis SH, Ducharme S, Albaugh MD, Hudziak JJ, Botteron KN, Lepage C, Zhao L, Khundrakpam B, Collins DL, Lerch JP, Wheeler A, Schachar R, Evans AC, Karama S. 2014. Cortical thickness, cortico-amygdalar networks, and externalizing

behaviors in healthy children. Biol Psychiatry. 75:65–72.

Amlien IK, Fjell AM, Tamnes CK, Grydeland H, Krogsrud SK, Chaplin TA, Rosa MGP, Walhovd KB. 2016. Organizing Principles of Human Cortical Development—Thickness and Area from 4 to 30 Years: Insights from Comparative Primate Neuroanatomy. Cereb Cortex. 26:257–267.

Anderson RS, Molnar P, Kessler MA. 2006. Features of glacial valley profiles simply explained. J Geophys Res. 111:F01004.

Andruff H, Carraro N, Thompson A, Gaudreau P. 2009. Latent Class Growth Modelling: A Tutorial, Tutorials in Quantitative Methods for Psychology.

Atladottir HO, Gyllenberg D, Langridge A, Sandin S, Hansen SN, Leonard H, Gissler M, Reichenberg A, Schendel DE, Bourke J, Hultman CM, Grice DE, Buxbaum JD, Parner ET. 2015. The increasing prevalence of reported diagnoses of childhood psychiatric disorders: a descriptive multinational comparison. Eur Child Adolesc Psychiatry. 24:173–183.

Attwell D, Iadecola C. 2002. The neural basis of functional brain imaging signals. Trends Neurosci. 25:621–625.

Ausderau KK, Dammann C, McManus K, Schneider M, Emborg ME, Schultz-Darken N. 2017. Cross-species comparison of behavioral neurodevelopmental milestones in the common marmoset monkey and human child. Dev Psychobiol. 59:807–821.

Avants BB, Hackman DA, Betancourt LM, Lawson GM, Hurt H, Farah MJ. 2015.

Relation of Childhood Home Environment to Cortical Thickness in Late Adolescence: Specificity of Experience and Timing. PLoS One. 10:e0138217.

Bailey A, Le Couteur A, Gottesman I, Bolton P, Simonoff E, Yuzda E, Rutter M. 1995. Autism as a strongly genetic disorder: evidence from a British twin study. Psychol Med. 25:63–77.

Baker KD, Loughman A, Spencer SJ, Reichelt AC. 2017. The impact of obesity and hypercaloric diet consumption on anxiety and emotional behavior across the lifespan. Neurosci Biobehav Rev. 83:173–182.

Bale TL, Baram TZ, Brown AS, Goldstein JM, Insel TR, McCarthy MM, Nemeroff CB, Reyes TM, Simerly RB, Susser ES, Nestler EJ. 2010. Early Life Programming and Neurodevelopmental Disorders. Biol Psychiatry. 68:314–319.

Ball G, Seal ML. 2019. Individual variation in longitudinal postnatal development of the primate brain. Brain Struct Funct. 1–17.

Banks SJ, Eddy KT, Angstadt M, Nathan PJ, Phan KL. 2007. Amygdala–frontal connectivity during emotion regulation. Soc Cogn Affect Neurosci. 2:303–312.

Belzung C, Le Pape G. 1994. Comparison of different behavioral test situations used in psychopharmacology for measurement of anxiety. Physiol Behav. 56:623–628.

Bentler PM. 1990. Comparative fit indexes in structural models. Psychol Bull. 107:238–246.

Bergdolt L, Dunaevsky A. 2019. Brain changes in a maternal immune activation model

of neurodevelopmental brain disorders. Prog Neurobiol. 175:1–19.

Bezgin G, Vakorin VA, van Opstal AJ, McIntosh AR, Bakker R. 2012. Hundreds of brain maps in one atlas: Registering coordinate-independent primate neuro-anatomical data to a standard brain. Neuroimage. 62:67–76.

Bilbo SD, Schwarz JM. 2009. Early-life programming of later-life brain and behavior: a critical role for the immune system. Front Behav Neurosci. 3:14.

Bouwmeester H, Smits K, Van Ree JM. 2002. Neonatal development of projections to the basolateral amygdala from prefrontal and thalamic structures in rat. J Comp Neurol. 450:241–255.

Bouwmeester H, Wolterink G, Van Ree JM. 2002. Neonatal development of projections from the basolateral amygdala to prefrontal, striatal, and thalamic structures in the rat. J Comp Neurol. 442:239–249.

Brambrink AM, Evers AS, Avidan MS, Farber NB, Smith DJ, Zhang X, Dissen GA, Creeley CE, Olney JW. 2010. Isoflurane-induced Neuroapoptosis in the Neonatal Rhesus Macaque Brain. Anesthesiology. 112:834–841.

Brito NH, Noble KG. 2014. Socioeconomic status and structural brain development. Front Neurosci. 8:276.

Bronson SL, Bale TL. 2014. Prenatal Stress-Induced Increases in Placental Inflammation and Offspring Hyperactivity Are Male-Specific and Ameliorated by Maternal Antiinflammatory Treatment. Endocrinology. 155:2635–2646.

Buhi E. 2008. Out of Sight, Not Out of Mind: Strategies for Handling Missing Data. Am J Health Behav. 32.

Buhle JT, Silvers JA, Wager TD, Lopez R, Onyemekwu C, Kober H, Weber J, Ochsner KN. 2014. Cognitive Reappraisal of Emotion: A Meta-Analysis of Human Neuroimaging Studies. Cereb Cortex. 24:2981–2990.

Buss C, Davis EP, Shahbaba B, Pruessner JC, Head K, Sandman CA. 2012. Maternal cortisol over the course of pregnancy and subsequent child amygdala and hippocampus volumes and affective problems. Proc Natl Acad Sci U S A. 109:E1312-9.

Buss DC, Entringer DS, Moog MNK, Toepfer MP, Fair DDA, Simhan DHN, Heim DCM, Wadhwa DPD. 2017. Intergenerational Transmission of Maternal Childhood Maltreatment Exposure: Implications for Fetal Brain Development. J Am Acad Child Adolesc Psychiatry. 56:373.

Careaga M, Murai T, Bauman MD. 2017. Maternal Immune Activation and Autism Spectrum Disorder: From Rodents to Nonhuman and Human Primates. Biol Psychiatry. 81:391–401.

Casimo K, Levinson LH, Zanos S, Gkogkidis CA, Ball T, Fetz E, Weaver KE, Ojemann JG. 2017. An interspecies comparative study of invasive electrophysiological functional connectivity. Brain Behav. 7:e00863.

Challis JR, Lockwood CJ, Myatt L, Norman JE, Strauss JF, Petraglia F. 2009. Inflammation and Pregnancy. Reprod Sci. 16:206–215.

Chavhan GB, Babyn PS, Thomas B, Shroff MM, Haacke EM. 2009. Principles, techniques, and applications of T2*-based MR imaging and its special applications. Radiographics. 29:1433–1449.

Clancy B, Darlington R., Finlay B. 2001. Translating developmental time across mammalian species. Neuroscience. 105:7–17.

Coleman K, Robertson ND, Bethea CL. 2011. Long-term ovariectomy alters social and anxious behaviors in semi-free ranging Japanese macaques. Behav Brain Res. 225:317–327.

Collins LM, Schafer JL, Kam CM. 2001. A comparison of inclusive and restrictive strategies in modern missing data procedures. Psychol Methods. 6:330–351.

Colucci F, Boulenouar S, Kieckbusch J, Moffett A. 2011. How does variability of immune system genes affect placentation? Placenta. 32:539–545.

Comstock SM, Pound LD, Bishop JM, Takahashi DL, Kostrba AM, Smith MS, Grove KL. 2013. High-fat diet consumption during pregnancy and the early post-natal period leads to decreased α cell plasticity in the nonhuman primate. Mol Metab. 2:10–22.

Contu L, Hawkes CA. 2017. A Review of the Impact of Maternal Obesity on the Cognitive Function and Mental Health of the Offspring. Int J Mol Sci. 18:1093.

Costello EJ, Mustillo S, Erkanli A, Keeler G, Angold A. 2003. Prevalence and Development of Psychiatric Disorders in Childhood and Adolescence. Arch Gen

Psychiatry. 60:837.

Crinnion WJ. 2009. Maternal levels of xenobiotics that affect fetal development and childhood health. Altern Med Rev. 14:212–222.

Curran PJ, Obeidat K, Losardo D. 2010. Twelve Frequently Asked Questions About Growth Curve Modeling. J Cogn Dev. 11:121–136.

Cuthbert BN. 2014. The RDoC framework: facilitating transition from ICD/DSM to dimensional approaches that integrate neuroscience and psychopathology. World Psychiatry. 13:28–35.

Dale AM, Fischl B, Sereno MI. 1999. Cortical Surface-Based Analysis. Neuroimage. 9:179–194.

de Zeeuw P, Schnack HG, van Belle J, Weusten J, van Dijk S, Langen M, Brouwer RM, van Engeland H, Durston S. 2012. Differential Brain Development with Low and High IQ in Attention-Deficit/Hyperactivity Disorder. PLoS One. 7:e35770.

DeCapo M, Thompson JR, Dunn G, Sullivan EL. 2019. Perinatal Nutrition and Programmed Risk for Neuropsychiatric Disorders: A Focus on Animal Models. Biol Psychiatry. 85:122–134.

Donahue CJ, Glasser MF, Preuss TM, Rilling JK, Van Essen DC. 2018. Quantitative assessment of prefrontal cortex in humans relative to nonhuman primates. Proc Natl Acad Sci U S A. 115:E5183–E5192.

Donahue CJ, Sotiropoulos SN, Jbabdi S, Hernandez-Fernandez M, Behrens TE, Dyrby

TB, Coalson T, Kennedy H, Knoblauch K, Van Essen DC, Glasser MF. 2016. Using Diffusion Tractography to Predict Cortical Connection Strength and Distance: A Quantitative Comparison with Tracers in the Monkey. J Neurosci. 36:6758–6770.

dos Santos JF, de Melo Bastos Cavalcante C, Barbosa FT, Gitaí DLG, Duzzioni M, Tilelli CQ, Shetty AK, de Castro OW. 2018. Maternal, fetal and neonatal consequences associated with the use of crack cocaine during the gestational period: a systematic review and meta-analysis. Arch Gynecol Obstet. 298:487–503.

Dosenbach NUF, Koller JM, Earl EA, Miranda-Dominguez O, Klein RL, Van AN, Snyder AZ, Nagel BJ, Nigg JT, Nguyen AL, Wesevich V, Greene DJ, Fair DA. 2017. Real-time motion analytics during brain MRI improve data quality and reduce costs. Neuroimage. 161:80–93.

Doucet G, Naveau M, Petit L, Delcroix N, Zago L, Crivello F, Jobard G, Tzourio-Mazoyer N, Mazoyer B, Mellet E, Joliot M. 2011. Brain activity at rest: a multiscale hierarchical functional organization. J Neurophysiol. 105:2753–2763.

Dunn GA, Nigg JT, Sullivan EL. 2019. Neuroinflammation as a risk factor for attention deficit hyperactivity disorder. Pharmacol Biochem Behav. 182:22–34.

Eggers S, Sinclair A. 2012. Mammalian sex determination-insights from humans and mice. Chromosom Res. 20:215–238.

Eklund A, Nichols TE, Knutsson H. 2016. Cluster failure: Why fMRI inferences for spatial extent have inflated false-positive rates. Proc Natl Acad Sci U S A. 113:7900–7905.

Elsabbagh M, Divan G, Koh Y-J, Kim YS, Kauchali S, Marcín C, Montiel-Nava C, Patel V, Paula CS, Wang C, Yasamy MT, Fombonne E. 2012. Global prevalence of autism and other pervasive developmental disorders. Autism Res. 5:160–179.

Enayati M, Solati J, Hosseini M-H, Shahi H-R, Saki G, Salari A-A. 2012. Maternal infection during late pregnancy increases anxiety- and depression-like behaviors with increasing age in male offspring. Brain Res Bull. 87:295–302.

Enders CK. 2001. A Primer on Maximum Likelihood Algorithms Available for Use With Missing Data. Struct Equ Model A Multidiscip J. 8:128–141.

England LJ, Bunnell RE, Pechacek TF, Tong VT, McAfee TA. 2015. Nicotine and the Developing Human: A Neglected Element in the Electronic Cigarette Debate. Am J Prev Med. 49:286–293.

Entringer S. 2007. Exposure to prenatal psychosocial stress : implications for long-term disease susceptibility. 1st ed. Göttingen: Cuvillier Verlag.

Entringer S, Buss C, Wadhwa PD. 2015. Prenatal stress, development, health and disease risk: A psychobiological perspective—2015 Curt Richter Award Paper. Psychoneuroendocrinology. 62:366–375.

Escudero I, Johnstone M. 2014. Genetics of Schizophrenia. Curr Psychiatry Rep. 16:502.

Estes ML, McAllister AK. 2015. Immune mediators in the brain and peripheral tissues in autism spectrum disorder. Nat Rev Neurosci. 16:469–486.

Estes ML, McAllister AK. 2016. Maternal immune activation: Implications for

neuropsychiatric disorders. Science (80-). 353.

Fair DA, Nigg JT, Iyer S, Bathula D, Mills KL, Dosenbach NUF, Schlaggar BL, Mennes M, Gutman D, Bangaru S, Buitelaar JK, Dickstein DP, Di Martino A, Kennedy DN, Kelly C, Luna B, Schweitzer JB, Velanova K, Wang Y-F, Mostofsky S, Castellanos FX, Milham MP. 2012. Distinct neural signatures detected for ADHD subtypes after controlling for micro-movements in resting state functional connectivity MRI data. Front Syst Neurosci. 6:80.

Faraone S V., Perlis RH, Doyle AE, Smoller JW, Goralnick JJ, Holmgren MA, Sklar P. 2005. Molecular Genetics of Attention-Deficit/Hyperactivity Disorder. Biol Psychiatry. 57:1313–1323.

Fischl B, Sereno MI, Dale AM. 1999. Cortical Surface-Based Analysis. Neuroimage. 9:195–207.

Foulkes L, Blakemore S-J. 2018. Studying individual differences in human adolescent brain development. Nat Neurosci. 21:315–323.

Friedman LA, Rapoport JL. 2015. Brain development in ADHD. Curr Opin Neurobiol. 30:106–111.

Gennatas ED, Avants BB, Wolf DH, Satterthwaite TD, Ruparel K, Ciric R, Hakonarson H, Gur RE, Gur RC. 2017. Age-Related Effects and Sex Differences in Gray Matter Density, Volume, Mass, and Cortical Thickness from Childhood to Young Adulthood. J Neurosci. 37:5065–5073.

Glasser MF, Sotiropoulos SN, Wilson JA, Coalson TS, Fischl B, Andersson JL, Xu J, Jbabdi S, Webster M, Polimeni JR, Van Essen DC, Jenkinson M. 2013. The minimal preprocessing pipelines for the Human Connectome Project. Neuroimage. 80:105–124.

Glaus J, von Känel R, Lasserre AM, Strippoli M-PF, Vandeleur CL, Castelao E, Gholam-Rezaee M, Marangoni C, Wagner E-YN, Marques-Vidal P, Waeber G, Vollenweider P, Preisig M, Merikangas KR. 2017. Mood disorders and circulating levels of inflammatory markers in a longitudinal population-based study. Psychol Med. 1–13.

Gogtay N, Greenstein D, Lenane M, Clasen L, Sharp W, Gochman P, Butler P, Evans A, Rapoport J. 2007. Cortical Brain Development in Nonpsychotic Siblings of Patients With Childhood-Onset Schizophrenia. Arch Gen Psychiatry. 64:772.

Goodkind M, Eickhoff SB, Oathes DJ, Jiang Y, Chang A, Jones-Hagata LB, Ortega BN, Zaiko Y V., Roach EL, Korgaonkar MS, Grieve SM, Galatzer-Levy I, Fox PT, Etkin A. 2015. Identification of a Common Neurobiological Substrate for Mental Illness. JAMA Psychiatry. 72:305.

Gordon EM, Laumann TO, Adeyemo B, Huckins JF, Kelley WM, Petersen SE. 2016. Generation and Evaluation of a Cortical Area Parcellation from Resting-State Correlations. Cereb Cortex. 26:288–303.

Gorgolewski KJ, Auer T, Calhoun VD, Craddock RC, Das S, Duff EP, Flandin G, Ghosh SS, Glatard T, Halchenko YO, Handwerker DA, Hanke M, Keator D, Li X, Michael

Z, Maumet C, Nichols BN, Nichols TE, Pellman J, Poline J-B, Rokem A, Schaefer G, Sochat V, Triplett W, Turner JA, Varoquaux G, Poldrack RA. 2016. The brain imaging data structure, a format for organizing and describing outputs of neuroimaging experiments. Sci Data. 3:160044.

Gottlieb DH, Capitanio JP. 2013. Latent Variables Affecting Behavioral Response to the Human Intruder Test in Infant Rhesus Macaques (Macaca mulatta). Am J Primatol. 75:314–323.

Graham AM, Buss C, Rasmussen JM, Rudolph MD, Demeter D V., Gilmore JH, Styner M, Entringer S, Wadhwa PD, Fair DA. 2016. Implications of newborn amygdala connectivity for fear and cognitive development at 6-months-of-age. Dev Cogn Neurosci. 18:12–25.

Graham AM, Pfeifer JH, Fisher PA, Carpenter S, Fair DA. 2015. Early life stress is associated with default system integrity and emotionality during infancy. J Child Psychol Psychiatry. 56:1212–1222.

Graham AM, Pfeifer JH, Fisher PA, Lin W, Gao W, Fair DA. 2015. The potential of infant fMRI research and the study of early life stress as a promising exemplar. Dev Cogn Neurosci. 12:12–39.

Graham AM, Rasmussen JM, Entringer S, Ben Ward E, Rudolph MD, Gilmore JH, Styner M, Wadhwa PD, Fair DA, Buss C. 2019. Maternal Cortisol Concentrations During Pregnancy and Sex-Specific Associations With Neonatal Amygdala Connectivity and Emerging Internalizing Behaviors. Biol Psychiatry. 85:172–181.

Graham AM, Rasmussen JM, Rudolph MD, Heim CM, Gilmore JH, Styner M, Potkin SG, Entringer S, Wadhwa PD, Fair DA, Buss C. 2018. Maternal Systemic Interleukin-6 During Pregnancy Is Associated With Newborn Amygdala Phenotypes and Subsequent Behavior at 2 Years of Age. Biol Psychiatry. 83:109–119.

Graham JW. 2003. Adding Missing-Data-Relevant Variables to FIML-Based Structural Equation Models. Struct Equ Model A Multidiscip J. 10:80–100.

Grayson DS, Fair DA. 2017. Development of large-scale functional networks from birth to adulthood: A guide to the neuroimaging literature. Neuroimage. 160:15–31.

Grayson DSS, Bliss-Moreau E, Machado CJJ, Bennett J, Shen K, Grant KAA, Fair DAA, Amaral DGG. 2016. The Rhesus Monkey Connectome Predicts Disrupted Functional Networks Resulting from Pharmacogenetic Inactivation of the Amygdala. Neuron. 91:453–466.

Greve DN, Fischl B. 2018. False positive rates in surface-based anatomical analysis. Neuroimage. 171:6–14.

Guma E, Plitman E, Chakravarty MM. 2019. The role of maternal immune activation in altering the neurodevelopmental trajectories of offspring: A translational review of neuroimaging studies with implications for autism spectrum disorder and schizophrenia. Neurosci Biobehav Rev. 104:141–157.

Gumusoglu SB, Fine RS, Murray SJ, Bittle JL, Stevens HE. 2017. The role of IL-6 in neurodevelopment after prenatal stress. Brain Behav Immun. 65:274–283.

Gumusoglu SB, Stevens HE. 2019. Maternal Inflammation and Neurodevelopmental Programming: A Review of Preclinical Outcomes and Implications for Translational Psychiatry. Biol Psychiatry. 85:107–121.

Gustafsson HC, Sullivan EL, Nousen EK, Sullivan CA, Huang E, Rincon M, Nigg JT, Loftis JM. 2018. Maternal prenatal depression predicts infant negative affect via maternal inflammatory cytokine levels. Brain Behav Immun.

Gustavson K, von Soest T, Karevold E, Røysamb E. 2012. Attrition and generalizability in longitudinal studies: findings from a 15-year population-based study and a Monte Carlo simulation study. BMC Public Health. 12:918.

Haak K V., Marquand AF, Beckmann CF. 2018. Connectopic mapping with resting-state fMRI. Neuroimage. 170:83–94.

Habets P, Marcelis M, Gronenschild E, Drukker M, van Os J, Genetic Risk and Outcome of Psychosis (G.R.O.U.P). 2011. Reduced Cortical Thickness as an Outcome of Differential Sensitivity to Environmental Risks in Schizophrenia. Biol Psychiatry. 69:487–494.

Hajek T, Kopecek M, Kozeny J, Gunde E, Alda M, Höschl C. 2009. Amygdala volumes in mood disorders--meta-analysis of magnetic resonance volumetry studies. J Affect Disord. 115:395–410.

Hardan AY, Libove RA, Keshavan MS, Melhem NM, Minshew NJ. 2009. A Preliminary Longitudinal Magnetic Resonance Imaging Study of Brain Volume and Cortical Thickness in Autism. Biol Psychiatry. 66:320–326.

Hardan AY, Muddasani S, Vemulapalli M, Keshavan MS, Minshew NJ. 2006. An MRI study of increased cortical thickness in autism. Am J Psychiatry. 163:1290–1292.

Hava G, Vered L, Yael M, Mordechai H, Mahoud H. 2006. Alterations in behavior in adult offspring mice following maternal inflammation during pregnancy. Dev Psychobiol. 48:162–168.

Hawi Z, Cummins TDR, Tong J, Johnson B, Lau R, Samarrai W, Bellgrove MA. 2015. The molecular genetic architecture of attention deficit hyperactivity disorder. Mol Psychiatry. 20:289–297.

Hazlett HC, Gu H, Munsell BC, Kim SH, Styner M, Wolff JJ, Elison JT, Swanson MR, Zhu H, Botteron KN, Collins DL, Constantino JN, Dager SR, Estes AM, Evans AC, Fonov VS, Gerig G, Kostopoulos P, McKinstry RC, Pandey J, Paterson S, Pruett JR, Schultz RT, Shaw DW, Zwaigenbaum L, Piven J, Piven J, Hazlett HC, Chappell C, Dager SR, Estes AM, Shaw DW, Botteron KN, McKinstry RC, Constantino JN, Pruett Jr JR, Schultz RT, Paterson S, Zwaigenbaum L, Elison JT, Wolff JJ, Evans AC, Collins DL, Pike GB, Fonov VS, Kostopoulos P, Das S, Gerig G, Styner M, Gu CH. 2017. Early brain development in infants at high risk for autism spectrum disorder. Nature. 542:348–351.

Hedrick A, Lee Y, Wallace GL, Greenstein D, Clasen L, Giedd JN, Raznahan A. 2012. Autism Risk Gene *MET* Variation and Cortical Thickness in Typically Developing Children and Adolescents. Autism Res. 5:434–439.

Higgins L, Greenwood SL, Wareing M, Sibley CP, Mills TA. 2011. Obesity and the

placenta: A consideration of nutrient exchange mechanisms in relation to aberrant fetal growth. Placenta. 32:1–7.

Homan ER, Zendzian RP, Schott LD, Levy HB, Adamson RH. 1972. Studies on Poly I : C Toxicity in Experimental AnimalslJ Studies on Poly I: C Toxicity in Experimental Animals.

Hoogman M, Bralten J, Hibar DP, Mennes M, Zwiers MP, Schweren LSJ, van Hulzen KJE, Medland SE, Shumskaya E, Jahanshad N, Zeeuw P de, Szekely E, Sudre G, Wolfers T, Onnink AMH, Dammers JT, Mostert JC, Vives-Gilabert Y, Kohls G, Oberwelland E, Seitz J, Schulte-Rüther M, Ambrosino S, Doyle AE, Høvik MF, Dramsdahl M, Tamm L, van Erp TGM, Dale A, Schork A, Conzelmann A, Zierhut K, Baur R, McCarthy H, Yoncheva YN, Cubillo A, Chantiluke K, Mehta MA, Paloyelis Y, Hohmann S, Baumeister S, Bramati I, Mattos P, Tovar-Moll F, Douglas P, Banaschewski T, Brandeis D, Kuntsi J, Asherson P, Rubia K, Kelly C, Martino A Di, Milham MP, Castellanos FX, Frodl T, Zentis M, Lesch K-P, Reif A, Pauli P, Jernigan TL, Haavik J, Plessen KJ, Lundervold AJ, Hugdahl K, Seidman LJ, Biederman J, Rommelse N, Heslenfeld DJ, Hartman CA, Hoekstra PJ, Oosterlaan J, Polier G von, Konrad K, Vilarroya O, Ramos-Quiroga JA, Soliva JC, Durston S, Buitelaar JK, Faraone S V, Shaw P, Thompson PM, Franke B. 2017. Subcortical brain volume differences in participants with attention deficit hyperactivity disorder in children and adults: a cross-sectional mega-analysis. The Lancet Psychiatry. 4:310–319.

Hoogman M, Muetzel R, Guimaraes JP, Shumskaya E, Mennes M, Zwiers MP,

Jahanshad N, Sudre G, Wolfers T, Earl EA, Soliva Vila JC, Vives-Gilabert Y, Khadka S, Novotny SE, Hartman CA, Heslenfeld DJ, Schweren LJS, Ambrosino S, Oranje B, de Zeeuw P, Chaim-Avancini TM, Rosa PGP, Zanetti M V., Malpas CB, Kohls G, von Polier GG, Seitz J, Biederman J, Doyle AE, Dale AM, van Erp TGM, Epstein JN, Jernigan TL, Baur-Streubel R, Ziegler GC, Zierhut KC, Schrantee A, Høvik MF, Lundervold AJ, Kelly C, McCarthy H, Skokauskas N, O'Gorman Tuura RL, Calvo A, Lera-Miguel S, Nicolau R, Chantiluke KC, Christakou A, Vance A, Cercignani M, Gabel MC, Asherson P, Baumeister S, Brandeis D, Hohmann S, Bramati IE, Tovar-Moll F, Fallgatter AJ, Kardatzki B, Schwarz L, Anikin A, Baranov A, Gogberashvili T, Kapilushniy D, Solovieva A, El Marroun H, White T, Karkashadze G, Namazova-Baranova L, Ethofer T, Mattos P, Banaschewski T, Coghill D, Plessen KJ, Kuntsi J, Mehta MA, Paloyelis Y, Harrison NA, Bellgrove MA, Silk TJ, Cubillo AI, Rubia K, Lazaro L, Brem S, Walitza S, Frodl T, Zentis M, Castellanos FX, Yoncheva YN, Haavik J, Reneman L, Conzelmann A, Lesch K-P, Pauli P, Reif A, Tamm L, Konrad K, Oberwelland Weiss E, Busatto GF, Louza MR, Durston S, Hoekstra PJ, Oosterlaan J, Stevens MC, Ramos-Quiroga JA, Vilarroya O, Fair DA, Nigg JT, Thompson PM, Buitelaar JK, Faraone S V., Shaw P, Tiemeier H, Bralten J, Franke B. 2019. Brain Imaging of the Cortex in ADHD: A Coordinated Analysis of Large-Scale Clinical and Population-Based Samples. Am J Psychiatry. 176:531–542.

Hsiao EY, Patterson PH. 2012. Placental regulation of maternal-fetal interactions and brain development. Dev Neurobiol. 72:1317–1326.

Huettel SA, Song AW, McCarthy G. 2008. Functional magnetic resonance imaging.

Sinauer Associates.

Hunter CA, Jones SA. 2015. IL-6 as a keystone cytokine in health and disease. Nat Immunol.

Hutchison RM, Everling S. 2012. Monkey in the middle: why non-human primates are needed to bridge the gap in resting-state investigations. Front Neuroanat. 6:29.

Insel T, Cuthbert B, Garvey M, Heinssen R, Pine DS, Quinn K, Sanislow C, Wang P. 2010. Research domain criteria (RDoC): toward a new classification framework for research on mental disorders. Am J Psychiatry. 167:748–751.

Jansen AG, Mous SE, White T, Posthuma D, Polderman TJC. 2015. What Twin Studies Tell Us About the Heritability of Brain Development, Morphology, and Function: A Review. Neuropsychol Rev. 25:27–46.

Jeličić H, Phelps E, Lerner RM. 2009. Use of missing data methods in longitudinal studies: The persistence of bad practices in developmental psychology. Dev Psychol. 45:1195–1199.

Jenkinson M, Beckmann CF, Behrens TEJ, Woolrich MW, Smith SM. 2012. FSL. Neuroimage. 62:782–790.

Kahm M, Hasenbrink RG, Lichtenberg-Fraté H, Ludwig J, Rheinahrcampus MK. 2010. grofit: Fitting Biological Growth Curves with R. JSS J Stat Softw. 33.

Kalin NH, Shelton SE, Takahashi LK. 1991. Defensive Behaviors in Infant Rhesus Monkeys: Ontogeny and Context-dependent Selective Expression. Child Dev.

62:1175–1183.

Kalmady SV, Venkatasubramanian G, Shivakumar V, Gautham S, Subramaniam A, Jose DA, Maitra A, Ravi V, Gangadhar BN. 2014. Relationship between Interleukin-6 Gene Polymorphism and Hippocampal Volume in Antipsychotic-Naïve Schizophrenia: Evidence for Differential Susceptibility? PLoS One. 9:e96021.

Karalunas SL, Fair D, Musser ED, Aykes K, Iyer SP, Nigg JT. 2014. Subtyping attention-deficit/hyperactivity disorder using temperament dimensions: toward biologically based nosologic criteria. JAMA psychiatry. 71:1015–1024.

Karalunas SL, Gustafsson HC, Dieckmann NF, Tipsord J, Mitchell SH, Nigg JT. 2017. Heterogeneity in development of aspects of working memory predicts longitudinal attention deficit hyperactivity disorder symptom change. J Abnorm Psychol. 126:774–792.

Kessler RC, Berglund P, Demler O, Jin R, Merikangas KR, Walters EE. 2005. Lifetime Prevalence and Age-of-Onset Distributions of DSM-IV Disorders in the National Comorbidity Survey Replication. Arch Gen Psychiatry. 62:593.

Khundrakpam BS, Lewis JD, Kostopoulos P, Carbonell F, Evans AC. 2017. Cortical Thickness Abnormalities in Autism Spectrum Disorders Through Late Childhood, Adolescence, and Adulthood: A Large-Scale MRI Study. Cereb Cortex. 27:1721–1731.

Kiecolt-Glaser JK, Derry HM, Fagundes CP. 2015. Inflammation: Depression Fans the Flames and Feasts on the Heat. Am J Psychiatry. 172:1075–1091.

Knuesel I, Chicha L, Britschgi M, Schobel SA, Bodmer M, Hellings JA, Toovey S, Prinssen EP. 2014. Maternal immune activation and abnormal brain development across CNS disorders. Nat Rev Neurol. 10:643–660.

Kodituwakku PW. 2007. Defining the behavioral phenotype in children with fetal alcohol spectrum disorders: A review. Neurosci Biobehav Rev. 31:192–201.

Kolb B, Gibb R. 2011. Brain plasticity and behaviour in the developing brain. J Can Acad Child Adolesc Psychiatry. 20:265–276.

Krakowiak P, Walker CK, Bremer AA, Baker AS, Ozonoff S, Hansen RL, Hertz-Picciotto I. 2012. Maternal Metabolic Conditions and Risk for Autism and Other Neurodevelopmental Disorders. Pediatrics. 129:e1121–e1128.

Kwon EJ, Kim YJ. 2017. What is fetal programming?: a lifetime health is under the control of in utero health. Obstet Gynecol Sci. 60:506.

Langs G, Golland P, Tie Y, Rigolo L, Golby AJ. 2010. Functional Geometry Alignment and Localization of Brain Areas. Adv Neural Inf Process Syst. 1:1225–1233.

Larsen R. 2011. Missing Data Imputation versus Full Information Maximum Likelihood with Second-Level Dependencies. Struct Equ Model A Multidiscip J. 18:649–662.

Laumann TO, Gordon EM, Adeyemo B, Snyder AZ, Joo SJ, Chen M-Y, Gilmore AW, McDermott KB, Nelson SM, Dosenbach NUF, Schlaggar BL, Mumford JA, Poldrack RA, Petersen SE. 2015. Functional System and Areal Organization of a Highly Sampled Individual Human Brain. Neuron. 87:657–670.

Lee BR, Thompson R. 2009. Examining Externalizing Behavior Trajectories of Youth in Group Homes: Is there Evidence for Peer Contagion? J Abnorm Child Psychol. 37:31–44.

Lenz KM, McCarthy MM. 2015. A Starring Role for Microglia in Brain Sex Differences. Neurosci. 21:306–321.

Levy F, Hay FA, Mcstephen M, Wood C, Waldman I. 1997. Attention-Deficit Hyperactivity Disorder: A Category or a Continuum? Genetic Analysis of a Large-Scale Twin Study. J Am Acad Child Adolesc Psychiatry. 36:737–744.

Li G, Lin W, Gilmore JH, Shen D. 2015. Spatial Patterns, Longitudinal Development, and Hemispheric Asymmetries of Cortical Thickness in Infants from Birth to 2 Years of Age. J Neurosci. 35:9150–9162.

Lichtenstein P, Yip BH, Björk C, Pawitan Y, Cannon TD, Sullivan PF, Hultman CM. 2009. Common genetic determinants of schizophrenia and bipolar disorder in Swedish families: a population-based study. Lancet. 373:234–239.

Liu C, Tian X, Liu H, Mo Y, Bai F, Zhao X, Ma Y, Wang J. 2015. Rhesus monkey brain development during late infancy and the effect of phencyclidine: A longitudinal MRI and DTI study. Neuroimage. 107:65–75.

Lohse C, Bassett DS, Lim KO, Carlson JM. 2014. Resolving Anatomical and Functional Structure in Human Brain Organization: Identifying Mesoscale Organization in Weighted Network Representations. PLoS Comput Biol. 10:e1003712.

Lucchina L, Carola V, Pitossi F, Depino AM. 2010. Evaluating the interaction between early postnatal inflammation and maternal care in the programming of adult anxiety and depression-related behaviors. Behav Brain Res. 213:56–65.

Lyall AE, Shi F, Geng X, Woolson S, Li G, Wang L, Hamer RM, Shen D, Gilmore JH. 2015. Dynamic Development of Regional Cortical Thickness and Surface Area in Early Childhood. Cereb Cortex. 25:2204–2212.

Maccallum RC, Browne MW, Sugawara HM. 1996. Power Analysis and Determination of Sample Size for Covariance Structure Modeling. 13.

Malkova L, Heuer E, Saunders RC. 2006. Longitudinal magnetic resonance imaging study of rhesus monkey brain development. Eur J Neurosci. 24:3204–3212.

Malonek D, Dirnagl U, Lindauer U, Yamada K, Kanno I, Grinvald A. 1997. Vascular imprints of neuronal activity: Relationships between the dynamics of cortical blood flow, oxygenation, and volume changes following sensory stimulation. Proc Natl Acad Sci U S A. 94:14826–14831.

Marcus DS, Harwell J, Olsen T, Hodge M, Glasser MF, Prior F, Jenkinson M, Laumann T, Curtiss SW, Van Essen DC. 2011. Informatics and Data Mining Tools and Strategies for the Human Connectome Project. Front Neuroinform. 5:4.

Marek S, Tervo-Clemmens B, Nielsen AN, Wheelock MD, Miller RL, Laumann TO, Earl E, Foran WW, Cordova M, Doyle O, Perrone A, Miranda-Dominguez O, Feczko E, Sturgeon D, Graham A, Hermosillo R, Snider K, Galassi A, Nagel BJ, Ewing SWF, Eggebrecht AT, Garavan H, Dale AM, Greene DJ, Barch DM, Fair

DA, Luna B, Dosenbach NUF. 2019. Identifying reproducible individual differences in childhood functional brain networks: An ABCD study. Dev Cogn Neurosci. 40.

Margulies DS, Ghosh SS, Goulas A, Falkiewicz M, Huntenburg JM, Langs G, Bezgin G, Eickhoff SB, Castellanos FX, Petrides M, Jefferies E, Smallwood J. 2016. Situating the default-mode network along a principal gradient of macroscale cortical organization. Proc Natl Acad Sci U S A. 113:12574–12579.

Markett S, Montag C, Melchers M, Weber B, Reuter M. 2016. Anxious personality and functional efficiency of the insular-opercular network: A graph-analytic approach to resting-state fMRI. Cogn Affect Behav Neurosci. 16:1039–1049.

Markov NT, Ercsey-Ravasz MM, Ribeiro Gomes AR, Lamy C, Magrou L, Vezoli J, Misery P, Falchier A, Quilodran R, Gariel MA, Sallet J, Gamanut R, Huissoud C, Clavagnier S, Giroud P, Sappey-Marinier D, Barone P, Dehay C, Toroczkai Z, Knoblauch K, Van Essen DC, Kennedy H. 2014. A weighted and directed interareal connectivity matrix for macaque cerebral cortex. Cereb Cortex. 24:17–36.

McArdle JJ, Epstein D. 1987. Latent growth curves within developmental structural equation models. Child Dev. 58:110–133.

McCarthy MM. 2019. Sex differences in neuroimmunity as an inherent risk factor. Neuropsychopharmacology. 44:38–44.

McCarthy MM, Wright CL. 2017. Convergence of Sex Differences and the Neuroimmune System in Autism Spectrum Disorder. Biol Psychiatry. 81:402–410.

McCurdy CE, Bishop JM, Williams SM, Grayson BE, Smith MS, Friedman JE, Grove KL. 2009. Maternal high-fat diet triggers lipotoxicity in the fetal livers of nonhuman primates. J Clin Invest. 119:323–335.

Mensen VT, Wierenga LM, van Dijk S, Rijks Y, Oranje B, Mandl RCW, Durston S. 2017. Development of cortical thickness and surface area in autism spectrum disorder. NeuroImage Clin. 13:215–222.

Meredith W, Tisak J. 1990. Latent Curve Analysis.

Milham MP, Ai L, Koo B, Xu T, Amiez C, Balezeau F, Baxter MG, Blezer ELA, Brochier T, Chen A, Croxson PL, Damatac CG, Dehaene S, Everling S, Fair DA, Fleysher L, Freiwald W, Froudist-Walsh S, Griffiths TD, Guedj C, Hadj-Bouziane F, Ben Hamed S, Harel N, Hiba B, Jarraya B, Jung B, Kastner S, Klink PC, Kwok SC, Laland KN, Leopold DA, Lindenfors P, Mars RB, Menon RS, Messinger A, Meunier M, Mok K, Morrison JH, Nacef J, Nagy J, Rios MO, Petkov CI, Pinsk M, Poirier C, Procyk E, Rajimehr R, Reader SM, Roelfsema PR, Rudko DA, Rushworth MFS, Russ BE, Sallet J, Schmid MC, Schwiedrzik CM, Seidlitz J, Sein J, Shmuel A, Sullivan EL, Ungerleider L, Thiele A, Todorov OS, Tsao D, Wang Z, Wilson CRE, Yacoub E, Ye FQ, Zarco W, Zhou Y, Margulies DS, Schroeder CE. 2018. An Open Resource for Non-human Primate Imaging. Neuron. 100:61-74.e2.

Milham MP, Ai L, Koo B, Xu T, Balezeau F, Baxter MG, Croxson PL, Damatac CG, Harel N, Freiwald W, al. et. 2017. An open resource for nonhuman primate imaging. bioRxiv.

Miller GA, Rockstroh B. 2013. Endophenotypes in Psychopathology Research: Where Do We Stand? Annu Rev Clin Psychol. 9:177–213.

Mills BD, Pearce HL, Khan O, Jarrett BR, Fair DA, Lahvis GP. 2016. Prenatal domoic acid exposure disrupts mouse pro-social behavior and functional connectivity MRI. Behav Brain Res. 308:14–23.

Mills KL, Goddings A-L, Herting MM, Meuwese R, Blakemore S-J, Crone EA, Dahl RE, Güroğlu B, Raznahan A, Sowell ER, Tamnes CK. 2016. Structural brain development between childhood and adulthood: Convergence across four longitudinal samples. Neuroimage. 141:273–281.

Miranda-Dominguez O, Mills BD, Carpenter SD, Grant KA, Kroenke CD, Nigg JT, Fair DA. 2014. Connectotyping: Model Based Fingerprinting of the Functional Connectome. PLoS One. 9:e111048.

Miranda-Dominguez O, Mills BD, Grayson D, Woodall A, Grant KA, Kroenke CD, Fair DA. 2014. Bridging the gap between the human and macaque connectome: a quantitative comparison of global interspecies structure-function relationships and network topology. J Neurosci. 34:5552–5563.

Morrison JL, Regnault TRH. 2016. Nutrition in Pregnancy: Optimising Maternal Diet and Fetal Adaptations to Altered Nutrient Supply. Nutrients. 8.

Motzkin JC, Philippi CL, Wolf RC, Baskaya MK, Koenigs M. 2015. Ventromedial Prefrontal Cortex Is Critical for the Regulation of Amygdala Activity in Humans. Biol Psychiatry. 77:276–284.

Musser ED, Karalunas SL, Dieckmann N, Peris TS, Nigg JT. 2016. Attention-deficit/hyperactivity disorder developmental trajectories related to parental expressed emotion. J Abnorm Psychol. 125:182–195.

Muthén B, Asparouhov T, Muthén M&. 2002. Latent Variable Analysis With Categorical Outcomes: Multiple-Group And Growth Modeling In Mplus.

Muthén BO. 2002. Beyond SEM: General Latent Variable Modeling, Behaviormetrika.

Muthén LK, Muthén BO. 2017. Mplus User's Guide. 1998-2017.

Natu VS, Gomez J, Barnett M, Jeska B, Kirilina E, Jaeger C, Zhen Z, Cox S, Weiner KS, Weiskopf N, Grill-Spector K. 2019. Apparent thinning of human visual cortex during childhood is associated with myelination. Proc Natl Acad Sci U S A. 201904931.

Nayak D, Roth TL, McGavern DB. 2014. Microglia Development and Function. Annu Rev Immunol. 32:367–402.

Nenning K-H, Liu H, Ghosh SS, Sabuncu MR, Schwartz E, Langs G. 2017. Diffeomorphic functional brain surface alignment: Functional demons. Neuroimage. 156:456–465.

Nordahl CW, Scholz R, Yang X, Buonocore MH, Simon T, Rogers S, Amaral DG. 2012. Increased rate of amygdala growth in children aged 2 to 4 years with autism spectrum disorders: a longitudinal study. Arch Gen Psychiatry. 69:53–61.

Nugent TF, Herman DH, Ordonez A, Greenstein D, Hayashi KM, Lenane M, Clasen L,

Jung D, Toga AW, Giedd JN, Rapoport JL, Thompson PM, Gogtay N. 2007. Dynamic mapping of hippocampal development in childhood onset schizophrenia. Schizophr Res. 90:62–70.

O'Brien LM, Ziegler DA, Deutsch CK, Frazier JA, Herbert MR, Locascio JJ. 2011. Statistical adjustments for brain size in volumetric neuroimaging studies: some practical implications in methods. Psychiatry Res. 193:113–122.

O'Roak BJ, State MW. 2008. Autism genetics: strategies, challenges, and opportunities. Autism Res. 1:4–17.

Ogawa S, Lee TM, Kay AR, Tank DW. 1990. Brain magnetic resonance imaging with contrast dependent on blood oxygenation. Proc Natl Acad Sci. 87:9868–9872.

Orban GA, Van Essen D, Vanduffel W. 2004. Comparative mapping of higher visual areas in monkeys and humans. Trends Cogn Sci. 8:315–324.

Ostrea EM, Morales V, Ngoumgna E, Prescilla R, Tan E, Hernandez E, Ramirez GB, Cifra HL, Manlapaz ML. 2002. Prevalence of Fetal Exposure to Environmental Toxins as Determined by Meconium Analysis. Neurotoxicology. 23:329–339.

Owen MJ, O'Donovan MC. 2017. Schizophrenia and the neurodevelopmental continuum:evidence from genomics. World Psychiatry. 16:227–235.

Panizzon MS, Fennema-Notestine C, Eyler LT, Jernigan TL, Prom-Wormley E, Neale M, Jacobson K, Lyons MJ, Grant MD, Franz CE, Xian H, Tsuang M, Fischl B, Seidman L, Dale A, Kremen WS. 2009. Distinct Genetic Influences on Cortical Surface Area

and Cortical Thickness. Cereb Cortex. 19:2728–2735.

Parker-Athill EC, Tan J. 2010. Maternal Immune Activation and Autism Spectrum Disorder: Interleukin-6 Signaling as a Key Mechanistic Pathway. Neurosignals. 18:113–128.

Patterson PH. 2009. Immune involvement in schizophrenia and autism: Etiology, pathology and animal models. Behav Brain Res. 204:313–321.

Petersen SE, Sporns O. 2015. Brain Networks and Cognitive Architectures. Neuron. 88:207–219.

Peyre H, Leplège A, Coste J. 2011. Missing data methods for dealing with missing items in quality of life questionnaires. A comparison by simulation of personal mean score, full information maximum likelihood, multiple imputation, and hot deck techniques applied to the SF-36 in the French 2003 decennial health survey. Qual Life Res. 20:287–300.

Piontkewitz Y, Arad M, Weiner I. 2011. Abnormal Trajectories of Neurodevelopment and Behavior Following In Utero Insult in the Rat. Biol Psychiatry. 70:842–851.

Polanczyk G V, Willcutt EG, Salum GA, Kieling C, Rohde LA. 2014. ADHD prevalence estimates across three decades: an updated systematic review and meta-regression analysis. Int J Epidemiol. 43:434–442.

Popova S, Lange S, Probst C, Gmel G, Rehm J. 2017. Estimation of national, regional, and global prevalence of alcohol use during pregnancy and fetal alcohol syndrome: a

systematic review and meta-analysis. Lancet Glob Heal. 5:e290–e299.

Power JD, Barnes KA, Snyder AZ, Schlaggar BL, Petersen SE. 2012. Spurious but systematic correlations in functional connectivity MRI networks arise from subject motion. Neuroimage. 59:2142–2154.

Power JD, Cohen AL, Nelson SM, Wig GS, Barnes KA, Church JA, Vogel AC, Laumann TO, Miezin FM, Schlaggar BL, Petersen SE. 2011. Functional Network Organization of the Human Brain. Neuron. 72:665–678.

Power JD, Mitra A, Laumann TO, Snyder AZ, Schlaggar BL, Petersen SE. 2014. Methods to detect, characterize, and remove motion artifact in resting state fMRI. Neuroimage. 84:320–341.

Power JD, Schlaggar BL, Petersen SE. 2015. Recent progress and outstanding issues in motion correction in resting state fMRI. Neuroimage. 105:536–551.

Prigge MBD, Bigler ED, Travers BG, Froehlich A, Abildskov T, Anderson JS, Alexander AL, Lange N, Lainhart JE, Zielinski BA. 2018. Social Responsiveness Scale (SRS) in Relation to Longitudinal Cortical Thickness Changes in Autism Spectrum Disorder. J Autism Dev Disord. 48:3319–3329.

Pulli EP, Kumpulainen V, Kasurinen JH, Korja R, Merisaari H, Karlsson L, Parkkola R, Saunavaara J, Lähdesmäki T, Scheinin NM, Karlsson H, Tuulari JJ. 2019. Prenatal exposures and infant brain: Review of magnetic resonance imaging studies and a population description analysis. Hum Brain Mapp. 40:1987–2000.

Qiu A, Anh TT, Li Y, Chen H, Rifkin-Graboi A, Broekman BFP, Kwek K, Saw S-M, Chong Y-S, Gluckman PD, Fortier M V, Meaney MJ. 2015a. Prenatal maternal depression alters amygdala functional connectivity in 6-month-old infants. Transl Psychiatry. 5:e508.

Qiu A, Anh TT, Li Y, Chen H, Rifkin-Graboi A, Broekman BFP, Kwek K, Saw S-M, Chong Y-S, Gluckman PD, Fortier M V, Meaney MJ. 2015b. Prenatal maternal depression alters amygdala functional connectivity in 6-month-old infants. Transl Psychiatry. 5:e508–e508.

Ramirez JSB, Graham AM, Thompson JR, Zhu JY, Sturgeon D, Bagley JL, Thomas E, Papadakis S, Bah M, Perrone A, Earl E, Miranda-Dominguez O, Feczko E, Fombonne EJ, Amaral DG, Nigg JT, Sullivan EL, Fair DA. 2019. Maternal Interleukin-6 Is Associated With Macaque Offspring Amygdala Development and Behavior. Cereb Cortex. 1–52.

Raper J, Wallen K, Sanchez MM, Stephens SBZ, Henry A, Villareal T, Bachevalier J. 2013. Sex-dependent role of the amygdala in the development of emotional and neuroendocrine reactivity to threatening stimuli in infant and juvenile rhesus monkeys. Horm Behav. 63:646–658.

Rapoport JL, Giedd JN, Gogtay N. 2012. Neurodevelopmental model of schizophrenia: update 2012. Mol Psychiatry. 17:1228–1238.

Rasmussen JM, Graham AM, Entringer S, Gilmore JH, Styner M, Fair DA, Wadhwa PD, Buss C. 2018. Maternal Interleukin-6 concentration during pregnancy is associated

with variation in frontolimbic white matter and cognitive development in early life. Neuroimage.

Raykov T. 2005. Analysis of Longitudinal Studies With Missing Data Using Covariance Structure Modeling With Full-Information Maximum Likelihood. Struct Equ Model A Multidiscip J. 12:493–505.

Raznahan A, Shaw P, Lalonde F, Stockman M, Wallace GL, Greenstein D, Clasen L, Gogtay N, Giedd JN. 2011. How does your cortex grow? J Neurosci. 31:7174–7177.

Raznahan A, Toro R, Daly E, Robertson D, Murphy C, Deeley Q, Bolton PF, Paus T, Murphy DGM. 2010. Cortical Anatomy in Autism Spectrum Disorder: An In Vivo MRI Study on the Effect of Age. Cereb Cortex. 20:1332–1340.

Rees S, Harding R. 2004. Brain development during fetal life: influences of the intra-uterine environment. Neurosci Lett. 361:111–114.

Rees S, Inder T. 2005. Fetal and neonatal origins of altered brain development. Early Hum Dev. 81:753–761.

Reisinger S, Khan D, Kong E, Berger A, Pollak A, Pollak DD. 2015. The Poly(I:C)-induced maternal immune activation model in preclinical neuropsychiatric drug discovery. Pharmacol Ther.

Remer J, Croteau-Chonka E, Dean DC, D'Arpino S, Dirks H, Whiley D, Deoni SCL. 2017. Quantifying cortical development in typically developing toddlers and young children, 1–6 years of age. Neuroimage. 153:246–261.

Reynolds LP, Borowicz PP, Caton JS, Vonnahme KA, Luther JS, Hammer CJ, Maddock Carlin KR, Grazul-Bilska AT, Redmer DA. 2010. Developmental programming: The concept, large animal models, and the key role of uteroplacental vascular development1,2. J Anim Sci. 88:E61–E72.

Rimol LM, Nesvåg R, Hagler DJ, Bergmann Ø, Fennema-Notestine C, Hartberg CB, Haukvik UK, Lange E, Pung CJ, Server A, Melle I, Andreassen OA, Agartz I, Dale AM. 2012. Cortical Volume, Surface Area, and Thickness in Schizophrenia and Bipolar Disorder. Biol Psychiatry. 71:552–560.

Rivera HM, Christiansen KJ, Sullivan EL. 2015. The role of maternal obesity in the risk of neuropsychiatric disorders. Front Neurosci. 9:194.

Rivera HM, Kievit P, Kirigiti MA, Bauman LA, Baquero K, Blundell P, Dean TA, Valleau JC, Takahashi DL, Frazee T, Douville L, Majer J, Smith MS, Grove KL, Sullivan EL. 2015. Maternal high-fat diet and obesity impact palatable food intake and dopamine signaling in nonhuman primate offspring. Obesity. 23:2157–2164.

Robinson EC, Jbabdi S, Glasser MF, Andersson J, Burgess GC, Harms MP, Smith SM, Van Essen DC, Jenkinson M. 2014. MSM: A new flexible framework for Multimodal Surface Matching. Neuroimage. 100:414–426.

Ronald A, Pennell CE, Whitehouse AJO. 2010. Prenatal Maternal Stress Associated with ADHD and Autistic Traits in early Childhood. Front Psychol. 1:223.

Rudolph MD, Graham A, Feczko E, Miranda-Dominguez O, Rasmussen J, Nardos R, Entringer S, Wadhwa PD, Buss C, Fair DA. 2018. Maternal IL-6 during pregnancy

can be estimated from the newborn brain connectome and predicts future working memory performance in offspring. Nat Neurosci. 1–36.

Sawiak SJ, Shiba Y, Oikonomidis L, Windle CP, Santangelo AM, Grydeland H, Cockcroft G, Bullmore ET, Roberts AC. 2018. Trajectories and Milestones of Cortical and Subcortical Development of the Marmoset Brain From Infancy to Adulthood. Cereb Cortex. 28:4440–4453.

Schatz DB, Rostain AL. 2006. ADHD With Comorbid Anxiety. J Atten Disord. 10:141–149.

Schlomer GL, Bauman S, Card NA. 2010. Best practices for missing data management in counseling psychology. J Couns Psychol. 57:1–10.

Schumacker R, Lomax R. 2004. A beginner's guide to structural equation modeling.

Schwarz JM, Sholar PW, Bilbo SD. 2012. Sex differences in microglial colonization of the developing rat brain. J Neurochem. 120:948–963.

Scola G, Duong A. 2017. Prenatal maternal immune activation and brain development with relevance to psychiatric disorders. Neuroscience. 346:403–408.

Scott JA, Grayson D, Fletcher E, Lee A, Bauman MD, Schumann CM, Buonocore MH, Amaral DG. 2016a. Longitudinal analysis of the developing rhesus monkey brain using magnetic resonance imaging: birth to adulthood. Brain Struct Funct. 221:2847–2871.

Scott JA, Grayson D, Fletcher E, Lee A, Bauman MD, Schumann CM, Buonocore MH,

Amaral DG. 2016b. Longitudinal analysis of the developing rhesus monkey brain using magnetic resonance imaging: birth to adulthood. Brain Struct Funct. 221:2847–2871.

Seki F, Hikishima K, Komaki Y, Hata J, Uematsu A, Okahara N, Yamamoto M, Shinohara H, Sasaki E, Okano H. 2017. Developmental trajectories of macroanatomical structures in common marmoset brain. Neuroscience. 364:143–156.

Selemon LD, Zecevic N. 2015. Schizophrenia: A tale of two critical periods for prefrontal cortical development. Transl Psychiatry.

Semple BD, Blomgren K, Gimlin K, Ferriero DM, Noble-Haeusslein LJ. 2013. Brain development in rodents and humans: Identifying benchmarks of maturation and vulnerability to injury across species. Prog Neurobiol.

Shaw P, Eckstrand K, Sharp W, Blumenthal J, Lerch JP, Greenstein D, Clasen L, Evans A, Giedd J, Rapoport JL. 2007. Attention-deficit/hyperactivity disorder is characterized by a delay in cortical maturation. Proc Natl Acad Sci U S A. 104:19649–19654.

Shaw P, Gogtay N, Rapoport J. 2010. Childhood psychiatric disorders as anomalies in neurodevelopmental trajectories. Hum Brain Mapp. 31:917–925.

Shaw P, Lerch J, Greenstein D, Sharp W, Clasen L, Evans A, Giedd J, Castellanos FX, Rapoport J. 2006. Longitudinal Mapping of Cortical Thickness and Clinical Outcome in Children and Adolescents With Attention-Deficit/Hyperactivity

Disorder. Arch Gen Psychiatry. 63:540.

Shaw P, Malek M, Watson B, Greenstein D, de Rossi P, Sharp W. 2013. Trajectories of Cerebral Cortical Development in Childhood and Adolescence and Adult Attention-Deficit/Hyperactivity Disorder. Biol Psychiatry. 74:599–606.

Shin J, French L, Xu T, Leonard G, Perron M, Pike GB, Richer L, Veillette S, Pausova Z, Paus T. 2018. Cell-Specific Gene-Expression Profiles and Cortical Thickness in the Human Brain. Cereb Cortex. 28:3267–3277.

Short SJ, Lubach GR, Karasin AI, Olsen CW, Styner M, Knickmeyer RC, Gilmore JH, Coe CL. 2010. Maternal Influenza Infection During Pregnancy Impacts Postnatal Brain Development in the Rhesus Monkey. Biol Psychiatry. 67:965–973.

Sidman RL, Rakic P. 1973. Neuronal migration, with special reference to developing human brain: a review. Brain Res. 62:1–35.

Simanek AM, Meier HCS. 2015. Association Between Prenatal Exposure to Maternal Infection and Offspring Mood Disorders: A Review of the Literature. Curr Probl Pediatr Adolesc Health Care. 45:325–364.

Singer JD, Willett JB. 2003. Applied longitudinal data analysis : modeling change and event occurrence. Oxford University Press.

Smith SEP, Li J, Garbett K, Mirnics K, Patterson PH. 2007. Maternal immune activation alters fetal brain development through interleukin-6. J Neurosci. 27:10695–10702.

Smith SM, Jenkinson M, Woolrich MW, Beckmann CF, Behrens TEJ, Johansen-Berg H,

Bannister PR, De Luca M, Drobnjak I, Flitney DE, Niazy RK, Saunders J, Vickers J, Zhang Y, De Stefano N, Brady JM, Matthews PM. 2004a. Advances in functional and structural MR image analysis and implementation as FSL. Neuroimage. 23 Suppl 1:S208--19.

Smith SM, Jenkinson M, Woolrich MW, Beckmann CF, Behrens TEJ, Johansen-Berg H, Bannister PR, De Luca M, Drobnjak I, Flitney DE, Niazy RK, Saunders J, Vickers J, Zhang Y, De Stefano N, Brady JM, Matthews PM. 2004b. Advances in functional and structural MR image analysis and implementation as FSL. Neuroimage. 23:S208–S219.

Smith D V., Gseir M, Speer ME, Delgado MR. 2016. Toward a cumulative science of functional integration: A meta-analysis of psychophysiological interactions. Hum Brain Mapp. 37:2904–2917.

Smolders S, Notter T, Smolders SMT, Rigo JM, Brône B. 2018. Controversies and prospects about microglia in maternal immune activation models for neurodevelopmental disorders. Brain Behav Immun.

Spann MN, Monk C, Scheinost D, Peterson BS. 2018. Maternal Immune Activation During the Third Trimester Is Associated with Neonatal Functional Connectivity of the Salience Network and Fetal to Toddler Behavior. J Neurosci. 38:2877–2886.

Stafford JM, Jarrett BR, Miranda-Dominguez O, Mills BD, Cain N, Mihalas S, Lahvis GP, Lattal KM, Mitchell SH, David S V., Fryer JD, Nigg JT, Fair DA. 2014. Large-scale topology and the default mode network in the mouse connectome. Proc Natl

Acad Sci U S A. 111:18745–18750.

Stolp HB. 2013. Neuropoietic cytokines in normal brain development and neurodevelopmental disorders. Mol Cell Neurosci. 53:63–68.

Sullivan EL, Grayson B, Takahashi D, Robertson N, Maier A, Bethea CL, Smith MS, Coleman K, Grove KL. 2010. Chronic consumption of a high-fat diet during pregnancy causes perturbations in the serotonergic system and increased anxiety-like behavior in nonhuman primate offspring. J Neurosci. 30:3826–3830.

Sullivan EL, Kievit P. 2016. The Implications of Maternal Obesity on Offspring Physiology and Behavior in the Nonhuman Primate. In: Parental Obesity: Intergenerational Programming and Consequences. New York, NY: Springer New York. p. 201–234.

Sullivan EL, Nousen EK, Chamlou KA. 2014. Maternal high fat diet consumption during the perinatal period programs offspring behavior. Physiol Behav. 123:236–242.

Sullivan EL, Nousen EK, Chamlou KA, Grove KL. 2012. The Impact of Maternal High-Fat Diet Consumption on Neural Development and Behavior of Offspring. Int J Obes Suppl. 2:S7–S13.

Sullivan EL, Rivera HM, True CA, Franco JG, Baquero K, Dean TA, Valleau JC, Takahashi DL, Frazee T, Hanna G, Kirigiti MA, Bauman LA, Grove KL, Kievit P. 2017. Maternal and postnatal high-fat diet consumption programs energy balance and hypothalamic melanocortin signaling in nonhuman primate offspring. Am J Physiol Integr Comp Physiol. 313:R169–R179.

Tamnes CK, Herting MM, Goddings AL, Meuwese R, Blakemore SJ, Dahl RE, Güroğlu B, Raznahan A, Sowell ER, Crone EA, Mills KL. 2017. Development of the cerebral cortex across adolescence: A multisample study of inter-related longitudinal changes in cortical volume, surface area, and thickness. J Neurosci. 37:3402–3412.

Thomas E, Buss C, Rasmussen JM, Entringer S, Ramirez JSB, Marr M, Rudolph MD, Gilmore JH, Styner M, Wadhwa PD, Fair DA, Graham AM. 2019. Newborn amygdala connectivity and early emerging fear. Dev Cogn Neurosci. 37.

Thompson JR, Gustafsson HC, Decapo M, Takahashi DL. 2018. Maternal Diet , Metabolic State , and Inflammatory Response Exert Unique and Long-lasting Influences on Offspring Behavior in Non- human Primates. 1–29.

Thompson JR, Gustafsson HC, DeCapo M, Takahashi DL, Bagley JL, Dean TA, Kievit P, Fair DA, Sullivan EL. 2018. Maternal Diet, Metabolic State, and Inflammatory Response Exert Unique and Long-Lasting Influences on Offspring Behavior in Non-Human Primates. Front Endocrinol (Lausanne). 9:161.

Thompson JR, Valleau JC, Barling AN, Franco JG, DeCapo M, Bagley JL, Sullivan EL. 2017. Exposure to a High-Fat Diet during Early Development Programs Behavior and Impairs the Central Serotonergic System in Juvenile Non-Human Primates. Front Endocrinol (Lausanne). 8:164.

Toga AW, Thompson PM, Sowell ER. 2006. Mapping brain maturation. Trends Neurosci. 29:148–159.

Tohmi M, Tsuda N, Watanabe Y, Kakita A, Nawa H. 2004. Perinatal inflammatory

cytokine challenge results in distinct neurobehavioral alterations in rats: implication in psychiatric disorders of developmental origin. Neurosci Res. 50:67–75.

Tottenham N, Gabard-Durnam LJ. 2017. The developing amygdala: a student of the world and a teacher of the cortex. Curr Opin Psychol. 17:55–60.

True C, Arik A, Lindsley S, Kirigiti M, Sullivan E, Kievit P. 2018. Early High-Fat Diet Exposure Causes Dysregulation of the Orexin and Dopamine Neuronal Populations in Nonhuman Primates. Front Endocrinol (Lausanne). 9:508.

Uematsu A, Hata J, Komaki Y, Seki F, Yamada C, Okahara N, Kurotaki Y, Sasaki E, Okano H. 2017. Mapping orbitofrontal-limbic maturation in non-human primates: A longitudinal magnetic resonance imaging study. Neuroimage. 163:55–67.

Van Essen D. 2005. Surface-Based Comparisons of Macaque and Human Cortical Organization. In: Dehaene S,, Duhamel J,, Hauser M,, Rizzolatti G, editors. From monkey brain to human brain. 1st ed. Cambridge, MA: MIT Press. p. 3–19.

Van Essen DC, Glasser MF. 2018. Parcellating Cerebral Cortex: How Invasive Animal Studies Inform Noninvasive Mapmaking in Humans. Neuron. 99:640–663.

Van Lieshout RJ, GJJM S, M D. 2013. Role of maternal adiposity prior to and during pregnancy in cognitive and psychiatric problems in offspring. Nutr Rev. 71:S95–S101.

Van Lieshout RJ, Voruganti LP. 2008. Diabetes mellitus during pregnancy and increased risk of schizophrenia in offspring: a review of the evidence and putative

mechanisms. J Psychiatry Neurosci. 33:395–404.

Vijayakumar N, Allen NB, Youssef G, Dennison M, Yücel M, Simmons JG, Whittle S. 2016. Brain development during adolescence: A mixed-longitudinal investigation of cortical thickness, surface area, and volume. Hum Brain Mapp. 37:2027–2038.

Vincent JL, Patel GH, Fox MD, Snyder AZ, Baker JT, Van Essen DC, Zempel JM, Snyder LH, Corbetta M, Raichle ME. 2007. Intrinsic functional architecture in the anaesthetized monkey brain. Nature. 447:83–86.

Walhovd KB, Fjell AM, Giedd J, Dale AM, Brown TT. 2016. Through Thick and Thin: a Need to Reconcile Contradictory Results on Trajectories in Human Cortical Development. Cereb Cortex. 27:bhv301.

Warnell KR, Pecukonis M, Redcay E. 2017. Developmental relations between amygdala volume and anxiety traits: Effects of informant, sex, and age. Dev Psychopathol. 1–13.

Warning JC, McCracken SA, Morris JM. 2011. A balancing act: Mechanisms by which the fetus avoids rejection by the maternal immune system. Reproduction.

White SW, Oswald D, Ollendick T, Scahill L. 2009. Anxiety in children and adolescents with autism spectrum disorders. Clin Psychol Rev. 29:216–229.

Willette AA, Lubach GR, Knickmeyer RC, Short SJ, Styner M, Gilmore JH, Coe CL. 2011. Brain enlargement and increased behavioral and cytokine reactivity in infant monkeys following acute prenatal endotoxemia. Behav Brain Res. 219:108–115.

Williamson DE, Coleman K, Bacanu S-A, Devlin BJ, Rogers J, Ryan ND, Cameron JL. 2003. Heritability of fearful-anxious endophenotypes in infant rhesus macaques: a preliminary report. Biol Psychiatry. 53:284–291.

Wong H, Hoeffer C. 2017. Maternal IL-17A in autism.

Woolrich MW, Jbabdi S, Patenaude B, Chappell M, Makni S, Behrens T, Beckmann C, Jenkinson M, Smith SM. 2009. Bayesian analysis of neuroimaging data in FSL. Neuroimage. 45:S173–S186.

Workman AD, Charvet CJ, Clancy B, Darlington RB, Finlay BL. 2013. Modeling Transformations of Neurodevelopmental Sequences across Mammalian Species. J Neurosci. 33:7368–7383.

Wu WL, Hsiao EY, Yan Z, Mazmanian SK, Patterson PH. 2017. The placental interleukin-6 signaling controls fetal brain development and behavior. Brain Behav Immun. 62:11–23.

Xu T, Falchier A, Sullivan EL, Linn G, Ramirez JSB, Ross D, Feczko E, Opitz A, Bagley J, Sturgeon D, Earl E, Miranda-Domínguez O, Perrone A, Craddock RC, Schroeder CE, Colcombe S, Fair DA, Milham MP. 2018. Delineating the Macroscale Areal Organization of the Macaque Cortex In Vivo. Cell Rep. 23:429–441.

Xu T, Nenning K-H, Schwartz E, Hong S-J, Vogelstein JT, Fair DA, Schroeder CE, Margulies DS, Smallwood J, Milham MP, Langs G. 2019. Cross-species Functional Alignment Reveals Evolutionary Hierarchy Within the Connectome. bioRxiv. 692616.

Xu T, Sturgeon D, Ramirez JSB, Froudist-Walsh S, Margulies DS, Schroeder CE, Fair DA, Milham MP. 2019a. Interindividual Variability of Functional Connectivity in Awake and Anesthetized Rhesus Macaque Monkeys. Biol Psychiatry Cogn Neurosci Neuroimaging. 4:543–553.

Xu T, Sturgeon D, Ramirez JSB, Froudist-Walsh S, Margulies DS, Schroeder CE, Fair DA, Milham MP. 2019b. Interindividual Variability of Functional Connectivity in Awake and Anesthetized Rhesus Macaque Monkeys. Biol Psychiatry Cogn Neurosci Neuroimaging. 4:543–553.

Xu T, Sturgeon D, Ramirez JSB, Froudist-Walsh S, Margulies DS, Schroeder CE, Milham MP. 2019. Interindividual Variability of Functional Connectivity in Awake and Anesthetized Rhesus Macaque Monkeys. Biol Psychiatry Cogn Neurosci Neuroimaging. 4:543–553.

Yeo BTT, Krienen FM, Sepulcre J, Sabuncu MR, Lashkari D, Hollinshead M, Roffman JL, Smoller JW, Zöllei L, Polimeni JR, Fischl B, Liu H, Buckner RL, Ahn Y, Bagrow J, Lehmann S, Amano K, Wandell B, Dumoulin S, Amunts K, Lenzen M, Friederici A, Schleicher A, Morosan P, Palomero-Gallagher N, Zilles K, Amunts K, Malikovic A, Mohlberg H, Schormann T, Zilles K, Amunts K, Schleicher A, Bürgel U, Mohlberg H, Uylings H, Zilles K, Andersen R, Asanuma C, Essick G, Siegel R, Andersen R, Buneo C, Andrews-Hanna J, Reidler J, Sepulcre J, Poulin R, Buckner R, Baizer J, Ungerleider L, Desimone R, Balasubramanian M, Polimeni J, Schwartz E, Barbas H, Pandya D, Basser P, Mattiello J, LeBihan D, Beckmann C, DeLuca M, Devlin J, Smith S, Beckmann C, Smith S, Bellec P, Rosa-Neto P, Lyttelton O,

Benali H, Evans A, Ben-Hur A, Elisseeff A, Guyon I, Binkofski F, Buccino G, Posse S, Seitz R, Rizzolatti G, Freund H, Binkofski F, Dohle C, Posse S, Stephan K, Hefter H, Seitz R, Freund H, Biswal B, Yetkin F, Haughton V, Hyde J, Biswal B, Mennes M, Zuo X, Gohel S, Kelly C, Smith S, Beckmann C, Adelstein J, Buckner R, Colcombe S, Dogonowski A, Ernst M, Fair D, Hampson M, Hoptman M, Hyde J, Kiviniemi V, Kötter R, Li S, Lin C, Lowe M, Mackay C, Madden D, Madsen K, Margulies D, Mayberg H, McMahon K, Monk C, Mostofsky S, Nagel B, Pekar J, Peltier S, Petersen S, Riedl V, Rombouts S, Rypma B, Schlaggar B, Schmidt S, Seidler R, Siegle G, Sorg C, Teng G, Veijola J, Villringer A, Walter M, Wang L, Weng X, Whitfield-Gabrieli S, Williamson P, Windischberger C, Zang Y, Zhang H, Castellanos F, Milham M, Blinkov S, Glezer I, Brewer A, Liu J, Wade A, Wandell B, Brodmann K, Buckner R, Andrews-Hanna J, Schacter D, Buckner R, Krienen F, Castellanos A, Diaz J, Yeo B, Buckner R, Sepulcre J, Talukdar T, Krienen F, Liu H, Hedden T, Andrews-Hanna J, Sperling R, Johnson K, Buckner R, Bullmore E, Sporns O, Cabeza R, Ciaramelli E, Olson I, Moscovitch M, Carmichael S, Price J, Caspers S, Eickhoff S, Geyer S, Scheperjans F, Mohlberg H, Zilles K, Amunts K, Caspers S, Geyer S, Schleicher A, Mohlberg H, Amunts K, Zilles K, Catani M, ffytche D, Cavada C, Goldman-Rakic P, Cavada C, Goldman-Rakic P, Choi H, Zilles K, Mohlberg H, Schleicher A, Fink G, Armstrong E, Amunts K, Cohen A, Fair D, Dosenbach N, Miezin F, Dierker D, Essen D Van, Schlaggar B, Petersen S, Colby C, Goldberg M, Connolly J, Goodale M, Desouza J, Menon R, Vilis T, Connolly J, Goodale M, Menon R, Munoz D, Corbetta M, Akbudak E, Conturo T, Snyder A, Ollinger J, Drury H, Linenweber M, Petersen S, Raichle M, Essen D Van,

Shulman G, Corbetta M, Shulman G, Cragg B, Culham J, Danckert S, DeSouza J, Gati J, Menon R, Goodale M, Culham J, Kanwisher N, Dale A, Fischl B, Sereno M, Damoiseaux J, Rombouts S, Barkhof F, Scheltens P, Stam C, Smith S, Beckmann C, Luca M De, Beckmann C, Stefano N De, Matthews P, Smith S, DeYoe E, Carman G, Bandettini P, Glickman S, Wieser J, Cox R, Miller D, Neitz J, Dickson J, Drury H, Essen D Van, Disbrow E, Litinas E, Recanzone G, Padberg J, Krubitzer L, Distler C, Boussaoud D, Desimone R, Ungerleider L, Dosenbach N, Fair D, Miezin F, Cohen A, Wenger K, Dosenbach R, Fox M, Snyder A, Vincent J, Raichle M, Schlaggar B, Petersen S, Dow B, Snyder A, Vautin R, Bauer R, Eickhoff S, Stephan K, Mohlberg H, Grefkes C, Fink G, Amunts K, Zilles K, Engel S, Glover G, Wandell B, Engel S, Rumelhart D, Wandell B, Lee A, Glover G, Chichilnisky E, Shadlen M, Evarts E, Thach W, Faillenot I, Sunaert S, Hecke P Van, Orban G, Felleman D, Essen D Van, Fischl B, Liu A, Dale A, Fischl B, Rajendran N, Busa E, Augustinack J, Hinds O, Yeo B, Mohlberg H, Amunts K, Zilles K, Fischl B, Sereno M, Dale A, Fischl B, Sereno M, Tootell R, Dale A, Fox M, Corbetta M, Snyder A, Vincent J, Raichle M, Fox M, Raichle M, Fox M, Snyder A, Vincent J, Corbetta M, Essen D Van, Raichle M, Frahm H, Stephan H, Baron G, Friedman D, Friston K, Geschwind N, Geyer S, Ledberg A, Schleicher A, Kinomura S, Schormann T, Bürgel U, Klingberg T, Larsson J, Zilles K, Roland P, Geyer S, Schleicher A, Zilles K, Geyer S, Gold J, Shadlen M, Goldman-Rakic P, Golland P, Golland Y, Malach R, Gould H, Cusick C, Pons T, Kaas J, Grefkes C, Geyer S, Schormann T, Roland P, Zilles K, Grefkes C, Weiss P, Zilles K, Fink G, Greicius M, Krasnow B, Reiss A, Menon V, Greicius M, Srivastava G, Reiss A, Menon V, Greve D, Fischl B, Grill-

Spector K, Malach R, Hadjikhani N, Liu A, Dale A, Cavanagh P, Tootell R, Hagler D, Riecke L, Sereno M, Hagmann P, Cammoun L, Gigandet X, Meuli R, Honey C, Wedeen V, Sporns O, Heide W, Binkofski F, Seitz R, Posse S, Nitschke M, Freund H, Kömpf D, Hilgetag C, O'Neill M, Young M, Hill J, Inder T, Neil J, Dierker D, Harwell J, Essen D Van, Hinds O, Polimeni J, Rajendran N, Balasubramanian M, Amunts K, Zilles K, Schwartz E, Fischl B, Triantafyllou C, Hinds O, Rajendran N, Polimeni J, Augustinack J, Wiggins G, Wald L, Rosas HD, Potthast A, Schwartz E, Fischl B, Honey C, Sporns O, Cammoun L, Gigandet X, Thiran J, Meuli R, Hagmann P, Hubel D, Wiesel T, Huk A, Dougherty R, Heeger D, Iwamura Y, James W, Jäncke L, Kleinschmidt A, Mirzazade S, Shah N, Freund H, Jenkinson M, Bannister P, Brady M, Smith S, Johansen-Berg H, Behrens T, Robson M, Drobnjak I, Rushworth M, Brady J, Smith S, Higham D, Matthews P, Johnston J, Vaishnavi S, Smyth M, Zhang D, He B, Zempel J, Shimony J, Snyder A, Raichle M, Jones E, Coulter J, Hendry S, Jones E, Powell T, Jones E, Wise S, Kaas J, Kemp J, Powell T, Killackey H, Gould H, Cusick C, Pons T, Kaas J, Kolster H, Peeters R, Orban G, Kondo H, Saleem K, Price J, Koyama M, Hasegawa I, Osada T, Adachi Y, Nakahara K, Miyashita Y, Kurata K, Kwong K, Belliveau J, Chesler D, Goldberg I, Weisskoff R, Poncelet B, Kennedy D, Hoppel B, Cohen M, Turner R, Cheng H, Brady T, Rosen B, Lancaster J, Tordesillas-Gutierrez D, Martinez M, Salinas F, Evans A, Zilles K, Mazziotta J, Fox P, Lange T, Roth V, Braun M, Buhmann J, Larsson J, Heeger D, Lashkari D, Vul E, Kanwisher N, Golland P, Lavenex P, Suzuki W, Amaral D, Levy I, Hasson U, Avidan G, Hendler T, Malach R, Logothetis N, Luna B, Thulborn K, Strojwas M, McCurtain B, Berman R, Genovese

C, Sweeney J, Luppino G, Matelli M, Camarda R, Rizzolatti G, Malach R, Reppas J, Benson R, Kwong K, Jiang H, Kennedy W, Ledden P, Brady T, Rosen B, Tootell R, Malikovic A, Amunts K, Schleicher A, Mohlberg H, Eickhoff S, Wilms M, Palomero-Gallagher N, Armstrong E, Zilles K, Marcus D, Fotenos A, Csernansky J, Morris J, Buckner R, Marcus D, Wang T, Parker J, Csernansky J, Morris J, Buckner R, Markov N, Misery P, Falchier A, Lamy C, Vezoli J, Quilodran R, Gariel M, Giroud P, Ercsey-Ravasz M, Pilaz L, Huissoud C, Barone P, Dehay C, Toroczkai Z, Essen D Van, Kennedy H, Knoblauch K, Matelli M, Camarda R, Glickstein M, Rizzolatti G, Matelli M, Luppino G, Rizzolatti G, Matelli M, Luppino G, Rizzolatti G, Maunsell J, Essen D Van, Maunsell J, Essen D Van, Medendorp W, Goltz H, Vilis T, Crawford J, Mesulam M, Mufson E, Mesulam M, Mesulam M, Mesulam M, Mesulam M, Moeller S, Nallasamy N, Tsao D, Freiwald W, Moran M, Mufson E, Mesulam M, Nelson S, Cohen A, Power J, Wig G, Miezin F, Wheeler M, Velanova K, Donaldson D, Phillips J, Schlaggar B, Petersen S, Ogawa S, Tank D, Menon R, Ellermann J, Kim S, Merkle H, Ugurbil K, Ojemann J, Akbudak E, Snyder A, McKinstry R, Raichle M, Conturo T, Orban G, Claeys K, Nelissen K, Smans R, Sunaert S, Todd J, Wardak C, Durand J, Vanduffel W, Orban G, Essen D Van, Vanduffel W, Pandya D, Kuypers H, Pandya D, Seltzer B, Pandya D, Vignolo L, Passingham R, Stephan K, Kötter R, Perry R, Zeki S, Petrides M, Pandya D, Petrides M, Pilbeam D, Young N, Polimeni J, Fischl B, Greve D, Wald L, Polimeni J, Hinds O, Balasubramanian M, Kouwe A van der, Wald L, Dale A, L ., Fischl B, Schwartz E, Pons T, Kaas J, Posner M, Petersen S, Fox P, Raichle M, Power J, Fair D, Schlaggar B, Petersen S, Preuss T, Rajkowska G, Goldman-Rakic P, Rizzolatti

G, Luppino G, Matelli M, Rockland K, Pandya D, Rosenbaum R, Stuss D, Levine B, Tulving E, Rottschy C, Eickhoff S, Schleicher A, Mohlberg H, Kujovic M, Zilles K, Amunts K, Rousseeuw P, Rovamo J, Virsu V, Saleem K, Kondo H, Price J, Saxe R, Powell L, Saxe R, Scheperjans F, Eickhoff S, Hömke L, Mohlberg H, Hermann K, Amunts K, Zilles K, Scheperjans F, Hermann K, Eickhoff S, Amunts K, Schleicher A, Zilles K, Schleicher A, Amunts K, Geyer S, Morosan P, Zilles K, Schormann T, Zilles K, Seeley W, Menon V, Schatzberg A, Keller J, Glover G, Kenna H, Reiss A, Greicius M, Ségonne F, Dale A, Busa E, Glessner M, Salat D, Hahn H, Fischl B, Ségonne F, Pacheco J, Fischl B, Selemon L, Goldman-Rakic P, Seltzer B, Pandya D, Seltzer B, Pandya D, Sepulcre J, Liu H, Talukdar T, Martincorena I, Yeo B, Buckner R, Sereno M, Dale A, Reppas J, Kwong K, Belliveau J, Brady T, Rosen B, Tootell R, Sereno M, Pitzalis S, Martinez A, Sestieri C, Corbetta M, Romani G, Shulman G, Shadlen M, Newsome W, Shikata E, Hamzei F, Glauche V, Knab R, Dettmers C, Weiller C, Büchel C, Shikata E, Hamzei F, Glauche V, Koch M, Weiller C, Binkofski F, Büchel C, Shulman G, McAvoy M, Cowan M, Astafiev S, Tansy A, d'Avossa G, Corbetta M, Shulman G, Ollinger J, Akbudak E, Conturo T, Snyder A, Petersen S, Corbetta M, Smith S, Fox P, Miller K, Glahn D, Fox P, Mackay C, Filippini N, Watkins K, Toro R, Laird A, Beckmann C, Smith S, Jenkinson M, Woolrich M, Beckmann C, Behrens T, Johansen-Berg H, Bannister P, Luca M De, Drobnjak I, Flitney D, Niazy R, Saunders J, Vickers J, Zhang Y, Stefano N De, Brady J, Matthews P, Stanton G, Bruce C, Goldberg M, Strick P, Suzuki W, Amaral D, Swisher J, Halko M, Merabet L, McMains S, Somers D, Taira M, Nose I, Inoue K, Tsutsui K, Talairach J, Tournoux P, Tanné-Gariépy J, Rouiller

E, Boussaoud D, Thirion B, Pinel P, Meriaux S, Roche A, Dehaene S, Poline J, Tootell R, Hadjikhani N, Hall E, Marrett S, Vanduffel W, Vaughan J, Dale A, Tootell R, Hadjikhani N, Tootell R, Reppas J, Kwong K, Malach R, Born R, Brady T, Rosen B, Belliveau J, Tootell R, Taylor J, Ungerleider L, Desimone R, Kouwe A van der, Benner T, Fischl B, Schmitt F, Salat D, Harder M, Sorensen A, Dale A, Kouwe A van der, Benner T, Salat D, Fischl B, Dijk K Van, Hedden T, Venkataraman A, Evans K, Lazar S, Buckner R, Essen D Van, Essen D Van, Overwalle F Van, Baetens K, Essen D Van, Anderson C, Felleman D, Essen D Van, Dierker D, Essen D Van, Zeki S, Vilberg K, Rugg M, Vincent J, Kahn I, Snyder A, Raichle M, Buckner R, Vincent J, Patel G, Fox M, Snyder A, Baker J, Essen D Van, Zempel J, Snyder L, Corbetta M, Raichle M, Vincent J, Snyder A, Fox M, Shannon B, Andrews J, Raichle M, Buckner R, Bonin G von, Bailey P, Wagner A, Shannon B, Kahn I, Buckner R, Wandell B, Brewer A, Dougherty R, Wandell B, Dumoulin S, Brewer A, Wessinger C, VanMeter J, Tian B, Lare J Van, Pekar J, Rauschecker J, Wilms M, Eickhoff S, Hömke L, Rottschy C, Kujovic M, Amunts K, Fink G, Yeo B, Sabuncu M, Vercauteren T, Ayache N, Fischl B, Golland P, Yeo B, Sabuncu M, Vercauteren T, Holt D, Amunts K, Zilles K, Golland P, Fischl B, Zeki S, Zilles K, Schlaug G, Matelli M, Luppino G, Schleicher A, Qü M, Dabringhaus A, Seitz R, Roland P. 2011. The organization of the human cerebral cortex estimated by intrinsic functional connectivity. J Neurophysiol. 106:1125–1165.

Zhao Y, Castellanos FX. 2016. Annual Research Review: Discovery science strategies in studies of the pathophysiology of child and adolescent psychiatric disorders - promises and limitations. J Child Psychol Psychiatry. 57:421–439.